

NATIONAL TECHNICAL UNIVERSITY OF UKRAINE
“IGOR SIKORSKY KYIV POLYTECHNIC INSTITUTE”
MINISTRY OF EDUCATION AND SCIENCE OF UKRAINE

NATIONAL TECHNICAL UNIVERSITY OF UKRAINE
“IGOR SIKORSKY KYIV POLYTECHNIC INSTITUTE”
MINISTRY OF EDUCATION AND SCIENCE OF UKRAINE

Qualifying scientific work
on the rights of the manuscript

Mane Kishor Vishwanath

UDC 536.248.2

DISSERTATION

**DETERMINATION OF PARAMETERS OF EFFECTIVE USE OF PULSATION
HEAT PIPES IN COOLING SYSTEMS OF ELECTRONIC EQUIPMENT**

144 - Heat-Power Engineering

14 – Electrical Engineering

Submitted for the degree of Philosophy Doctor

The dissertation contains the results of author own research. Using of ideas, results and texts of other authors is referenced to the appropriate source

_____/Mane Kishor/

Scientific supervisor: Kravets Volodymyr Yuriiiovych doct. techn. sci., prof.

Kyiv – 2025

ANNOTATION

Mane Kishor Vishwanath. Determination of parameters of effective use of pulsation heat pipes in cooling systems of electronic equipment.

Dissertation for a Philosophy Doctor degree in specialty 144 "Heat-Power Engineering". National Technical University of Ukraine "Igor Sikorsky Kyiv Polytechnic Institute" MES of Ukraine, Kyiv, 2025.

This dissertation work is dedicated on the study of heat transfer processes in pulsating heat pipes (PHPs) with different heat carriers at variation of operational and geometrical parameters.

The introduction highlights the relevance of this study, defining the research objectives, scientific novelty, the purpose, and goal of the study. Scientific positions and conclusions formulated in the thesis are validated. Information about: practical value of the work results, personal contribution of the author, approbation of dissertation results, publications on the topic of the dissertation, scope and structure of the thesis is presented.

Chapter 1 of the dissertation provides a comprehensive literature review on pulsating heat pipes (PHPs), examining their operational principles, geometrical configurations, working fluid properties, and key operational parameters. It starts with an introduction to PHPs, discussing their working mechanism, which relies on phase change and fluid oscillations for efficient heat transfer. The chapter then explores the influence of geometrical parameters, including inner diameter, number of turns, cross-section shape, channel design, and zone length, on PHP performance. The discussion on working fluid parameters highlights the importance of selecting appropriate fluids based on their physical properties, category, and filling ratio. These factors influence phase distribution, flow dynamics, and overall heat transport efficiency. The chapter also reviews key operational parameters, such as heat input and orientation, both of which significantly impact PHP functionality. Despite extensive studies, the literature review identifies gaps in existing research, particularly in aligning PHP designs with real-world applications, optimizing PHP configurations for compact electronics, and understanding the interplay

between geometrical parameters and fluid dynamics. This study aims to address these limitations by investigating the start-up and transient characteristics of PHPs under practical conditions, contributing to improved cooling and thermal management solutions in electronics equipment.

Chapter 2 contains the construction of an experimental setup, which was designed and developed to study the start-up and transient characteristics of pulsating heat pipes (PHPs). Experimental samples of copper PHPs with five turns were fabricated, ensuring compatibility with the height of modern CPU coolers. These samples were equipped with thermocouples placed at appropriate positions, allowing for temperature measurements. The design also incorporates adjustable heating zone lengths, enabling a detailed investigation of how heating zone dimensions influence PHP performance. An experimental setup was developed to facilitate research across various orientations, including vertical bottom heating (90°), horizontal (0°), top heating (-90°), and inclined positions ($+45^\circ$, -45°). The system allows for controlled variation of heat input, ensures stable cooling water temperature in the condenser, and enables systematic data acquisition. This setup enables the evaluation of PHP performance based on different heat carriers, heat flux densities, and heating zone lengths.

A well-defined experimental methodology was established, including the data acquisition process and data processing techniques. Uncertainty analysis of measuring instruments was performed, and potential sources of error were identified.

Chapter 3 investigates the various operational modes of PHPs, categorizing them into heat conductivity mode, thermosyphone mode, transition mode, pulsating mode, and dry-out mode. Additionally, it explores how heat carriers, PHP length ratios, and inclination angles influence PHP behavior. This chapter provides a comprehensive analysis of PHP dynamics, offering insights into the conditions required for efficient pulsating heat transfer.

Chapter 4 examines how the thermophysical properties of working fluids affect the start-up and transient behavior of pulsating heat pipes (PHPs). The study highlights that higher vapor density lowers start-up heat flux and temperature, making pulsation

initiation easier, while higher liquid physical properties (thermal conductivity, surface tension, and heat capacity) increase the energy required for start-up. Fluids with greater surface tension and viscosity introduce resistance to fluid movement, demanding higher energy input to form vapor bubbles and sustain oscillations of heat carrier. Pentane and methanol exhibit rapid start-up due to their lower boiling points and heat of vaporization but are prone to dry-out under high heat loads. Water, with its high heat capacity and latent heat, requires a greater start-up power but ensures stability under high thermal loads. The findings emphasize that working fluid selection should balance start-up ease, thermal capacity, and operational conditions to optimize PHP performance.

Chapter 5 investigates the impact of inclination angle and PHP length ratio (LR) on the start-up and transient behavior PHPs with different heat carriers. The study highlights that inclination angle plays a crucial role in PHP start-up, with horizontal orientation (0°) requiring the highest start-up heat flux, while vertical bottom heating ($+90^\circ$) facilitates start-up with lower heat flux requirements. The influence of LR on start-up heat flux density varies with inclination angle and working fluid. At $+90^\circ$, increasing LR reduces start-up heat flux by minimizing hydraulic resistance, while at $+45^\circ$, water and methanol show an optimal LR for efficient pulsations. Negative inclinations (-45° and -90°) prevent PHP start-up entirely, as gravity counteracts capillary forces, restricting liquid return to the heating zone. The transition to pulsation mode is favored by higher inclination angles and longer LRs, as larger heat transfer areas contain more nucleation sites. Among all working fluids, pentane requires the lowest transient heat flux density.

Chapter 6 examines the influence of length ratio (LR), inclination angle, and working fluid properties on the thermal performance of pulsating heat pipes (PHPs), focusing on average heating zone (HZ) temperature, temperature difference and thermal resistance. Increasing LR enhances thermal performance by promoting nucleation sites and reducing start-up heat flux, but it also raises heating zone (HZ) temperatures due to higher internal pressure. Inclination angle strongly affects PHP efficiency, with $+90^\circ$ (vertical bottom heating) providing the best heat transfer, while horizontal (0°) orientation results in vapor stagnation and increased thermal resistance. The choice of

working fluid significantly impacts PHP behavior. Methanol achieves the lowest thermal resistance, ensuring efficient heat transfer at lower heat flux densities, whereas water provides almost the same thermal resistance as methanol but at higher heat flux densities which makes it suitable for high-power applications. PHP with pentane, though the least start-up heat flux density, suffers from excessive vapor generation which due to incomplete condensation leads to higher HZ temperatures and reduced efficiency. Thermal resistance decreases with increasing heat flux, but excessive heat input can cause dry-out, which occurs at relatively low heat inputs for pentane and methanol.

The materials and results of the dissertation work have been implemented into the educational process at the Department of Nuclear Power Engineering of the Educational and Scientific Institute of Nuclear and Thermal Energy at the National Technical University of Ukraine "Igor Sikorsky Kyiv Polytechnic Institute."

Key words: pulsating heat pipe, heat and mass transfer, boiling, evaporation, heat transfer, length ratio, heat flux density, heat, start-up characteristics, transient characteristics, inclination angle, temperature difference, thermal resistance, electronics cooling, efficiency.

Publications presenting the main scientific results of the dissertation:

Journal Articles:

1. Mane, K.V., Alekseik, Y. Comprehensive parametric and design review for reducing pulsating heat pipes dependence on space orientation. Archives of Thermodynamics, 2024, 45(2), p. 165-182. DOI: <https://doi.org/10.24425/ather.2024.150863> (SCOPUS Q3).
2. Mane, K., & Alekseik, Y. The combined effect of heating zone length and inclination angle on start-up, transient, and operational characteristics of a pulsating heat pipe. Refrigeration Engineering and Technology, 2024, 60(3), p. 156-167. DOI: <https://doi.org/10.15673/ret.v60i3.2997>

Conference Proceedings:

1. Mane K.V., Alekseik Y. Influence of PHP channel design on start-up and gravity: a review. Modern Problems of Scientific Support of Energy. Materials of the XIX

- Scientific and Practical Conference of Young Scientists and Students, Kyiv, April 20–23, 2021, Kyiv: KPI, Polytechnic Publishing House, 2021, Vol. 1, p. 125-126.
2. Mane K., Alekseik Y. Influence of heating zone length on thermal performance of pulsating heat pipe. Modern Problems of Scientific Support for Energy. Proceedings of the XX International Scientific and Practical Conference of Young Scientists and Students, Kyiv, April 25–28, 2023. Kyiv: KPI, Polytechnic Publishing House, 2023, Vol. 1, p. 107-108.
 3. Mane K.V., Alekseik Y. Pulsating heat pipe sensitivity to space orientation: zone length and heat carrier influence. Modern Problems of Scientific Support for Energy. Proceedings of the XXI International Scientific and Practical Conference of Young Scientists and Students, Kyiv, April 23–26, 2024. Kyiv: KPI, Polytechnic Publishing House, 2024, Vol.1, p. 70-72.
 4. Alekseik Ye.S, Mane K.V. Influence of the heat carrier and the length of the heating zone of a pulsating heat pipe on the limits of the main operating modes at different inclination angles. Proceedings of the XXV International Scientific and Practical Conference of Modern Information and Electronic Technologies, May 27–29, 2024, Odessa, Ukraine, pp. 72-73.

АНОТАЦІЯ

Мане Кішор Вішванатх. Визначення параметрів ефективного застосування пульсаційних теплових труб в системах охолодження електронної техніки.

Дисертація на здобуття наукового ступеня доктора філософії за спеціальністю 144 «Теплоенергетика». - Національний технічний університет України "Київський політехнічний інститут імені Ігоря Сікорського", МОН України, Київ, 2025.

Дисертаційна робота присвячена дослідженню процесів теплопередачі в пульсуючих теплових трубах (ТТ) з різними теплоносіями при варіюванні режимних і геометричних параметрів.

У вступі висвітлено актуальність теми дослідження, визначено об'єкт, предмет, наукову новизну, мету та завдання дослідження. Обґрунтовано наукові положення та висновки, сформульовані в дисертації. Подано інформацію про: практичне значення результатів роботи, особистий внесок автора, апробацію результатів дисертації, публікації за темою дисертації, обсяг та структуру дисертації.

Розділ 1 дисертації містить огляд літератури з пульсуючих теплових труб (ПТТ), в якому розглядаються принципи їхньої роботи, геометричні конфігурації, властивості робочої рідини та ключові експлуатаційні параметри. Він починається зі вступу до, в якому описано робочий механізм ПТТ, який ґрунтується на фазових перетвореннях і пульсаційному русі теплоносія, що забезпечує ефективний теплообмін. Потім описується вплив геометричних параметрів, включаючи внутрішній діаметр, кількість витків, форму поперечного перерізу, конструкцію каналу і довжини зон, на теплопередавальні характеристики ПТТ. Підкреслено важливість вибору відповідних рідин в якості теплоносіїв на основі їх фізичних властивостей та коефіцієнта заповнення. Ці фактори впливають на розподіл фаз, динаміку потоку і загальну ефективність теплопередачі. У розділі також розглядаються ключові робочі параметри, такі як тепловий потік та орієнтація у просторі, які суттєво впливають на функціонування ПТТ. Незважаючи на велику

кількість досліджень, огляд літератури виявив прогалини в існуючих дослідженнях, зокрема, в узгодженні конструкцій РНР з реальними застосуваннями, оптимізації конфігурацій РНР для компактної електроніки та розумінні взаємодії між геометричними параметрами і гідродинамікою рідини. Це дослідження спрямоване на усунення цих прогалин шляхом вивчення пускових і перехідних характеристик ПТТ, що сприятиме вдосконаленню рішень з охолодження та терморегулювання електронної техніки.

Розділ 2 містить опис конструкції експериментальної установки, яка була спроектована і розроблена для дослідження пускових і перехідних характеристик ПТТ. Було виготовлено експериментальні зразки мідних ПТТ з п'ятьма витками, що забезпечує сумісність з висотою сучасних процесорних кулерів. Ці зразки були оснащені термопарами, розміщеними у відповідних місцях, що дозволило проводити вимірювання температури. Конструкція також включає регульовану довжину зони нагріву, що дозволяє детально дослідити, як розміри зони нагріву впливають на характеристики ПТТ. Розроблена експериментальна установка дозволяє проводити дослідження в різних положеннях, включаючи вертикальне положення з нижнім нагрівом ($+90^\circ$), горизонтальне (0°), вертикальне положення з верхнім нагрівом (-90°) і похилі положення ($+45^\circ$, -45°). Система дозволяє контролювати зміну теплового навантаження, забезпечує стабільну температуру охолоджувальної води в конденсаторі і дозволяє систематично збирати дані. Така установка дає змогу досліджувати характеристики ПТТ за різних теплоносіїв, густини теплового потоку та довжини зони нагріву.

Було розроблено експериментальну методику, включаючи процес збору даних та методику їх обробки. Проведено аналіз похибок.

У розділі 3 досліджуються різні режими роботи ПТТ, які поділяються на режим теплопровідності, термосифонний режим, перехідний режим, пульсаційний режим і режим осушення. Крім того, в ньому досліджено, як теплоносії, співвідношення довжин ПТТ та кути нахилу впливають на режими роботи ПТТ. У

цьому розділі представлено комплексний аналіз динаміки ПТТ, який дає уявлення про умови, необхідні для ефективного теплообміну.

У розділі 4 розглянуто, як теплофізичні властивості теплоносіїв впливають на пускові і перехідні характеристики ПТТ. Показано, що вища густина пари знижує пусковий тепловий потік і температуру, а також перехідний тепловий потік, тоді як вищі фізичні властивості рідини (теплопровідність, поверхневий натяг і теплоємність) збільшують кількість енергії, необхідну для запуску. Рідини з більшим поверхневим натягом і в'язкістю чинять опір руху рідини, потребуючи більших витрат енергії для утворення бульбашок пари і підтримки пульсацій теплоносія. Пентан і метанол демонструють швидкий запуск завдяки нижчим температурам кипіння і теплоті випаровування, але схильні до осушення при високих теплових навантаженнях. Вода, з її високою теплоємністю і прихованим теплом, вимагає більшої пускової густини теплового потоку, але забезпечує стабільність пульсацій при високих теплових навантаженнях. Отримані дані підкреслюють, що вибір теплоносія має бути збалансованим між легкістю запуску та стабільністю роботи ПТТ.

У розділі 5 досліджено вплив кута нахилу та співвідношення довжини зон (LR) на пускові та перехідні характеристики ПТТ з різними теплоносіями. Дослідження підкреслює, що кут нахилу відіграє вирішальну роль у запуску ПТ, причому горизонтальна орієнтація (0°) вимагає найбільшої пускової густини теплового потоку, тоді як вертикальне положення з нижнім нагрівом ($+90^\circ$) - найменшої. Вплив LR на густину пускового теплового потоку залежить від кута нахилу і теплоносія. При $+90^\circ$ збільшення LR зменшує густину пускового теплового потоку за рахунок мінімізації гідравлічного опору, тоді як при $+45^\circ$ для вода і метанолу існує оптимальний LR. Негативні кути нахилу (-45° і -90°) повністю унеможливають запуск ПТТ, оскільки сила тяжіння протидіє капілярним силам, обмежуючи повернення рідини в зону нагріву. Переходу в режим пульсації сприяють більші кути нахилу і довші LR, оскільки більші площі

теплообміну містять більше центрів пароутворення. Серед усіх робочих рідин пентан має найнижчу перехідну густину теплового потоку.

У розділі 6 розглядається вплив відношення довжини зон (LR), кута нахилу і властивостей теплоносія на теплопередавальні характеристики ПТТ, а саме: середню температуру зони нагріву (ЗН), температурний напір і термічний опір. Збільшення LR покращує теплопередавальні характеристики, збільшуючи кількість активних центрів пароутворення і зменшуючи густину пускового теплового потоку, але це також підвищує температуру ЗН через вищий внутрішній тиск. Кут нахилу сильно впливає на ефективність ПТТ, причому при куті нахилу $+90^\circ$ (вертикальне положення з нижнім нагрівом) забезпечується найкраща теплопередача, тоді як горизонтальна орієнтація (0°) призводить до застою пари в ЗН і підвищеного термічного опору. Вибір робочої рідини суттєво впливає на роботу ПТТ. Метанол забезпечує найнижчий термічний опір при меншій густині теплового потоку, тоді як ПТТ з водою має приблизно такий же опір, але при вищих густинах теплового потоку, що робить її придатною для високопотужних застосувань. ПТТ з пентаном, хоча і має найнижчу густину пускового теплового потоку, страждає від надмірного пароутворення, що, через неповну конденсацію утвореної пари, призводить до підвищення температури ЗН і зниження ефективності теплопередачі. Термічний опір зменшується зі збільшенням теплового потоку, але надмірне підведення тепла може призвести до осушення ЗН, що відбувається при відносно низькому підведеному тепловому потоці для пентану і метанолу.

Матеріали дисертації та результати досліджень впроваджено в освітній процес кафедри атомної енергетики Навчально-наукового інституту атомної та теплової енергетики Національного технічного університету України «Київський політехнічний інститут імені Ігоря Сікорського».

Ключові слова: пульсаційна тепла труба, тепло-масообмін, кипіння, випаровування, теплообмін відношення довжин, густина теплового потоку,

теплота, пускові характеристики, перехідні характеристики, кут нахилу, температурний напір, термічний опір, охолодження електроніки, ефективність.

Публікації, в яких представлено основні результати дисертаційного дослідження.

Статті:

1. Mane, K.V., Alekseik, Y. Comprehensive parametric and design review for reducing pulsating heat pipes dependence on space orientation. Archives of Thermodynamics, 2024, 45(2), p. 165-182. DOI: <https://doi.org/10.24425/ather.2024.150863> (SCOPUS Q3).
2. Mane, K., & Alekseik, Y. The combined effect of heating zone length and inclination angle on start-up, transient, and operational characteristics of a pulsating heat pipe. Refrigeration Engineering and Technology, 2024, 60(3), p. 156-167. DOI: <https://doi.org/10.15673/ret.v60i3.2997> (фах. кат. Б).

Матеріали конференцій:

1. Mane K.V., Alekseik Y. Influence of PHP channel design on start-up and gravity: a review. Modern Problems of Scientific Support of Energy. Materials of the XIX Scientific and Practical Conference of Young Scientists and Students, Kyiv, April 20–23, 2021, Kyiv: KPI, Polytechnic Publishing House, 2021, Vol. 1, p. 125-126.
2. Mane K., Alekseik Y. Influence of heating zone length on thermal performance of pulsating heat pipe. Modern Problems of Scientific Support for Energy. Proceedings of the XX International Scientific and Practical Conference of Young Scientists and Students, Kyiv, April 25–28, 2023. Kyiv: KPI, Polytechnic Publishing House, 2023, Vol. 1, p. 107-108.
3. Mane K.V., Alekseik Y. Pulsating heat pipe sensitivity to space orientation: zone length and heat carrier influence. Modern Problems of Scientific Support for Energy. Proceedings of the XXI International Scientific and Practical Conference of Young Scientists and Students, Kyiv, April 23–26, 2024. Kyiv: KPI, Polytechnic Publishing House, 2024, Vol.1, p. 70-72.

4. Alekseik Ye.S, Mane K.V. Influence of the heat carrier and the length of the heating zone of a pulsating heat pipe on the limits of the main operating modes at different inclination angles. Proceedings of the XXV International Scientific and Practical Conference of Modern Information and Electronic Technologies, May 27–29, 2024, Odessa, Ukraine, pp. 72-73.

TABLE OF CONTENTS

NOMENCLATURE.....	16
INTRODUCTION.....	19
Chapter 1 – Literature Review	24
1.1 Introduction	24
1.2 Pulsating heat pipe operating mechanism	26
1.3 Geometrical parameter	28
1.3.1 Inner diameter	28
1.3.2 Number of turns	31
1.3.3 Cross-section of PHP	32
1.3.4 PHP channel design	34
1.3.5 Zones length	41
1.4 Working fluid parameters.....	44
1.4.1 Physical properties of working fluid.....	44
1.4.2 Fluid category	47
1.4.3 Filling ratio.....	51
1.5 Operational parameters.....	53
1.5.1 Heat input.....	53
1.5.2 Orientation of PHP	60
1.6 Conclusions	63
Chapter 2 – Experimental Methodology	65
2.1 Selection of PHP parameters and factors under investigation	65
2.1.1 Inner diameter and number of turns selection	65
2.1.2 Zones Length Selection.....	66
2.2 Experimental set up	67
2.3 Experimental procedure.....	70
2.4 Methodology of data processing	71
2.5 Assessment of measurement errors	75
2.6 Conclusions	78

Chapter 3 – Operational Modes of Pulsating Heat Pipe.....	80
3.1 Operational modes.....	80
3.1.1 Heat conductivity mode	81
3.1.2 Thermosyphone mode.....	81
3.1.3 Transition from thermosyphone to pulsating mode.....	82
3.1.4 Pulsating mode.....	83
3.1.5 Dry-out mode	83
3.2 Effect of heat carriers, PHP length ratio, and inclination angles on PHP behaviour	84
3.3 Conclusions	102
Chapter 4 – Influence of Heat Carrier Physical Properties on Start-up and Transient Characteristics of Pulsating Heat Pipe.....	105
4.1 Influence of physical properties on start-up characteristics of pulsating heat pipe	106
4.1.1 Start-up heat flux density	106
4.1.2 Start-up temperature.....	109
4.2 Influence of Physical Properties on transient Heat Flux Density	112
4.3 Conclusions	116
Chapter 5 - Influence of Geometrical and Operating Parameters on Start-up and Transient Characteristics of Pulsating Heat Pipe.....	118
5.1 Influence on startup and transient characteristics	118
5.2 Generalization of experimental data.....	124
5.3 Conclusions	129
Chapter 6 - Heat Transfer Characteristics of Pulsating Heat Pipe	131
6.1 Average temperature of heating zone.....	131
6.2 Temperature difference	134
6.3 Thermal resistance.....	137
6.4 Conclusions	142
CONCLUSIONS	145

REFERENCES.....	149
ANNEX A: List of Publications.....	161
ANNEX B: The act of implementation in the educational process.....	163

NOMENCLATURE

Symbols:

C – heat capacity, $\text{J}/(\text{kg}\cdot\text{K})$;

F – heat transfer area, m^2 ;

G – mass flow rate, kg/s ;

L – length, m ;

N – number of measurements;

P – pressure, Pa ;

Q – heat flux, W ;

R – thermal resistance, $^{\circ}\text{C}/\text{W}$;

d – diameter, m ;

g – acceleration due to gravity, m/s^2 ;

n – number of turns;

q – heat flux density, W/m^2 ;

r – heat of vaporization, J/kg ;

t – temperature, $^{\circ}\text{C}$;

x – number of divisions on flowmeter.

Greek Letters:

δ – uncertainty;

λ – saturated liquid thermal conductivity, $\text{W}/(\text{m}\cdot\text{K})$;

ν – saturated liquid kinematic viscosity, m^2/s ;

ρ – density, kg/m^3 ;

σ – saturated liquid surface tension, N/m .

Dimensionless Complexes:

Bo – Bond number:

Bo* – modified Bond number;

Ga – Galileo number.

Subscripts:

a – adiabatic;

c – condensing;

cool – cooling;

cap – capillary;

eff – effective;

h – heating;

i – inner

in – inner;

l – liquid;

max – maximum;

out – outer;

puls – pulsation

sat – saturation;

start – start-up;

th – thermal;

therm – thermostat;

transf – transferred;

v – vapour.

Abbreviations:

ABPHP – additional branch pulsating heat pipe;

AZ – adiabatic zone;

CFD – computational fluid dynamics;

CLPHP – closed loop pulsating heat pipe;

CTPHP – capillary tube pulsating heat pipe;

CZ – condensation zone;

DI – deionized;

DLPHP – dual layer pulsating heat pipe;

FPPHP – flat plate pulsating heat pipe;

FR – filling ratio;

HZ – heating zone;

ID- inner diameter;

LR – length ratio;

MPHP – micro pulsating heat pipe;

PC – personal computer;

PHP – pulsating heat pipe.

INTRODUCTION

Relevance of the Work. The increasing demand for efficient thermal management in modern electronics has driven significant interest in pulsating heat pipes (PHPs) due to their compact size, lightweight structure, and high heat transfer efficiency. As electronic devices continue to evolve with higher power densities and reduced form factors, the need for advanced cooling technologies has become more pressing. PHPs offer a promising alternative to conventional cooling methods, delivering superior thermal performance without the need for mechanical pumps or complex configurations.

A critical aspect of PHP operation is its start-up and transient behavior, which directly influences the transition to an optimal pulsation mode. This transition is essential to maintaining consistent heat transfer performance, providing high heat transfer characteristics and preventing thermal instabilities. Start-up and transient characteristics are influenced by number of geometrical, physical and operational factors and this influence is studied insufficiently. This work is dedicated to comprehensive investigation of length ratio, heat carrier physical properties and inclination angle on the start-up and transient characteristics of PHP.

By addressing the limitations of prior studies and providing comprehensive experimental data on PHP start-up and transient behavior, this research advances the development of next-generation cooling solutions for high-performance electronic devices. The findings of this study are expected to play a crucial role in optimizing PHP designs for practical applications, thereby improving energy efficiency, enhancing device longevity, and ensuring overall system reliability.

Connection of work with research programmes, plans, topics.

Topic of the dissertation work corresponds to priority area of science and technology development “Energy and energy efficiency” (On Priority Branches of Science and Technology Development: Law of Ukraine №2623-III from 11.06.2001 with changes from 29.01.2021) and it is connected with investigation of heat transfer

processes in two-phase heat transfer devices, namely pulsating heat pipes, for increasing of efficiency of using them in practical applications. Some materials of dissertation work were part of research programmes and projects which were implemented in department of nuclear power engineering of National Technical University of Ukraine “Igor Sikorsky Kyiv Polytechnic Institute”, namely “Processes of heat and mass transfer and hydrodynamics in in miniature two-phase heat transfer systems” (state registration number 0118U003539) and “Heat and mass transfer and hydrodynamics in single and multiphase media of the latest heat transfer fluids for the development of heat exchangers for cryogenic technology and radar systems” (state registration number 0121U109681).

Purpose of the research: to study the impact of length ratio, inclination angle and type of heat carrier on the start-up, transient and operating characteristics of pulsating heat pipes (PHPs) for electronics cooling. Addressing these parameters is crucial for optimizing PHP performance and ensuring efficient thermal management in compact electronic systems.

Object of research: heat transfer processes and physical phenomena which take place in pulsating heat pipes.

Subject of research: influence of determining factors (length ratio, inclination angle, physical properties of heat carrier) on the start-up, transient and operating characteristics of pulsating heat pipes.

Method of research: experimental investigation of pulsating heat pipe characteristics.

The scientific novelty of the results is as follows:

1. Classification of the main operating modes of pulsating heat pipes was improved.
2. For the first time, complex investigation of influence of geometrical, physical and operational factors on the borders of main operational PHP modes was performed. Effect of length ratio, inclination angle and type of heat carrier on existence and borders of PHP operational modes, pulsation amplitude and dry-out limit was shown and explained.
3. For the first time, comprehensive study of influence of physical properties of liquid and vapor phase of heat carrier on start-up and transient characteristics of PHP was

performed. Obtained data were analyzed from the point of view of their effect on mechanical interaction between vapor plugs and liquid slugs inside PHP and on boiling beginning in PHP heating zone. These processes directly influence on PHP start-up and transient behavior.

4. New data on influence of geometrical and operational factors on start-up and transient characteristics of PHP was obtained. Recommendations for choosing of PHP length ratio and heat carrier for different working conditions are presented.

5. For the first time, an empirical dimensionless correlation for predicting start-up and transient heat flux density in PHPs has been developed. This correlation takes into account length ratio, physical properties of liquid and vapor phase of heat carrier, inclination angle and it is applicable for PHP with water, alcohols and organic liquids as a heat carrier.

6. New data on influence of length ratio, inclination angle and type of heat carrier on heat transfer characteristics of PHP (average heating zone temperature, temperature difference, thermal resistance) was obtained. Connection between PHP start-up and transient behavior and its heat transfer characteristics was shown.

Validation of scientific positions and conclusions. The validity of the obtained results is ensured through the use of confirmed and reliable experimental research methods and data processing techniques. To verify their accuracy, the results were systematically analyzed and compared with those reported by other researchers.

Practical values of the work results. This study enhances the design and application of pulsating heat pipes (PHPs) for efficient electronics cooling. Obtained results allow choosing length ratio and heat carrier for different working conditions. Proposed correlation can be used in engineering calculations of PHP to predict its start-up and transient characteristics. Materials of the dissertation can be useful for designers of novel effective electronics cooling systems based on two-phase heat transfer devices.

Materials of the dissertation are used in the educational process for training of PhD-students on specialty 142 Power engineering and 143 Nuclear energy and included to:

- discipline “Kinetics of phase transformations in power equipment”, lectures “Common heat pipes. Miniature and micro heat pipes. Design. Functioning peculiarities. Gas-regulated heat pipes. Loop heat pipes. Pulsating heat pipes. Design. Functioning peculiarities.” and “Heat transfer characteristics of pulsating heat pipes depending on operational parameters”.

Implementation of research results in the educational process was made to improve students' knowledge on heat transfer processes in pulsating heat pipes.

Personal contribution of the author. The scientific results presented in this dissertation were obtained by the author, including the following contributions: development of experimental samples and experimental test rig, formulation of experimental procedures and data processing techniques, processing, analysis, interpretation and generalization of experimental results, establishment of recommendations for PHP configuration.

The dissertation was performed at the Department of Nuclear Power Engineering of the Educational and Scientific Institute of Nuclear and Thermal Energy at the National Technical University of Ukraine "Igor Sikorsky Kyiv Polytechnic Institute" under scientific supervision of PhD Alekseik Ye.S. (2019-2022) and doct. techn. sci., prof. Kravets V.Yu. (2022-2025).

Approbation of dissertation results. The materials of the dissertation were reported and discussed at conferences: XIX Scientific and Practical Conference of Young Scientists and Students "Modern Problems of Scientific Support of Energy" (Ukraine, Kyiv, April 20–23, 2021), XX International Scientific and Practical Conference of Young Scientists and Students "Modern Problems of Scientific Support for Energy" (Ukraine, Kyiv, April 25–28, 2023), XXI International Scientific and Practical Conference of Young Scientists and Students "Modern Problems of Scientific Support for Energy" (Ukraine, Kyiv, April 23–26, 2024), XXV International Scientific and Practical Conference "Modern Information and Electronic Technologies" (Ukraine, Odessa, May 27–29, 2024).

Publications. The main results of the dissertation were published in 6 scientific publications including: 2 journal articles (one of which is SCOPUS (Q3) and Web of Science (Q3) indexed, while the other is published in a professional journal of Ukraine of category B), 4 conference papers.

Structure and Scope of Work. The dissertation consists of an introduction, six chapters, two annexes, and a list of references comprising 122 sources. The total volume of the work is 163 pages, including 57 figures and 7 tables.

Chapter 1 – Literature Review

1.1 Introduction

The evolution of electronic devices, as they become smaller, faster, and more efficient, has set a challenge before the electronic industry, to dissipate high heat flux from electronic chips. Modern technology demands miniaturized electronic components with high processing speed. This trend of miniaturizing electronic equipment has significantly reduced surface area, and, at the same time, improved processing speed has resulted in even more heat dissipation. Thus, diverting high heat flux from small surface area makes cooling task more challenging. As semiconductor industry still complies with the popular Moore's law (Moore, 1998) [1], the average power dissipation and heat flux from the high density and highly efficient microprocessor chips are expected to hit about 360 W and 190 W/cm², respectively by 2020 (Murshed and Castro, 2017) [2]. Therefore, this high heat flux must be removed to keep the chips under normal operating conditions. Unfortunately, this rapidly evolving electronic industry is far from being able to walk hand in hand with a device to provide thermal solutions to these problems. With the advent of high-speed processor electronic devices, conventional methods of forced convection cooling have already reached its maximum. Novel methods of cooling are continuously researched about better solutions of electronic cooling. One such method is the application of heat pipe, developed as an electronic equipment cooling technique by Gaugler in 1942, which provides a promising alternative to conventional cooling schemes. Heat pipe is a passive two-phase heat transfer system, capable of transmitting large amounts of heat with minimal drop in temperature. The wick, as represented in fig. 1.1, is an obligatory part of conventional heat pipe which is intended for transport of heat carrier from condensation to heating zone.

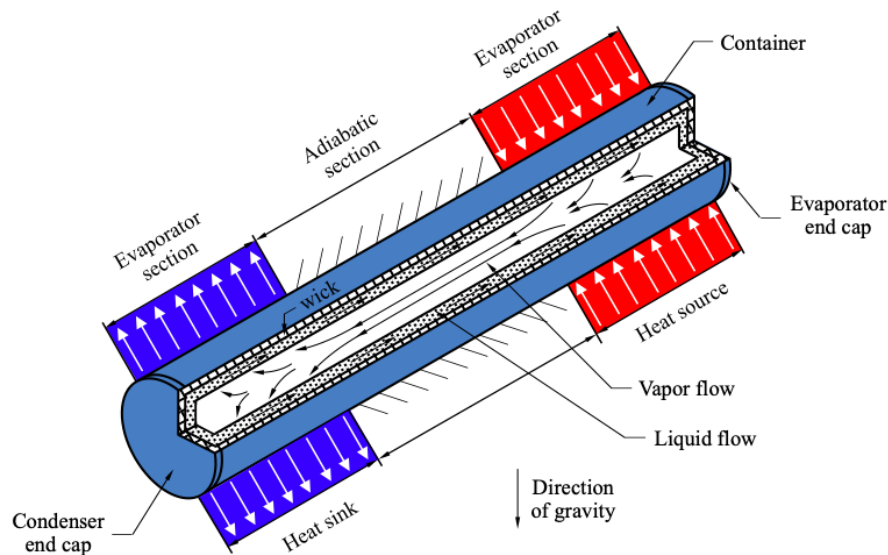


Figure 1.1 – Structure and operating mechanism in heat pipe (Faghri, 2014) [3]

It provides the heat carrier with the capillary forces needed for its continuous movement inside the loop and it also provides possibility of heat pipe working at any orientation with regards to gravity force. As such, the capillary limit is the most common disadvantage to the performance of a wicked heat pipe. This happens largely over a long transport distance as the wick fails to return enough liquid to the section of the evaporator to keep it saturated. The evaporator wall at this point starts experiencing a rapid, persistent rise in temperature (Faghri, 2014) [3].

Pulsating heat pipes (PHP), a novel idea proposed by (Akachi, 1990) [4], seems to fulfill all existing cooling requirements. Unlike conventional heat pipes, pulsating heat pipe have got simple structure and are completely free from the wick, which provides an advantage over the manufacturing aspect of it. PHP is made of a long capillary tube, which is bent into many turns. Due to the small inner diameter of the capillary tube, the size of the PHP heat transfer device can be very small too. Key benefits of PHP are its quick-thermal response, compact size, and simple construction. The downside of PHP, however, is that their operating philosophy cannot be adequately defined. It has gained the attention of many researchers since the development of PHP, as it is a versatile tool to transfer heat effectively. Therefore, it is considered to have application prospects in

areas of electronics cooling, solar energy utilization, waste heat recovery, and aerospace thermal management (Han et al., 2016) [5].

1.2 Pulsating heat pipe operating mechanism

According to the tube's structure, the PHP can be marked as closed PHP with or without a check valve and open PHP, as shown in fig 1-1. The apparatus is first evacuated and then it is filled partially with a heat carrier. The surface tension of working fluid and wetting of the meandering channel walls causes it to disperse into a characteristic chain of liquid slugs and vapour bubbles. The heat transfer phenomenon in the PHP occurs due to oscillations of liquid slugs and vapour plugs, which are produced as a result of evaporation, boiling and condensation of the heat carrier. The input heat flux accelerates the pressure of the vapor plug in the evaporator portion, forcing the adjacent vapor plugs and liquid slugs towards the condenser, keeping the heat carrier in motion (Shafi, et al., 2001) [6]. As the diameter of the capillary is small, the size of the PHP heat transfer device can be very small too. If the PHP operation carried out in isothermal condition, then the liquid and vapor phases inside the system must remain in equilibrium at the saturated pressure corresponding to the specified isothermal temperature. This thermodynamic state of all liquid plugs and vapor bubbles can be represented by a pressure-enthalpy diagram with points A and B respectively in fig. 1.3. Suppose the temperature of the whole PHP framework is now quasi-statically elevated to a new constant value, then a device can again find a new equilibrium A' and B' corresponding to the saturation pressure of newly attained temperature. A Similar equilibrium state A'' and B'' will be achieved if the system is cooled to a new value. Every time in doing so there will be some heat and mass exchange from liquid will occur until the system attains a new equilibrium state (Khandekar et al., 2002) [7].

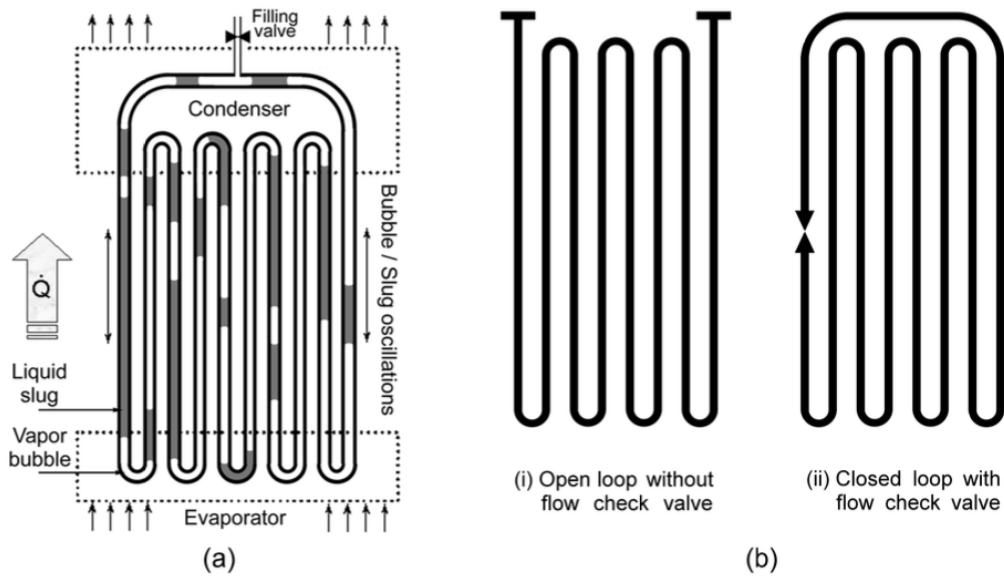


Figure 1.2 – Schematic of PHPs: (a) closed PHP; (b) PHP with open-loop and check valve (Groll, 2003) [8]

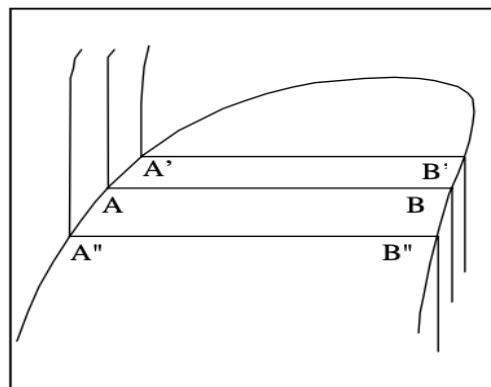


Figure 1.3 – P-h diagram of working fluid in PHP (Khandekar et al., 2002) [7]

PHP response is decided strongly by various parameters, such as tube diameter, fill ratio, number of turns, inclination angle, channel configuration and the type of heat carrier (Cai, 2006; Charoensawan, 2003; Han et al., 2016) [9] [10] [11]. Comprehensive information about PHP's thermal dependency on critical design and fluid parameters will be discussed in the next following sections.

The PHP's thermal performance is heavily affected by the different parameters, which can be divided into three basic categories, and are interdependent as shown in fig.

1.4. The past 30 years have seen increasingly rapid developments, both experimentally and numerically in the field of PHP, to make it an efficient heat transfer device. The following sections will provide a detailed description of the effect of all these parameters on PHP thermal efficiency.

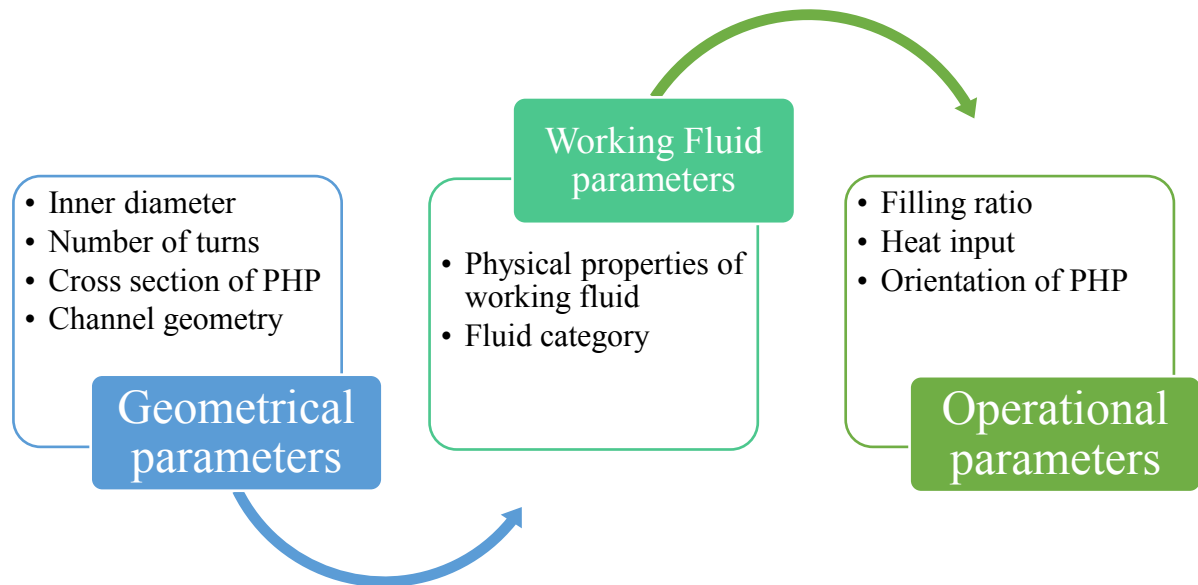


Figure 1.4 – Interdependence of parameters affecting thermal performance of PHP

1.3 Geometrical parameter

1.3.1 Inner diameter

The PHP's distinctive feature is its ability to produce liquid slugs and vapor bubbles in the channels. When the inner diameter of the channels is less than a critical diameter, surface tension forces overpower gravitational forces and the working fluid spreads across the tube in the form of liquid slugs and vapour plugs (Akachi,1996) [12]. The major design restriction for PHP is the Bond number (Bo), which limits the capillary tube diameter and gives the minimum internal diameter required for the capillary tube to operate in its true nature:

$$Bo = \sqrt{\frac{g (\rho_l - \rho_v) D_i^2}{\sigma}} \quad (1.1)$$

where g - acceleration due to gravity, m/s^2

ρ_l - density of the liquid, kg/m^3

ρ_v - density of vapour, kg/m^3

D_i - inner Diameter of PHP, m

σ - surface Tension, N/m.

It is also proposed as a preliminary criterion that if $Bo \leq 2$ then the gravity effect is reduced in contrast to the surface tension forming a train of liquid plugs and vapour bubbles (Hosoda et al., 1999) [13]. The maximum PHP diameter can therefore be given by

$$D_{i \max} = 2 \sqrt{\frac{\sigma}{(\rho_l - \rho_v)g}} \quad (1.2)$$

If the inner diameter is very small, the frictional resistance increases considerably with decreased inner diameter. Thus the usual maximum diameter suggested to be within the following range (Dobson et al., 1999) [14]:

$$0.7 \sqrt{\frac{\sigma}{(\rho_l - \rho_v)g}} \leq D_{i \max} \leq 2 \sqrt{\frac{\sigma}{(\rho_l - \rho_v)g}} \quad (1.3)$$

Very few researchers studied the sole effect of inner diameter on PHP performance but rather they put more emphasis on the effect of a variety of other parameters coupled with an inner diameter that affects the output of PHP. Thermal resistance of the PHP was distinctly reduced with the increase of the inner diameter and this was attributed to the fact that a smaller inner diameter provided a greater resistance to friction (Charoensawan and Terdtoon, 2008; Yang et al., 2008; Yang et al., 2009; Wang and Nishio, 2005) [15]–[18]. PHP's ability to manage large heat flux is also found to be closely related to

diameter. In this regard, a larger choice of diameter would be advantageous, as for the same filling ratio, PHP with 2 mm ID tube in horizontal mode could withstand a heat input of 350 W (evaporator temperature: 165⁰ C) before its dry-out, whereas, 1 mm ID tube catches dry-out at a very low heat input of 120 W (evaporator temperature: 90⁰ C) [16]. Likewise, with rising diameter the heat transfer efficiency was found to increase (Shafii et al., 2002) [19]. However, Comparison between two studies on open PHP revealed that PHP with an inner diameter of 0.9 mm could perform better than the PHP with an inner diameter of 1.5 mm. (Saha et al., 2012; R. Riehl, 2004) [20] [21] . The PHP was evaluated for space application (Mangini et al., 2015) [22] and concluded that PHP could act as a true oscillating system under microgravity conditions when the PHP diameter (3mm) was used more than the static critical diameter that was 1.68 mm.

PHP's operational characteristics have also been improved by a larger hydraulic diameter, even in microgravity conditions. Recently, (Ayel et al., 2015) [23] concluded that the effect of gravity is more in a vertical position when experiments are carried out under conditions of hyper and microgravity, whereas, the performance of PHP remained undeterred in a horizontal positions, largely attributed to higher hydraulic dimeters; results of this paper were compared with experimental work by (Mameli et al., 2014) [24] in the same working environment. In order to solve this problem, a theoretical model was developed by (Qu et al., 2016) [25], to provide the absolute limit of the inner diameter, which could allow PHP to work under conditions of microgravity and stated that the tube diameter should be greater than the maximum diameter set by the criterion of the Bond number. A study reported by (Rittidech et al., 2003) [26] found that thermal performance is not just a function of inner diameter but it is greatly affected by the properties of working fluid, as an experimental investigation revealed that heat transfer efficiency for R123 was higher, while ethanol performed poorly at a larger internal diameter. Additionally, it was noted that the choice of working fluid, especially those with higher reduced pressure, can allow for a reduction in the required inner diameter without compromising performance.

All in all, operating characteristics of PHP can be improved with the use right choice of working fluid and novel channel geometry. Although the precise value of the internal diameter that yields optimum performance is still in doubt, researchers agree that the physical properties of the working fluid play a major role in influencing the internal diameter of PHP's thermal performance.

1.3.2 Number of turns

The operating, starting, and transient behaviour of Pulsating Heat Pipes (PHPs) are strongly influenced by the internal fluid dynamics, pressure oscillations, and thermal interactions between the evaporator and condenser. One key factor that impacts these behaviours is the number of turns in the PHP, which has been extensively studied since the technology's inception. Research shows that increasing the number of turns can enhance the pressure disturbances within the PHP ([Akachi et al., 1996](#)) [12] facilitating stronger oscillations during both start-up and steady operation. But a higher number of turns of PHP takes up more space, thus restricting the demand ([Quan and Jia, 2009](#)) [27]. However, this contributes to a more reliable initiation of the pulsating mechanism, even under various external conditions, including different orientations. For instance, as the number of turns approaches 20 or more, the thermal resistance of the PHP tends to become independent of orientation, enhancing its operational stability ([Lee et al., 2018](#)) [28]. During the starting phase, a higher number of turns leads to more distinct regions for nucleation and liquid-vapor interactions, helping the PHP overcome gravitational influences more effectively ([Mameli et al., 2014](#)) [29]. Experimental studies have shown that devices with fewer than 20 turns struggle with startup, especially in horizontal or adverse heat flow orientations, where gravitational effects are more pronounced ([Yang et al., 2008](#)) [16]. This indicates that turn number plays a crucial role in the starting characteristics, particularly in systems designed for operation across multiple orientations.

In terms of transient characteristics, which describe the behaviour of the PHP during shifts between operating states, the number of turns again influences performance. PHPs

with more turns tend to show smoother transitions during changes in thermal load, as the increased number of oscillating liquid plugs enhances the system's ability to quickly adapt to temperature differentials (Li et al., 2018) [30]. This transient behaviour is critical in applications where rapid thermal response is necessary.

Despite these advantages, higher turn numbers result in larger PHPs, which contradicts the trend toward miniaturization in modern applications. Therefore, achieving efficient PHP operation with fewer turns (less than 20) remains a challenge. Recent research has explored ways to optimize PHPs with fewer turns by adjusting other design parameters, such as diameter, filling ratio, or working fluid, to compensate for the reduced oscillatory activity. (Kammuang-lee et al., 2018) [31] (Noh and Kim, 2020) [32]. According to the literature, PHPs with 20 or more turns have demonstrated consistent and stable operation across a wide range of conditions, including varying thermal loads and orientations (Charoensawan et al., 2003; Lee et al., 2018; Li et al., 2018; Yun 2020) [10], [28], [30], [32]. To improve operational stability, especially during start-up and transient phases, it is essential to develop designs that maintain high heat transfer performance with fewer turns. This requires further investigation into internal pressure dynamics and innovative approaches to enhance the pulsating mechanism, even in compact designs. Such optimizations would make PHPs more efficient and suitable for applications where space is limited, without compromising their overall thermal performance.

1.3.3 Cross-section of PHP

When PHPs are built of the same hydraulic diameter with circular, square, and triangular segments, their functionality with regards to flow behaviour through channel would be radically different. As it can be seen from the fig. 1.5 that sharp angled corners created because of the cross-section change, seem to accumulate more working fluid resulting in higher capillary action.

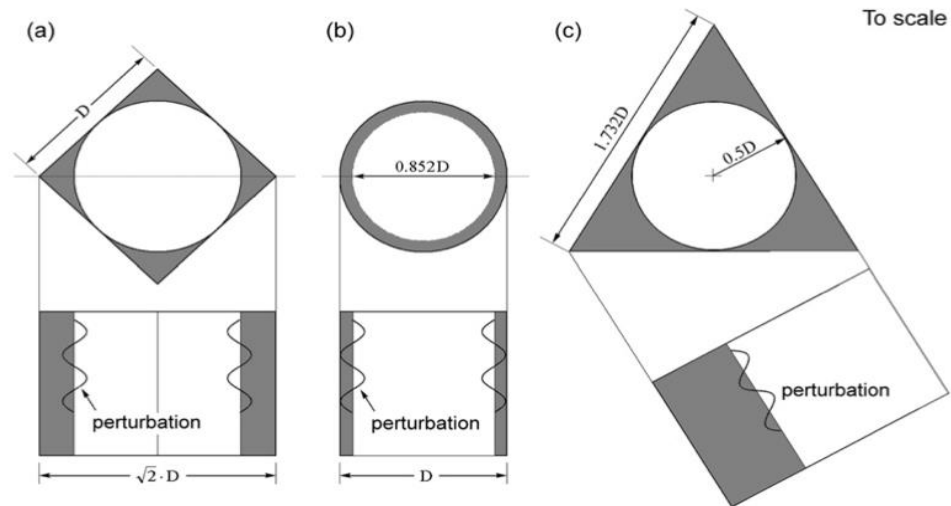


Figure 1.5 – Effect of tube cross-section with the same hydraulic diameter but different cross- shapes (a) Square, (b) circular, and (c) triangular (Yang et al., 2009) [17].

Beyond the commonly used circular cross-section, many researchers have explored alternative cross-sections to improve the start-up and operating characteristics of PHPs. (Khandekar et al., 2003) [33] compared PHPs with rectangular and circular cross-sections, both having the same hydraulic diameter. It was observed that the rectangular cross-section exhibited lower thermal resistance, particularly when the filling ratio (FR) was less than 10%, indicating improved start-up behaviour and heat transfer efficiency. (Hua et al., 2017) [34] also reported improved start-up characteristics, with a significant 60-70% reduction in thermal resistance when using a rectangular cross-section. A silicon-based micro PHP with trapezoidal channels could increase temperature uniformity in the evaporator section considerably (Qu et al., 2012) [35]. Moreover, the PHP performance with a triangular cross-section resulted in a lower thermal resistance than a square channel as reported by (Li and Jia, 2013) [36]. A similar trend was also observed in comparative study carried out between square and circular channel (Lee and Kim, 2017; Mehta et al., 2020) [37], [38]. Nevertheless, a recent study carried out by (Takawale et al., 2018) [39], has come out with contradictory outcome to all the above observations; a comparative study carried out between PHP made of flat plate (FPPHP) and capillary tube (CTPHP) with ethanol as a working fluid revealed that the total

thermal resistance of CTPHP was around 48% higher than FPPHP for the same operating parameters. This was attributed to lateral conduction between the neighbouring channels and short perturbations in the amplitude of FPPHP. A recent study conducted by (Markal et al., 2021) [40] on flat plate PHPs (FPPHP) demonstrated that using a dual cross-section ratio, where the width of adjacent channels differs between the evaporator and condenser, significantly improved operational stability and heat transfer efficiency. This design optimization enhanced start-up performance and maintained consistent thermal performance across varying conditions. Majority of the past literature review suggest that the PHP operation with different cross section, when compared with influence of gravity, FPPHP has always proven to be the best choice than CTPHP (Ayel et al., 2015; Mameli et al., 2014) [23], [29].

Although extensive research has been conducted on the impact of cross-sectional geometry on the operational characteristics of PHPs, there is still no consensus on which cross-section offers the best thermal efficiency. Further investigation into how different cross-sections impact thermal performance, with a focus on start-up and steady-state behaviour, is necessary to develop more efficient PHP designs.

1.3.4 PHP channel design

PHP channel geometry plays a critical role in regulating fluid flow dynamics, which directly impacts start-up and overall thermal performance. In addition to different loop configurations, such as open and closed-loop PHPs, various channel geometries have been tested to improve PHP effectiveness. Studies have shown that closed-loop PHPs enhance flow circulation, leading to more efficient heat transfer and improved start-up characteristics compared to open-loop designs (Zhang and Faghri, 2008) [41]. Therefore, more attention has been directed towards optimizing channel configurations to boost start-up and operating stability. For instance, using uneven capillary forces by varying channel diameters was numerically demonstrated to enhance flow circulation and increase heat transfer efficiency (Holley and Faghri, 2005) [42]. Similar strategies were

experimentally tested on three CLPHPs with slightly different channel diameters and have been found to be effective in building and sustaining efficient heat carrier circulation (Liu et al., 2007) [43]. The novel PHP design was experimentally tested, perfectly in a circular ring with no turns and twelve subsequent cooling and heating parts, and found an increase in the oscillation movement (Park and Ma, 2007) [44]. Meanwhile flow circulation improvement was observed when PHP with an additional branch (AB-PHP) in evaporator was fabricated on Pyrex glass and compared it with conventional flat plate PHP (FP-PHP) (FR=50%). This also led to reduction in thermal resistance at higher heat flux as depicted in fig. 1.6c (Sedighi et al., 2018) [45].

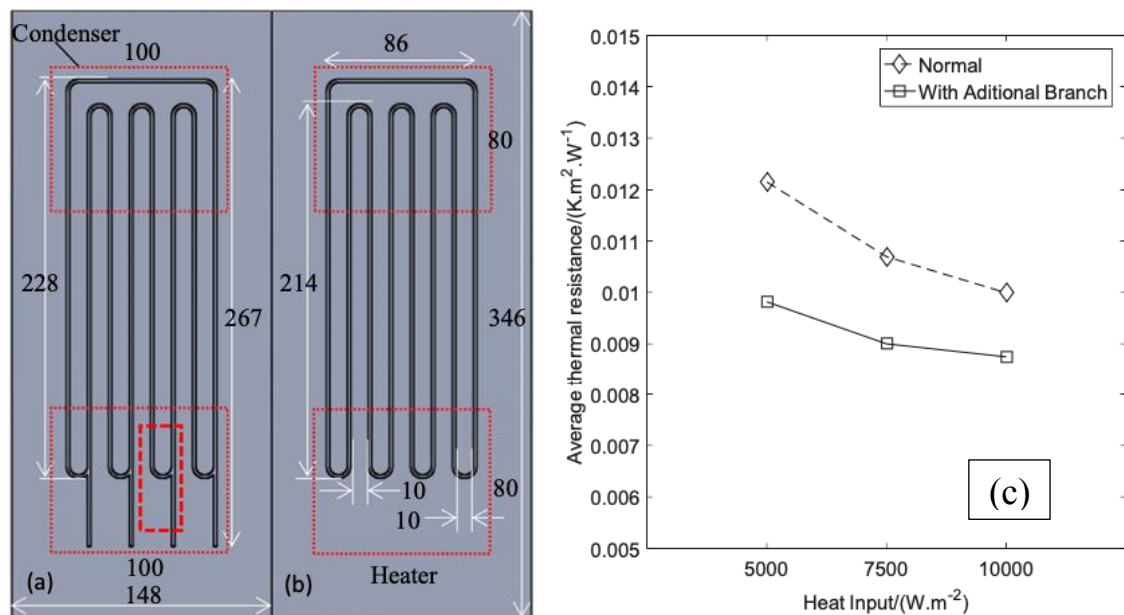


Figure 1.6 – Schematics related to experimental set-ups: (a) experimental set-up of the AB-FP-PHP and visualization area, (b) traditional FP-PHP experimental set-up; and (c) variation of thermal resistance versus heat flux (Sedighi et al., 2018) [45] (Morris, 2012) [46]

Author experimented dual layer PHP (DL-PHP; fig. 1.7) and found that compared to single layer PHP, DLPHP showed 85% less thermal resistance. But these findings are

limited to vertical position of PHP and no evidence of PHP working at horizontal position is mentioned.

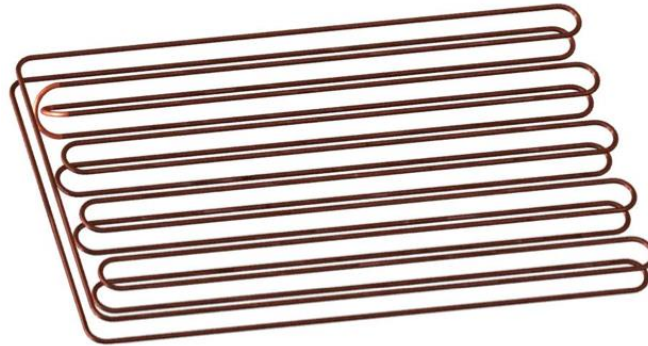


Figure 1.7 – Schematic of dual layer PHP (DL-PHP) (Morris, 2012) [46]

By experimental investigation on vertical top heated PHP, (Hathaway et al., 2012) [47] was able to improve the oscillations for top heating mode with uneven turn combinations (i.e. 20-turn evaporator and 14-turn condenser). Likewise, the PHP system could operate even at a horizontal orientation when square channels of alternate sizes were exercised in PHP but the same system could not operate in horizontal mode with uniform square channel arrangement (Chien et al., 2012) [48]. Building on these findings (Tseng et al., 2014) [49] proposed a strategy for optimizing closed-loop PHPs. They conducted a comparative analysis between standard circular tube diameters and alternative flattened tubes (alternative tubes were flattened to oval shape with a 1.5 mm minor diameter; fig. 1.8). with an oval cross-section (minor diameter of 1.5 mm). The alternative channel design allowed for faster initiation at lower heat inputs and resulted in significantly lower thermal resistance, improving both start-up and steady-state performance compared to conventional designs.

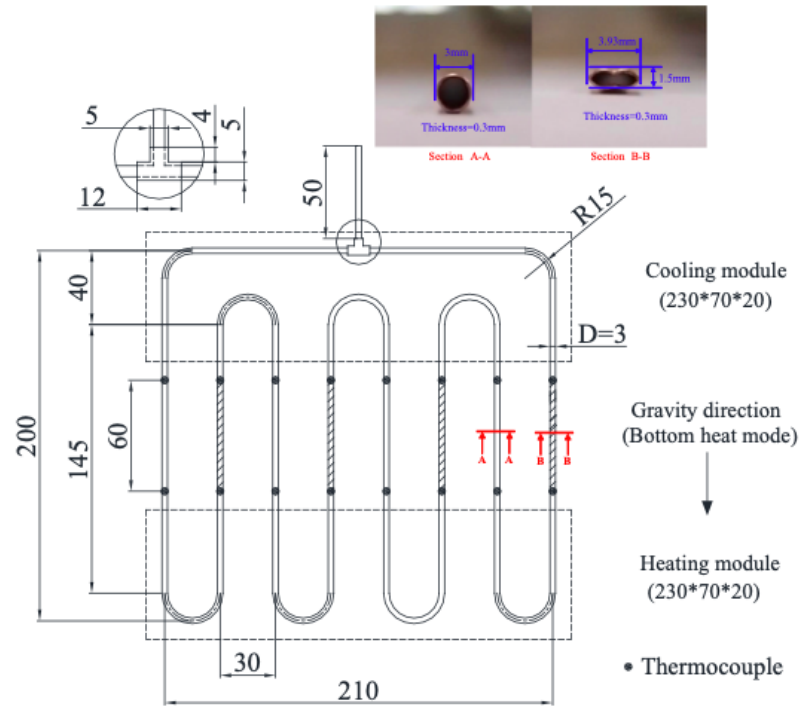


Figure 1.8 – Schematic of the tested PHP (Tseng et al., 2014) [49]

Even with various turns and geometric modifications, certain PHP designs struggle with efficient start-up and operation, particularly in demanding conditions. To address this issue, (Tseng et al., 2016) [50] introduced a novel PHP design utilizing a combination of alternate double-pipe tube diameters and extra open connections between the dual pipes. This innovative configuration enhanced fluid circulation by introducing an "extra unbalanced pressure force," which significantly improved start-up behaviour and overall operating stability as shown in fig. 1.9. The results of this new design were compared with (Tseng et al., 2014) [49] and found that, due to this new design, thermal resistance decreased to 0.0729 K/W compared to 0.17 K/W with traditional CLPHP. There was also a 54.6 percent improvement in thermal conductivity due to the double pipe tube diameter PHP, the results of which are shown below (fig. 1.10)

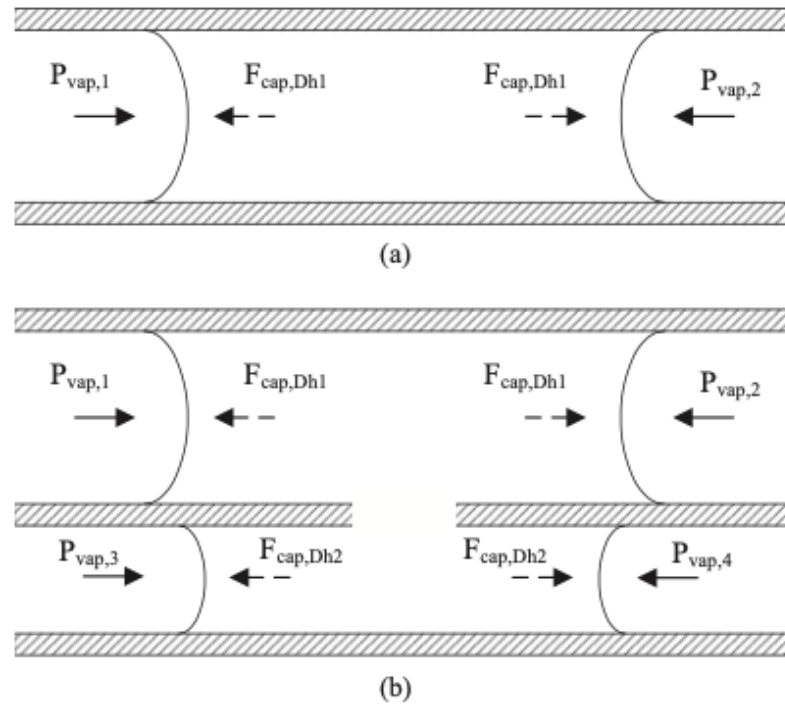


Figure 1.9 – Representation of unbalanced capillary forces acting on a vapor slug in the condensing section (a) PHP and (b) DPPHP (Tseng et al., 2016) [50]

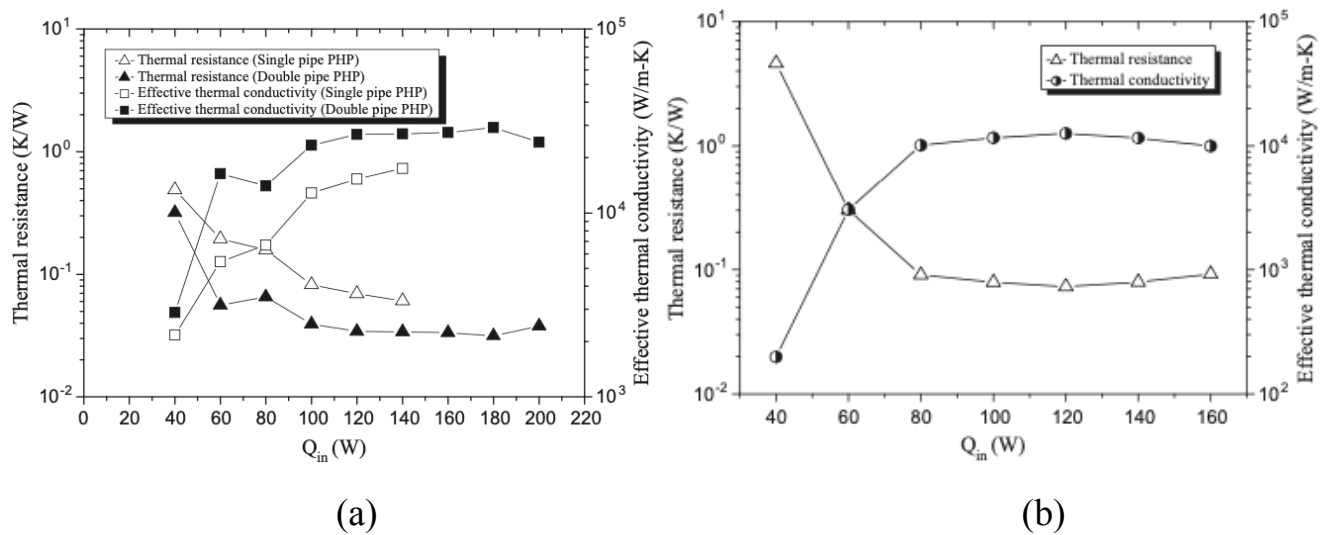


Figure 1.10 – Thermal resistance and effective thermal conductivity vs. heating power of various PHP when the heat source placed on (a) top heating mode (b) bottom heating mode (Tseng et al., 2016) [50].

To better answer the impact of channel configuration in order to find out what diameter difference could promote heat transfer to the maximum, (Kwon and Kim, 2014) [51] performed an experimental analysis on six different PHPs, three of which were symmetric PHPs (both tubes having same diameter in one turn or uniform diameter tube) and the other three were asymmetric PHPs (both tubes having different diameter in one turn or dual diameter tube) as can be seen in fig.1.11.

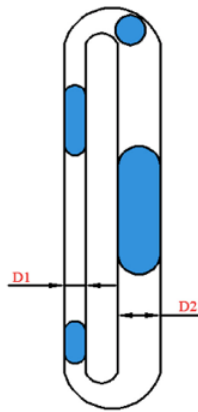


Figure 1.11 – Schematic of asymmetric PHP used for experimentation (Zhang et al., 2020) [52]

The “optimal dimensionless difference factor (ratio of diameter difference to average tube diameter)”, which was suggested to be between 0.25 and 0.4, was described. The use of asymmetric PHP showed 45% decrease in thermal resistance. The author used a single turn in this experimental work, and it was observed that PHP thermal resistance increased from vertical to horizontal operation. It was also verified through the proposed model that the flow circulation within PHP will increase with an increase in the number of turns and could allow asymmetric PHP work without gravity influence. Therefore, it was clearly stated that even in the case of horizontal operation, the use of non-uniformity in the channel layout could improve flow circulation. So in order to measure the effect of channel layout on thermal performance, the concept of effective dissimilarity was first introduced recently by (Lim and Kim, 2019) [53] and experimented micro pulsating heat pipe with HFE-7000 as a working fluid (50% FR) at

various values effective dissimilarity. Effective dissimilarity is a ratio between the extent to which the layout of the channel differs from the uniformly arranged channel layout to the extent that it differs from the decreasing channel layout. Due to the use of non-uniformity in channel layout the channel with maximum effective dissimilarity reported 32% higher thermal conductance than channel with minimum effective dissimilarity in horizontal operation, which can be articulated with help of fig. 1.12.

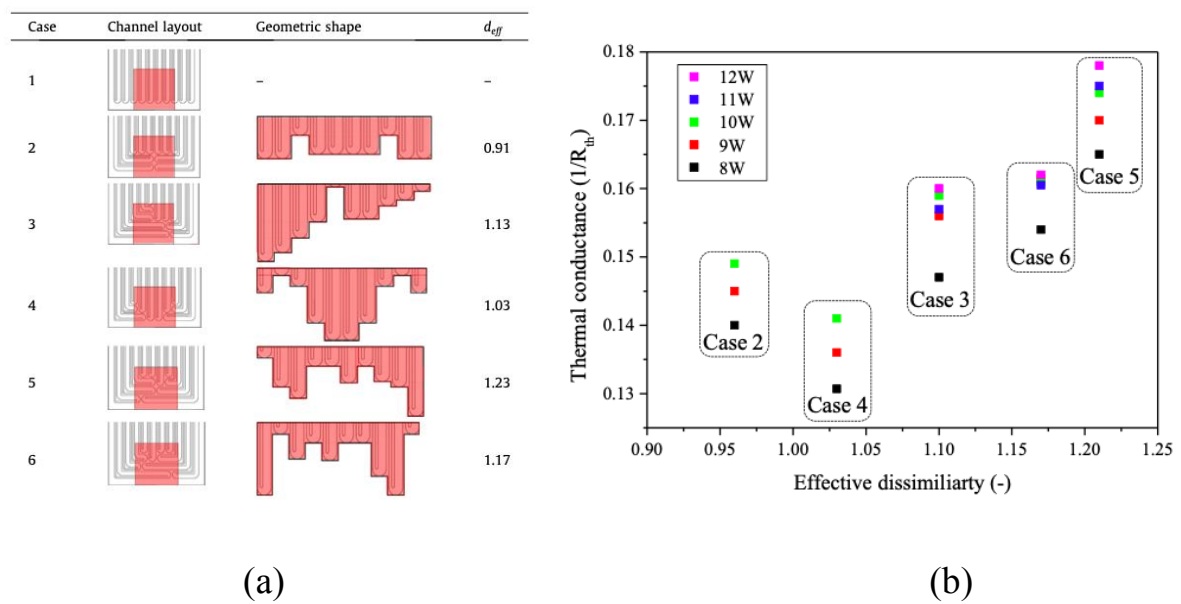


Figure 1.12 –Channel layout with effective dissimilarity (a). The thermal conductance of randomly arranged channel layouts of the MPHPs at various effective dissimilarities (b) (horizontal operation) (Lim and Kim, 2019) [53]

Most recently, the influence of the tandem tapered nozzle (fig. 1.13) on three-dimensional glass tube CLPHP was studied both experimentally and numerically (He et al., 2020) [54]. Results revealed that after the modification, the thermal resistance was decreased by 29.5 %, and the unidirectional flow was greatly encouraged. In addition, the dry-out condition that existed at 40% FR in the ordinary CLPHP was also removed in the tapered model.

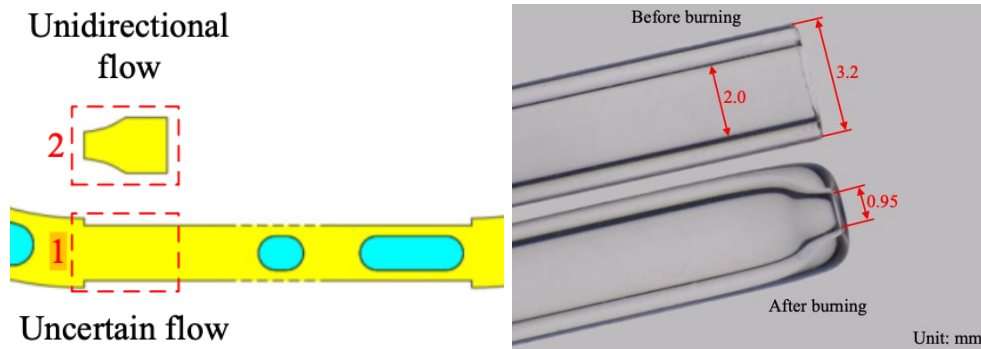


Figure 1.13 – 3D tapered model used in CFD research along with alteration of glass tubes for experimentation (He et al., 2020) [54]

Despite the promising benefits of using asymmetric PHP designs, few researchers have explored this approach to enhance start-up efficiency and operational stability by inducing unbalanced capillary forces. Further experimental work is needed to investigate these untried PHPs with non-uniform channel layouts, using various working fluids and diameters, to optimize their start-up and operational characteristics across different conditions.

1.3.5 Zones length

In addition to utilizing asymmetry in channels to improve circulation, researchers have explored the impact of varying evaporator, adiabatic, and condenser zone lengths on PHP start-up and transient operating characteristics. The ratio of heating section length to cooling section length was found to accelerate start-up and reduce thermal resistance under constant filling ratio and heat input, as demonstrated via CFD simulations (Wang et al., 2015) [55] (fig. 1.14). The influence of condenser length was also tested on micro-PHPs, revealing the existence of an optimal condenser length that resulted in the lowest evaporator temperature under constant condenser conditions (Kim and Kim., 2018) [56].

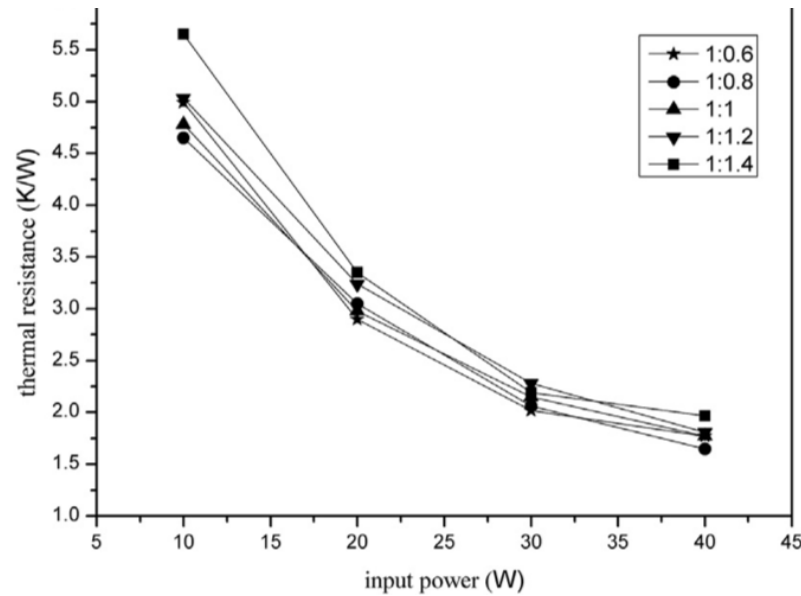


Figure 1.14 – Effect of evaporator to condenser length ratio on thermal resistance (Wang et al., 2015) [55]

In terms of the influence of adiabatic length, all researchers have come to a common conclusion that the wider the length of the adiabatic region, the greater the thermal resistance (Arab et al 2012; Dilawar and Pattmatta., 2013) [55], [57]. It was also recorded that thermal resistance was increased by just 30% by increasing adiabatic zone length by 500%, showing the possible benefits of PHPs to transmit heat over a long distance efficiently (Gan et al., 2019) [58]. The combined effect of the adiabatic section length and its convective heat transfer coefficient on the start-up and heat transfer efficiency was evaluated using two phase flow CFD model (Li et al., 2020) [59]. The start-up time of the PHP was reduced as the adiabatic section length was increased, but the thermal resistance of the PHP was increased, and the PHP's anti-dry-out capability was lowered.

To improve PHP performance, the effect of PHP zone length was also investigated in terms of its real-life potential application. Considering the entire length of PHP (evaporator to condenser), it is experimentally established that with increasing PHP length, thermal performance deteriorates (Deng et al., 2017) [60]. But PHP performance in terms of thermal resistance has given varying responses when it comes to variation in

individual evaporator, adiabatic and condenser zone lengths. A comprehensive study was performed on flat plate solar collectors in combination with pulsating heat pipes (Kargarsharifabad et al., 2013) [61]. It was observed that the longer the length of the evaporator, the higher the temperature of the outlet (fig. 1.15). Therefore, an increase in the evaporator's length resulted in more heat being added to the tank.

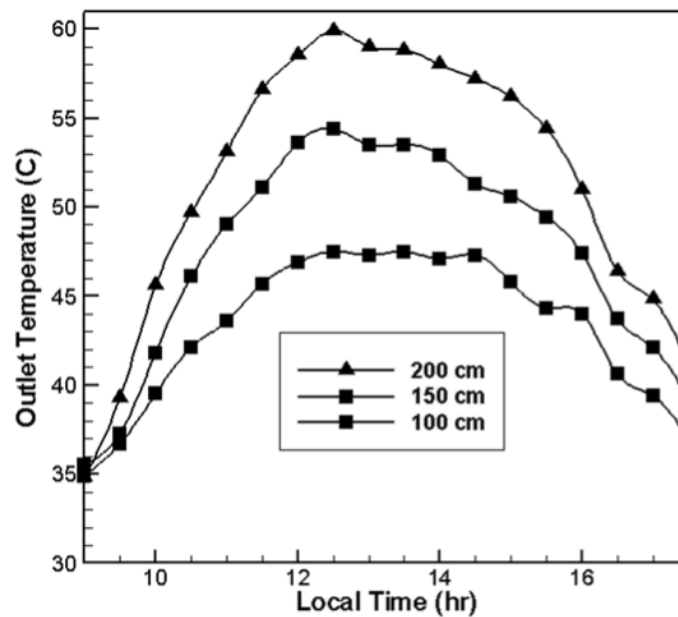


Figure 1.15 – Effect of different evaporator length on outlet temperature
(Kargarsharifabad et al., 2013) [61]

However, these findings are in complete contradiction with those obtained by (Charoenasawan et al., 2008) [15], which stated that, as can be seen in fig. 1.16, the thermal resistance decreased with decrease in evaporator length and maximum performance occurred at 50 mm evaporator length.

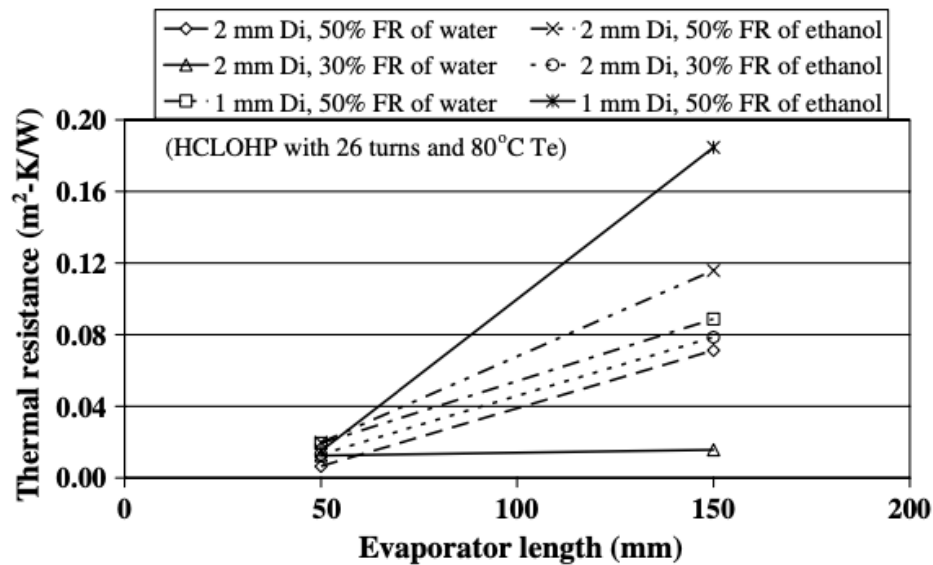


Figure 1.16 – Effect of evaporator length on thermal resistance by (Chaoenasawan et al., 2008) [15]

Considering the past literature work it is clear that influence of zone length was investigated mostly on particular application but true operational and start up characteristics of PHP with regards to zone length can only be studied if more attention is given to individual parameter. Research on individual zone length (evaporator, condenser, and adiabatic zone) is needed to investigate its efficacy. More targeted research into the interplay between zone length and fluid dynamics can provide the insights needed to design PHPs that perform efficiently across a variety of applications, ensuring rapid start-up and stable, consistent heat transfer under dynamic operating conditions.

1.4 Working fluid parameters

1.4.1 Physical properties of working fluid

A PHP's work and thermal performance depend enormously on the properties of the working fluid. The fluid attributes to be accounted while choosing the working fluid are surface tension, dynamic viscosity, latent heat, specific heat, thermal conductivity, and the rate of pressure variance over-temperature under saturated conditions $(dP/dT)_{\text{sat}}$. The

following section will pay attention to all these properties and list their impact on PHP thermal performance.

Surface tension: As specified in equation (1-1) the maximum permissible PHP diameter occurs when the gravitational force roughly equals the capillary force. It is a well-known fact that higher surface tension generates a large capillary force and allows the heat pipe to operate in any orientation, but at the same time blocks the flow during liquid slug oscillation. In support of these theoretical postulates, numerical and experimental study were carried out by (Bastakoti et al., 2018) [62] and (Kumar et al., 2019) [63] respectively, revealed that lower surface tension was found to increase thermal efficiency. On the other hand, fluid with greater surface tension tends to increase the diameter of the operating tube which, due to lower frictional resistance, in effect, decreases the pressure drop. Many researchers have started using surfactant solution to lower the surface tension. PHP thermal efficiency with surfactant aqueous solution of cetyl trimethyl ammonium bromide (CTAB) in the concentration range of 0.025% to 0.25% has been studied recently (Xing et al., 2018) [64]. It is noted that it can significantly reduce surface tension and increase wettability by adding surfactant solution. Due to the addition of surfactant to heat inputs of 100 W, thermal resistance decreased by 48.5 percent. Likewise, several researchers have recently made the same attempt to reduce surface tension with the aid of surfactant solution and have found positive results with regard to PHP thermal performance (Gandomkar et al., 2020; Wang et al., 2019; Bao et al., 2020) [65]–[67]. A detailed review conducted by (Nazari et al., 2018) [68], reported that it was lower surface tension that helped to increase heat transfer rate.

Dynamic viscosity: In line with the fact that a small value of viscosity can minimize channel shear stress, Experimental research documented by (Liu et al., 2013) [69], stated that low dynamic viscosity helped boost start-up performance. Whereas, in terms of heat transfer performance, lower dynamic viscosity was found to be the dominant property at lower heat input but its effect at higher heat input weakened (Han et al., 2014) [5]. A similar trend was observed even in silicon-based micro pulsating heat pipe fabricated

with different hydraulic diameter, as at low heat input, working fluid with lower dynamic viscosity (FC-72 and R113) could start up PHP operation, while fluid with high a value of dynamic viscosity (Water and ethanol) failed to start up (Qu et al., 2012) [70].

Latent heat: Low latent heat fluids exhibit better oscillation and start-up characteristics but are likely to dry out if the heat input continues to increase (Han et al., 2014) [5]. In terms of working fluid, PHP demonstrated comparatively better thermal properties for methanol than all other fluids, for both closed and open loops. For open-loop PHP, Methanol is considered the best fit working fluid in horizontal operation, pertaining to its high thermal conductance (Saha et al., 2012) [20]. Circular tube cross-section with 0.9 mm diameter was used in this experiment and performance is compared with water and acetone. Using DI water and methanol, (Srikrishna et al., 2019) [71] investigated the effect on closed-loop PHP (2.2 mm x 2 mm). Better heat transfer results were obtained for methanol than DI vapor at 70% FR. So, it's better to use small latent heat fluids for low heat flux applications and high latent heat fluids for high heat flux. Fluids that display both extremities have also experimented, to be discussed in the next section. The thermal conductivity of the fluid and the specific heat are two other parameters that have a great influence on thermal performance, as its higher value is likely to increase the rate of heat transfer. Another important parameter that was given utmost importance due to its unique characteristic is $(dP/dT)_{sat}$. Larger its value, higher the difference in vapor pressure between evaporator and condenser for small temperature change (Zhang and Faghri, 2008) [41]. Ammonia as a working fluid experimentally tested using glass tube PHP (ID = 2 mm) that has higher $(dP/dT)_{sat}$ than water found that during horizontal operation it was easy for PHP to start up at low heat input, but circulation was not that effective (Zhihu and Wei, 2014) [72]. To put all these properties into perspective literature analysis indicates that low surface tension, low dynamic viscosity, high specific heat, and thermal conductivity are expected for the smooth operation of PHP. The effect of surface tension is controversial, and to take benefit of surface tension property with regards to its influence on capillary force, liquid must be selected, which provides a compromise between the useful and blocking action of

capillary force. It also states that the latent heat and dynamic viscosity of the fluid should be decided based on high or low heat flux applications.

1.4.2 Fluid category

The most commonly used working fluids in PHP operation are water, ethanol, methanol, acetone, R123, and FC-72 (Khandekar et al., 2003; Qu et al., 2012; Han et al., 2014) [73] [70] [5]. Past studies have shown that one specific working fluid cannot meet all the requirements mentioned in the above section. In terms of required thermophysical properties, the combination of different fluids has shown improvement. It can be broken down into the following categories.

Binary mixtures: Experimental work carried out on PHP (2mm ID) with a binary mixture of water and acetone, in the mixing ratio of 13:1, 4:1, 1:1, 1:4, 1:13 found that start-up characteristics of a binary mixture (13:1, 1:1, 1:4, 1:13) were comparatively better than those of pure working fluids at low FR, but at high FR and high heat input, it shows no noticeable improvement (Zhu et al., 2014) [74]. A similar study was conducted by (Pachghare and Mahalle, 2014) [75] using a binary mixture of water with ethanol, methanol and acetone (with a mixing ratio of 1:1) and found that binary mixture comparatively reduced thermal resistance than single working fluid. Water- acetone mixture resulted in best combination with regards to lower thermal resistance. In another study, it was found that, at higher FR and heat input, thermal performance of PHP with binary mixtures largely becomes a function of the energy carrying capacity of fluid which is largely a function of latent heat value and specific heat of the fluid (Han et al., 2016) [76]; Experimental work was carried out on water-based binary zoetrope of methanol, ethanol, and acetone at varied mixing ratios (13:1, 4:1, 2:1, 1:1, 1:4, 1:13). At low FR and low heat input, the thermal performance was in accord to all other above discussed findings, but at high FR, water-methanol mixture showed excellent performance, which was largely attributed to its comparatively high latent heat and specific heat than all other mixtures. Experimental probe by (Wang et al., 2017) [77] on PHP with acetone-based mixtures (2:1, 4:1, 7:1) of water, methanol and ethanol reported

that at both low and medium FR, acetone-water binary mixture outperformed all other fluid mixtures with regards to its dry out features, but reverse effects were observed at high FR, and pure acetone exhibited better thermal performance.

Recently, the effect of some other immiscible binary mixtures such as not discussed in the above findings are also tested on PHP. (Xu et al., 2019) [78] used a combination of deionized water and HFE-7100 at different proportions (4:1, 2:1, 1:1; 1:2, 1:4), whereas FR (50%) was kept constant and heat input was given between 20-250 W. It was found that binary mixture with 1:2 proportion performed exceptionally well at all heat input range. When experimented at different heat inputs. At low heat inputs such as 20 W, binary mixture with 1:1 ratio performed comparatively well in terms of thermal resistance, whereas binary mixture with 1:4 ratio showed good results at high heat input (fig. 1.17).

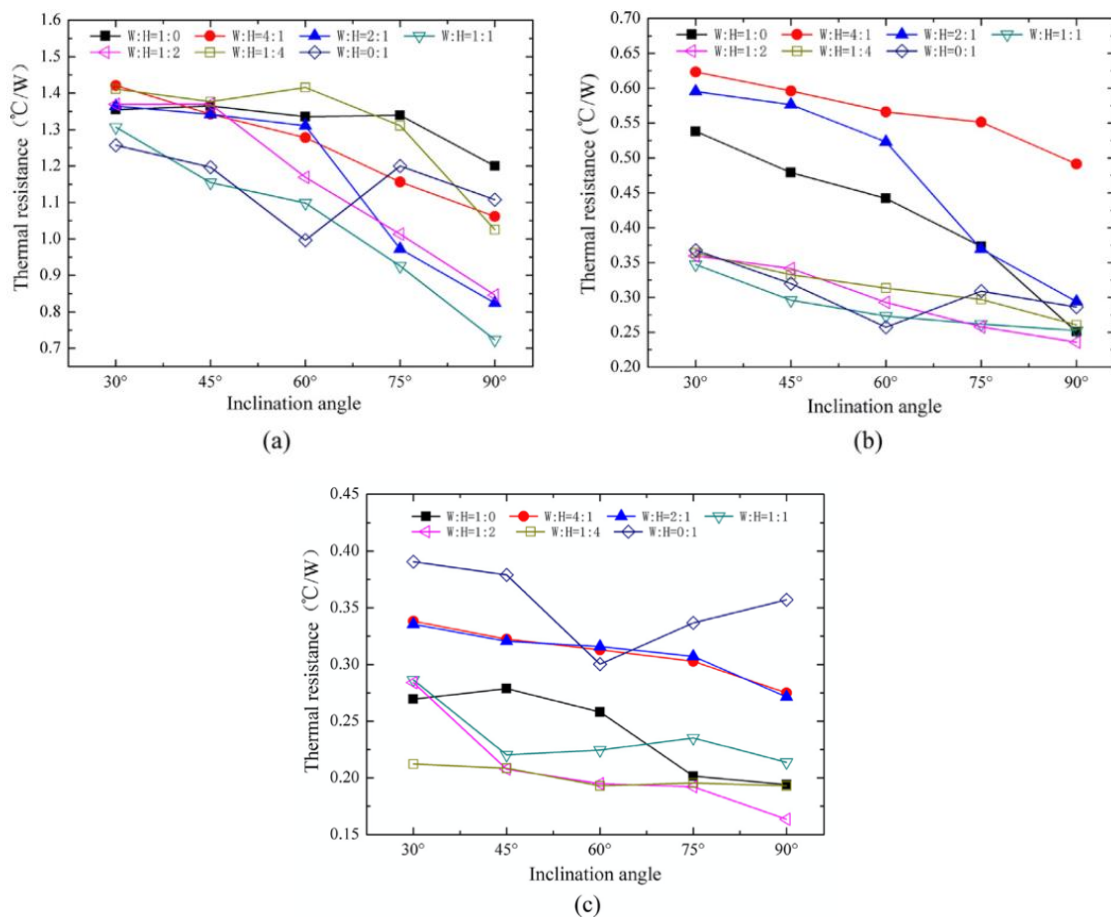


Figure 1.17 – (a) Thermal resistance at different inclination angles (a) 20 W, (b) 130 W and (c) 250 W (Xu et al., 2019) [78]

Apart from soluble mixtures like acetone and ethanol in water, a comparative study of insoluble mixtures such as toluene and hexane in water was also carried out by (Zamani et al., 2019). [79] Mixing ratio utilized was 3:1, 1:1, and 1:3, and once again acetone-water (3:1), displaying consistent trend, outperformed all other combinations, in terms of overall results. Although, these findings showed the dominance of binary mixtures to enhance PHP's thermal performance in comparison with traditional pure working fluids, much research still need to be done, to study operational modes of PHP across different heat carriers.

Nanofluids: Adding nanoparticles in the working fluid at an optimal proportion can effectively increase the thermal conductivity of the fluid, and hence the rate of heat transfer. Initially, during its development, many researchers used nanoparticles made primarily of gold, diamond, silver, Al_2O_3 and copper (Tsai et al., 2004; Ma et al., 2006; Lin et al., 2008; Ji and Ma, 2011; Riehl and Santos, 2012; Karthikeyan et al., 2014) [80]–[84]. All the researchers have come with a common conclusion that the use of nanofluids in PHP operation can certainly improve its performance due to its better thermal conducting properties. Later on, many researchers began using combinations of novel nanoparticles due to its improved heat transfer characteristics. One such comparative experimental work was carried out by (Qu and Wu, 2011; Rudresha and Kumar, 2014) [85], [86]. Both authors used Al_2O_3 and SiO_2 nanoparticles and found that Al_2O_3 nanoparticles give rise to better thermal performance compared to SiO_2 particles. However, its effect depends precisely on its concentration. When PHP was experimented with graphene oxide as a nanofluid in water (in the concentration of 0.25-1.5 g/lit), it is found that thermal resistance of PHP was reduced to 42% with 2.5 g/lit concentration, but the reverse trend was observed with a higher concentration (Nazari et al., 2018) [87]. Moreover, the stability of working fluid is another factor that affects its performance, as reported by (Akbari and Saidi, 2018) [88]. It is observed that the lower value of thermal resistance was obtained with Titania- water (TiO_2) nanofluid than graphene-water nanofluid, as the former had more stability than later. Nanoparticles have also shown its dependence on input heat flux, as thermal resistance was at its low when heat input was

lower, while reverse trend was observed with higher heat input (Gonzalez and Kim, 2014) [89].

In addition, thermal conductivity, which is the root cause of heat transfer enhancement, particularly given the effect of nanofluid, is strongly affected by both the size and shape of the nanoparticles. It is reported that fluid with large nanoparticles tends to promote the conductivity of a working fluid (Ali et al., 2013) [90]. Whereas, out of four shapes (platelet, blade, cylinder and, brick) of Al_2O_3 nanoparticles which were experimented, cylindrical shape outperformed all other shapes in terms its thermal performance; Nonetheless, this pattern changed by applying more heat ($> 125\text{W}$) to PHP, such that brick-shaped nanoparticles surpassed the best of all (Kim et al. 2015) [91].

While much attention was given towards improving thermal performance of PHP in vertical position using nanofluid, experimental research on CLPHP with DI-water and CuO nanofluid was carried out (Karthikeyan et al., 2015) [92] in order to study the impact of gravity. However, in horizontal operation, the tested PHP could not perform, suggesting that although nanofluid improves PHP thermal performance, it has very little impact on gravity. However, PHP with water based ferrofluid was able to operate at any orientation in presence of magnetic field as experimented by (Mohammadi et al., 2012) [93]. Thermal performance was significantly elevated in horizontal operation at a larger filling ratio and heat input (fig. 1.18).

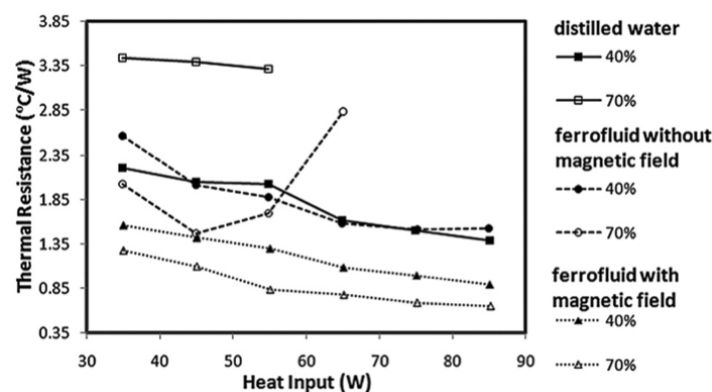


Figure 1.18 – Thermal resistance as a function of FR and heat input (Mohammadi et al., 2012) [93]

Under similar investigation, (Goshayeshi et al., 2016) [94] dispersed Fe_2O_3 nanoparticles into kerosene and studied its effect on closed-loop copper PHP under magnetic field. Even in horizontal operation, the PHP functioned successfully, although its thermal resistance decreased from vertical to horizontal.

In previous research, the influence of nanofluids on the operational characteristics of PHPs, especially concerning start-up behavior and transient performance, remains largely underexplored. While initial studies suggest that nanofluids alone have not significantly improved horizontal operation, promising results have been observed when combined with a magnetic field, which enhances fluid circulation and overall stability. This highlights the need for further investigation into how nanofluids can be leveraged to improve the operational efficiency of PHPs, particularly in optimizing start-up and transient phases across different orientations. Exploring these factors could lead to more robust designs and broader application potential for PHPs.

1.4.3 Filling ratio

Filling ratio is the volume filled by the working fluid in PHP to the total volume of PHP. FR of 0% means PHP without any form of working fluid, such that heat thermal resistance, in this case, is very high as heat transfer takes place only through the conduction mode of PHP material. Whereas FR of 100% means, PHP completely filled with the working fluid. In case it is 100% filled, the PHP does not hold its unique operating characteristic, rather it behaves much like a single phase thermosyphone with heat transfer occurring originally by convection due to density difference, hence it varies between these two extremities. Past studies have shown that for PHP to show its true nature, FR should range between 20% to 80% (Zhang and Faghri, 2008) [41]. However, critical review carried out by (Han et al., 2016) [76], showed that the majority of authors used FR of between 35% to 65% as investigation believes that it shows optimum performance for almost all the working fluids. The properties of working fluid have a significant influence on the optimum FR of working fluid. Experimental work reported by (Han et al., 2014) [5], revealed that for the same FR working fluid with low latent

heat value was easier to dry out. Results also revealed that (as can be seen from fig. 1.19) with regards to low thermal resistance, at low heat flux, FR of 60% to 80% is a fair choice for acetone, whereas, at high heat flux, the optimal filling ratio for methanol and DI water ranges from 90% or higher and 55% to 70%, respectively.

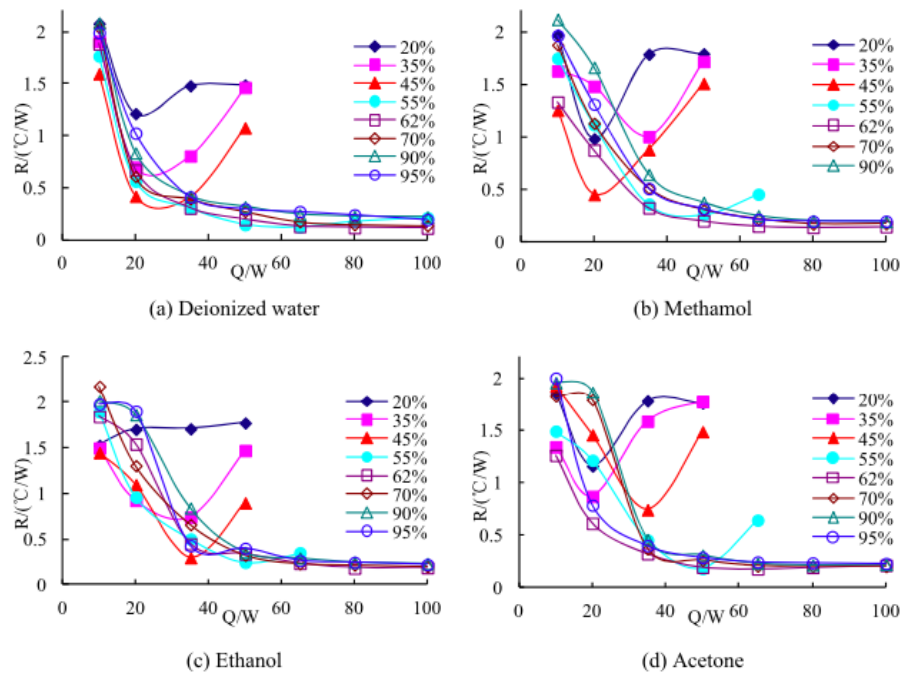


Figure 1.19 – Thermal resistance value of various working fluids at different FR (Han et al., 2014) [5]

Similar behavior was observed for acetone, as it displayed a lower thermal resistance value at 60% FR, when PHP was evaluated for FR ranging from 50% to 90% (Babu et al., 2018) [95]. Ethanol on the other hand exhibited optimum performance at FR of 50% to 70% (Rahman et al., 2016) [96]. For ammonia it was 70% - 80%, in order to avoid burn out of evaporator (Zhihu and Wei., 2014) [72]. Beside working fluid properties, PHP performance in terms of FR often varies with PHP system orientation and cross section. When a flat plate aluminum PHP was operated with ethanol as a working fluid, the optimum FR was found to be 50% - 65% in horizontal and top heated positions, whereas, it was between 40% - 70% with bottom heated mode (Yang et al., 2009) [17]. At close horizontal orientations, the performance of water as a working fluid

is lower than methanol with the same fill ratio and also, methanol displayed less thermal resistance when measured at 40% FR for inclination angles from 90^0 to 7.5^0 (Srikrishna et al., 2019) [71]. In another investigation, PHP with a circular channel showed the lowest thermal resistance at FR of 0.4 while, rectangular channel showed the lowest thermal resistance at 0.3 FR (Hua et al., 2016) [34].

Although, FR is a crucial parameter to decide heat transfer characteristics of PHP devices, past studies show that optimum FR of a working fluid varies with a particular experimental design, which again is a function of many other parameters that were discussed. Theoretical studies are also rare that could establish the optimum FR for optimizing heat transfer characteristics. Recently, one such study was carried out by (Yin et al., 2014) [97], and developed a mathematical model to predict the effect of FR on startup heat flux. The study found that heat input required to start the oscillation depends on FR, but the upper limit of FR is again considered to be a function of the type of fluid. It is therefore imperative that many experimental or computational tests need to be carried out in terms of FR to create a database that will help design future PHP devices at optimum FR.

1.5 Operational parameters

1.5.1 Heat input

The heat input to the PHP system relates directly to its operating temperature. With regard to the application of PHP in electronic devices, the reliability of electronic components is closely linked to the failure factor (failure rate ratio at any temperature to failure rate at 75^0 C), which increases exponentially with the system temperature (Murshed and Castro, 2017) [2], as shown in fig. 1.20. It is therefore of utmost importance to build a PHP that can be operated over a wide range of temperatures and prevent electronic components from raising their temperature beyond its failure threshold.

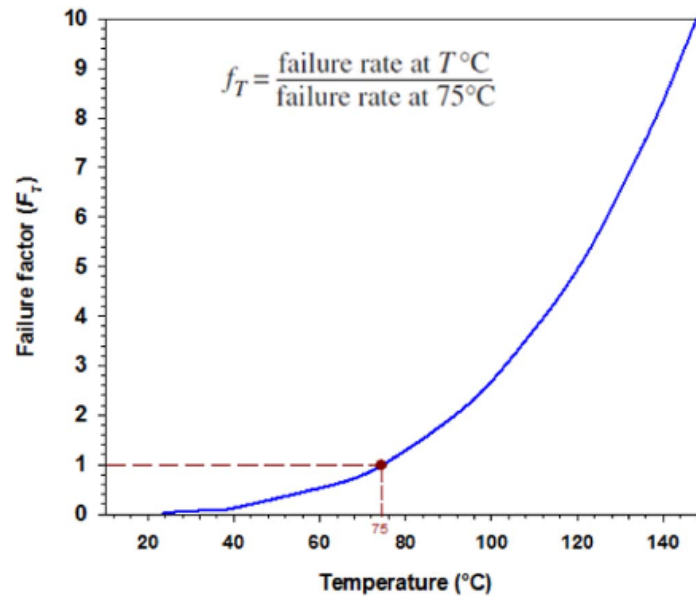


Figure 1.20– Plot of temperature effect on the failure rate of the electronic component (Murshed and Castro, 2017) [2]

Moreover, the contribution of an individual parameter from the list of FR, number of turns, zone length, working fluid, heat input diameter is evaluated recently based on the normalized coefficient approach (Patel and Mehta, 2019) and found that more than 50% of the overall thermal performance is regulated by heat intake. Therefore, PHP performance is largely affected by input heat flux. Efficient PHP is expected to start oscillations at low heat inputs and, avoid drying out at high inputs. Awareness of the thermo-hydrodynamics of flow within PHP is of paramount importance to fully understand the effect of input heat flux. For PHP, flow visualization using Pyrex glass (ID = 1.8 mm) was performed by (Tong et al., 2001) [98] and thermodynamics of bubble nucleation in evaporator to bubble coalescence in condenser was observed (fig. 1.21). Small bubble developed into Taylor bubble in the evaporator due to continuous heating, and long slugs were split into short slugs, whereas the vapour rise velocity in the condenser is highly dependent on the buoyancy force due to the density difference of the two phases. As vapour Plug B penetrates and overtakes the short slug to coalesce with vapour plug A, the short slug appears to merge with the slug upstream or vanish; after

two bubbles have coalesced, the density of the newly formed bubble is changed, which gradually restores the force of circulation and hence the oscillation of fluid.

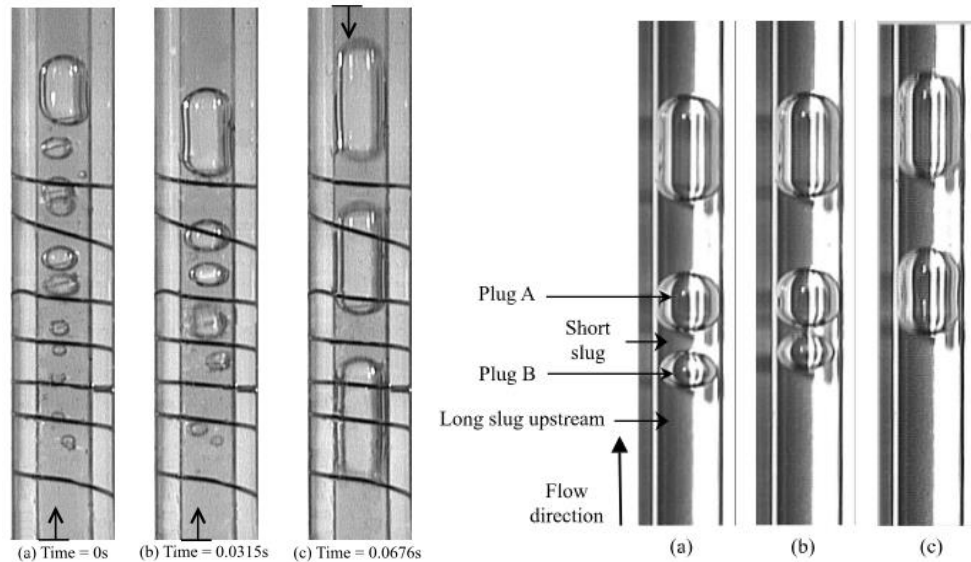


Figure 1.21 – Expansion and coalescence of bubbles in evaporator and condenser respectively (Tong et al., 2001) [98]

The operational and thermofluidic characteristics of working fluid inside PHP was also experimentally evaluated by (Pachghare and Mahalle, 2014) [75]. Study carried out on copper CLPHP (ID = 2 mm) using water, ethanol, methanol, and acetone. It was verified that after slug boiling, bubbly and slug flow patterns were observed in the upward flow under the influence of gravity up to 40 W, and semi annular and annular flows were found in the downward flow. At high heat flux, the gravity effect showed no impact (70 to 80 W). In particular, thin film evaporation has been shown to be the largest portion of the overall local heat transfer coefficient for all the conditions studied and can thus be considered as the prevailing heat transfer process (Spinato et al., 2016) [99]. All this research suggested that the collective activity of bubble nucleation, agglomeration and condensation is responsible for the two-phase flow movement. Channel wise examination of thermo-hydrodynamic characteristics too was carried out using acetone as a working fluid on 9 turn copper PHP (ID= 2mm) (Patel et al., 2019) [100] and it was

verified that numerous steady states were observed at 50 W, which is harmful to stable long-term PHP results. In the upward channels, mean velocity was observed to be double that of the downward channel; it was also found that the exact shape of the meniscus is maintained while flow becomes briefly sluggish or stationary during the pulsation, and slug flow mediated by surface tension is observed below 2.25 m/s. The shape of the meniscus is observed to deform with extreme flow motion (velocity ≥ 2.25 m/s) and semi-annular/annular flow mediated by inertia is observed. For the semi-annular/annular flow regime (which was observed at 125-200 W), average thermal output is observed to improve by 70 percent relative to slug-plug flow. Fig. 1.22 shows the velocity and frequency distribution inside PHP against heat input provided. However, data for the average velocity of all working fluids within PHP is not yet available.

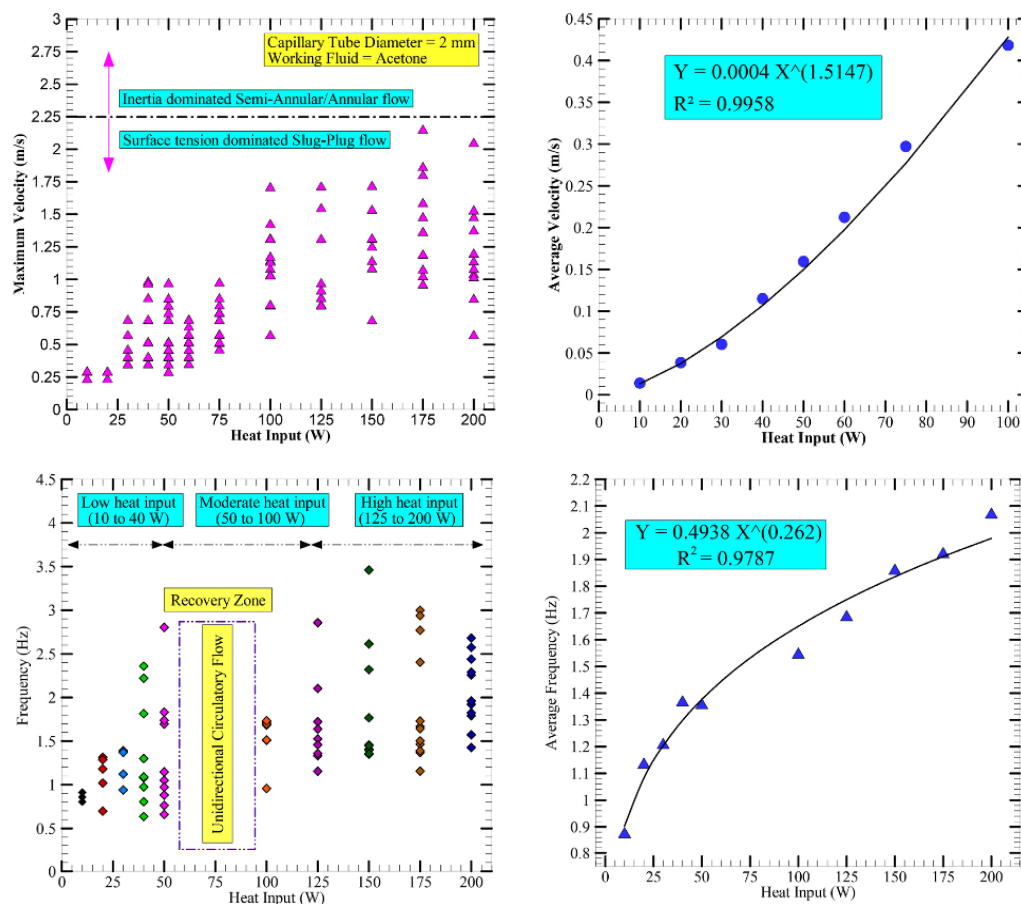


Figure 1.22 – Channel wise velocity and frequency distribution against heat input (Patel et al., 2019) [100]

For a decade now, the contribution of latent heat and sensible heat to the total heat transfer phenomenon has been studied and several researchers have concluded that the key heat transfer mechanism is sensible heat transfer by oscillation of liquid slugs and latent heat transfer has played a negligible role in terms of total heat transfer inside PHP (Shafi et al., 2002; Zhang and Faghri, 2008; Cheng and Ma, 2011) [19], [41], [101]. All these results were concluded with the aid of theoretical models. However, contradictory findings have recently been published regarding the contributions of sensible and latent heat transfer. Through his numerical investigation (Nikolayev, 2011) [102], found that it was latent that contributed to nearly 70 to 82% and not the sensible transfer of heat. Moreover, the first attempt to understand heat transfer mechanism experimentally was made by (Jo et al., 2019) [103], to their observation, the total contribution of latent heat transfer was experimentally calculated to be between 66% and 74%, and sensible heat transfer was hardly involved in the process of heat exchange.

An attempt was also made to find out the liquid and vapour volume fraction within PHP by experimenting with water-based PHP (6 turn) using neutron imaging technique. It was found that the average liquid volume fraction was always less than 2.5 percent and more than 80 percent in the evaporator and condenser, respectively, during the steady state oscillation within PHP (Yoon et al., 2012) [104]. The thermodynamic state of a vapour plug in the micro pulsating heat pipe (MPHP) was recently experimentally determined by (Jun and Kim, 2019) [105] and it was observed to be depend on the presence of the liquid film covering the vapour plug. If the vapour plug is surrounded by a liquid film, the vapour plug becomes saturated. In the other side, the vapour plug is superheated if the vapour plug is in close contact with the dry wall without the liquid film (fig. 1.23).

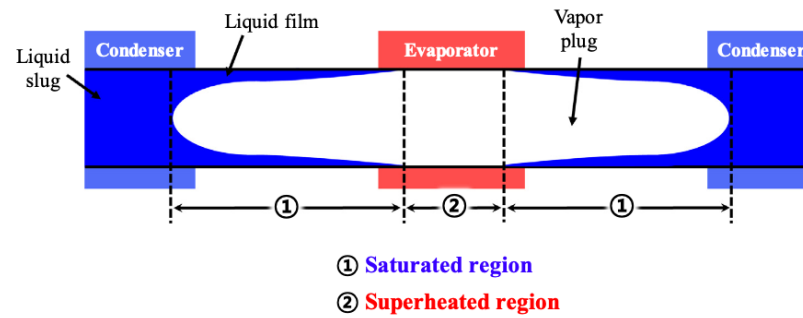


Figure 1.23 – Thermodynamic state of vapour hlug inside PHP (Jun and Kim, 2019)

[105]

The start-up analysis was conducted with binary fluids (acetone, ethanol, methanol) and surfactant solutions (Sodium dodecyl sulphate) based on water. It was found that the onset of pulsation remained the same even after using PHP for more than 7 hours, but with a rise in evaporator temperature. For all working fluids, start-up heat input values were depicted (fig. 1.24) in vertical orientation (Patel et al., 2016) [106]. Although heat flux is responsible for generating a driving force required to bring PHP into operation, start-up heat flux is different for different working fluids. Recently, a correlation is developed to estimate 'maximum permissible heat flux' for micro PHPs (Lee et al., 2018) [28], which can be extended to any number of turns and orientation. However, the effect of input heat flux duration on PHP thermal efficiency is a much less researched subject.

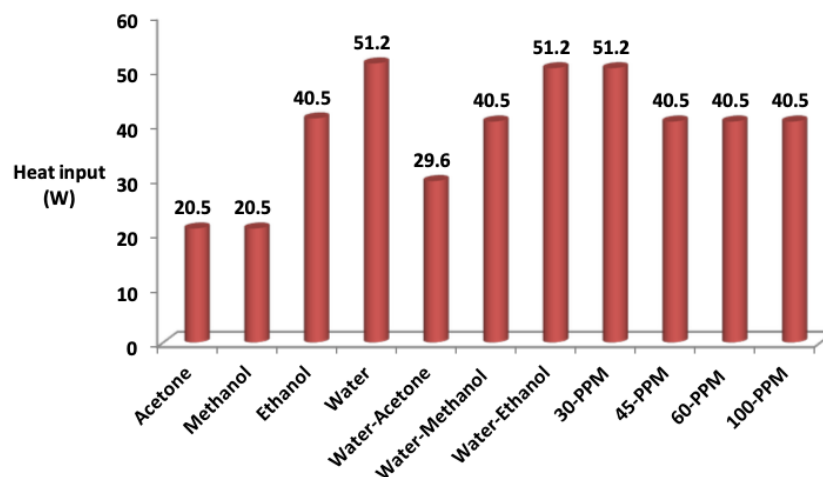


Figure 1.24 – Start-up heat input values for various working fluids (Patel et al., 2016)

[106]

PHP, when experimentally tested at different orientations from horizontal to vertical, PHP found that each tilting angle displayed different starting heat input level values. The heat flux required to enable the fluid motion was also dependent on the angle of inclination. Furthermore, the operational range of allowable heat fluxes adjusted to lower heat power values as the tilting angle increased (Mameli et al., 2014) [107]. Meanwhile heating patterns have shown significant influence on startup process and thermal resistance of PHP as indicated numerically by (Jiansheng et al., 2014) [108]. The PHP's start-up time and thermal resistance were decreased due to the non-uniform heating pattern (heating at one or many turns), which was attributed to the additional imbalance stimulating the device's start-up. Whereas a recent experimental analysis with non-uniform heating PHP carried out by (Jang et al., 2018) [109] reported contrary findings to the previous study. A concept of "dimensionless heat difference (ratio of difference in heat input between two sources to total heat input)" was used and thermal resistance was found to be increased due to early drying out on the higher side of the heat input with an increase in this factor. Most recently, a new double condenser pulsating heat pipe cooler configuration was studied (Torresin et al., 2017) [110] and confirmed the orientation-free PHP operation at high heat input (fig. 1.25).

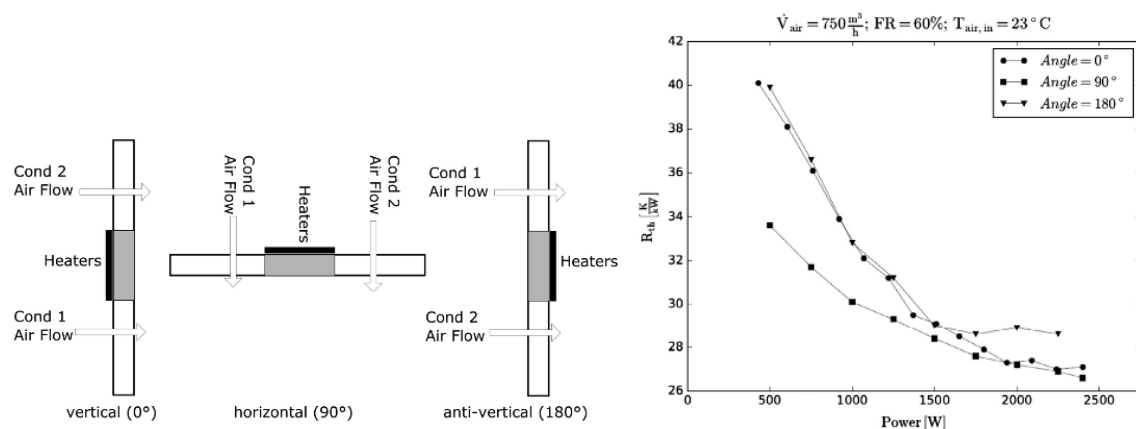


Figure 1.25 – Schematic of tested configuration and its performance against heat input at three different orientation (Torresin et al., 2017) [110]

Previous research has extensively focused on examining thermo-fluid dynamics in pulsating heat pipes (PHPs) at different heat inputs and orientations. However, the influence of heat input on geometric changes in PHPs, specifically in relation to their start-up and transient characteristics, remains largely unexplored. More research in terms of heat flux and operational modes of PHP is needed to understand the dynamics of the working fluid in both at vertical and horizontal orientation.

1.5.2 Orientation of PHP

Gravity adds to the unequal distribution of pressure in the OHP, which could increase the perturbation of the fluid and the enhanced heat transfer that follows it. Moreover, gravity facilitates the backflow of the liquid phase into the evaporator at low heat flux, which is a significant element in stopping the evaporator from drying out. One of those benefits is missed by PHP in a horizontal position and ultimately underperforms. Therefore, PHP orientation brings gravity indirectly into the picture and plays a very important role in evaluating its thermal performance, which can also be described using Equation (2-1). In the past several attempts have been made, to make PHP work independent of its orientation and weaken the influence of gravity.

During normal operation, the main working forces within a PHP include capillary, gravity, friction, and vapour pressure. The gravity force is marginal during horizontal PHP operation and frictional force plays no role during initialization as no detectable motion is observed. Capillary and vapour pressure, respectively, are therefore the main supporting factors to start PHP. And as such, in the past, several attempts have been made to raise the capillary and vapour pressure forces using new PHP designs to make PHP usable in either direction ([Chien et al., 2012](#); [Hathaway et al., 2012](#); [Tseng et al., 2014](#); [Tseng et al., 2016](#)) [47]–[50]

It is observed that although PHP's thermal performance becomes independent of the orientation using the number of turns as high as 80 ([Akachi et al., 1996](#)) [12], attempts have also been made to use a fewer number of turns (to minimize space) and yet be able to weaken the influence of gravity. First attempt to understand the role of gravity in the

operational characteristics of PHP is made by (Khandekar and Groll, 2004) [111]. A 'stop over' phenomenon was invented, described as repetitive activity phase occurrence (large amplitude oscillations) and static phase occurrence (very small amplitude oscillations). Liquid slugs oscillate with very small amplitude in the condenser segment during the static phase. This 'stop over' phenomenon is also explained clearly by (Jun and Kim, 2016) [112] (fig. 1.26). Due to this issue, the liquid slugs available there do not circulate to the heating zone, contributing to the evaporator drying out. In PHP with large number of turns, because of sustained high amplitude oscillations, this 'stop over' phenomenon seldom happens.

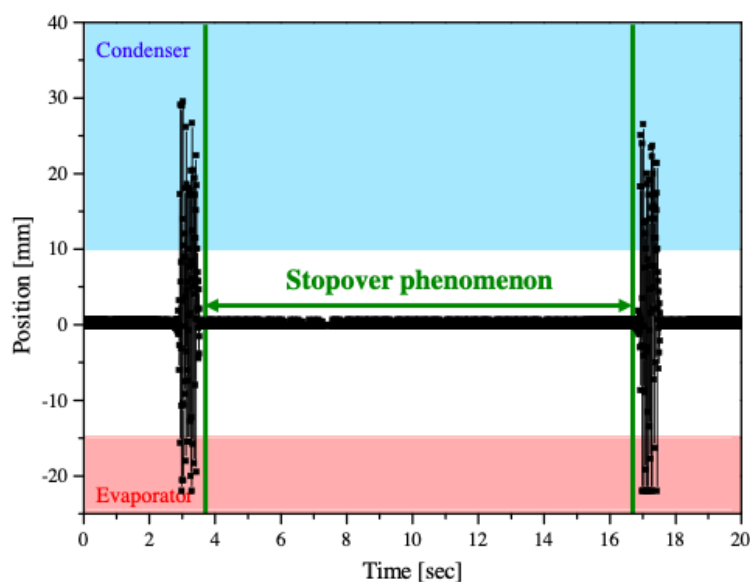


Figure 1.26 – Stop over phenomenon observed in 10 turn PHP during horizontal operation (Jun and Kim, 2016) [112]

It is also confirmed that during horizontal operation, this same issue appears in PHP. Therefore, quite recently (Jun and Kim, 2019) [113] established a criterion through theoretical and experimental investigation on MPHP (10 turns) to prevent this 'stop over' phenomenon and to allow PHP function in horizontal mode. For normal PHP operation in horizontal mode, a figure of merit was introduced (equation 1-4) which was the ratio of the minimum thermal resistance in a vertical orientation to that in a horizontal

orientation is proportional to the square of the ratio of the hydraulic diameter to the effective length of PHPs. It is also confirmed that to prevent a ‘stop over’ defect in horizontal operation, the ratio of hydraulic diameter to the effective length of PHPs must be greater than 0.03 (fig. 1.27).

$$\left(\frac{R_{th,V,min}}{R_{th,H,min}}\right) = \left(\frac{D_h}{L_{eff}}\right)^2, \quad (1.4)$$

where, $R_{th,V,min}$ - thermal resistance in vertical orientation, K/W;

$R_{th,H,min}$ - thermal resistance in horizontal orientation, K/W;

D_h - hydraulic diameter, m;

L_{eff} - effective length of the PHP, m.

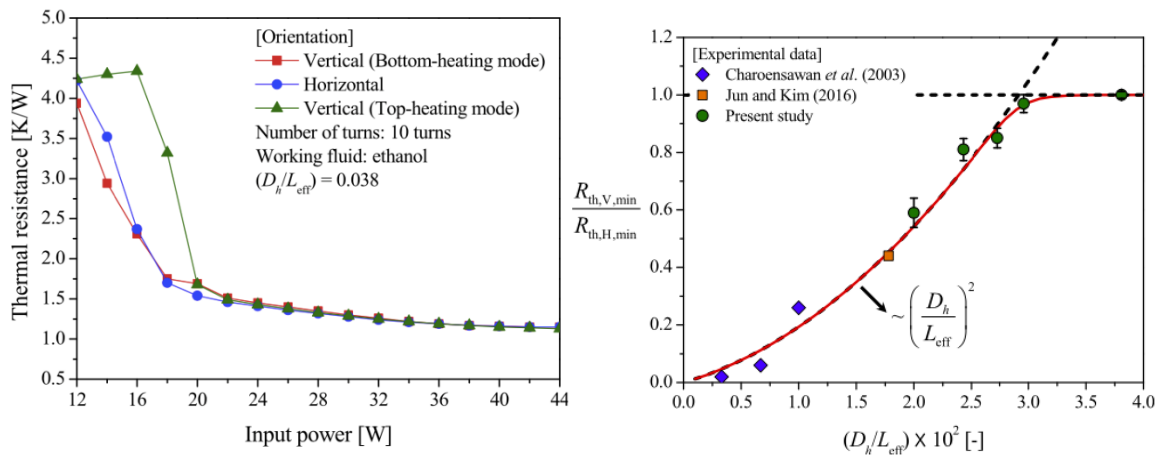


Figure 1.27 – Thermal resistance variation as a function of (D_h/D_{eff}) ratio (Jun and Kim, 2019) [113]

Simulation findings by (Nekarshevych et al., 2019) [114] reveals that the variation in PHP output is related to the difference in the phase distribution within the PHP evaporator at various orientations. Similar findings were observed previously by (Khandekar et al., 2009) [115] during experimental study.

Findings from the literature imply that, as indicated by previous scholars, PHP can be worked at any orientation even without using a significant number of turns, but study evidence available on this outcome is very limited and most of these tests are conducted on micro-pulsating heat pipes. In the future, outcomes of (Jun and Kim, 2019) [113] could be of good use when designing PHP which would operate independent of orientation.

1.6 Conclusions

The main findings of this literature review are listed below, and thereafter the future design of this research work may rely on the following guidelines.

1. In terms of geometrical parameter perspective, PHPs with an internal diameter (ID) less than 2 mm are known to exhibit increased thermal resistance, necessitating the development of strategies to reduce this drawback. However, there is still a significant lack of information regarding the influence of zone lengths on the thermal performance of PHPs. Studies focusing on the operational, transient, and start-up characteristics in relation to zone length are essential to enhance the understanding of PHP behavior. Additionally, PHPs with more than 20 turns have demonstrated effective operation, but their large size makes them unsuitable for modern electronic applications. Therefore, identifying methods to optimize PHPs with fewer turns, between 1 and 10, while maintaining performance is critical for advancing their use in compact electronic systems.

2. Investigating the physical properties of heat carriers, such as boiling point, viscosity, and surface tension, is essential to understand their influence on the start-up and transient behavior of pulsating heat pipes (PHPs). While binary mixtures like water-methanol, water-acetone etc. improve start-up characteristics, the reasons for these improvements remain unclear. A systematic study of pure liquids' properties is necessary to establish the foundation for understanding how they affect phase change dynamics and fluid circulation, ultimately guiding the optimization of mixtures and PHP designs for enhanced thermal performance.

3. The start-up and transient characteristics of pulsating heat pipes (PHPs) are significantly influenced by their inclination angle. Investigating this relationship is crucial for understanding how gravitational forces affect fluid circulation, phase change dynamics, and overall thermal performance. Such studies are necessary to optimize PHP designs for improved reliability and efficiency across a range of operational condition

Chapter 2 – Experimental Methodology

This chapter outlines the experimental methodology used to investigate the start-up and transient characteristics of pulsating heat pipes (PHPs) for varying geometrical, physical, and operating parameters.

2.1 Selection of PHP parameters and factors under investigation

The primary objective of this study is to assess the individual impact of various critical factors on the operating characteristics of pulsating heat pipes (PHPs). Table 2.1 presents a comprehensive overview of the key factors investigated, along with their corresponding values. These factors—such as heat zone length, working fluid, internal diameter, and filling ratio—were meticulously chosen based on an extensive review of existing literature. The selection ensures that each parameter plays a significant role in influencing the startup, transient, and overall thermal performance of PHPs. By isolating and examining these variables, the study aims to provide deeper insights into optimizing PHP design and enhancing its operational efficiency in real-world applications.

Table 2. 1– Factors to be investigated

Sr. No	Factor	Value
1	Heat carrier	Pure liquids: water, methanol, pentane
2	Filling ratio	Water, Methanol, Pentane:50±0.5%.
3	Heating zone length	10, 30, 50 mm
4	Inclination angle	+90°, +45°, 0°, -45°, -90°
5	Heat input	0-80 W

2.1.1 Inner diameter and number of turns selection

The selection of the inner capillary diameter for the PHP was based on two key considerations. Firstly, the critical diameter condition was considered, which determines the maximum inner capillary diameter for optimal PHP performance. Through

calculations, it was determined that the critical diameter for water is 4.5 mm, for methanol is 3.4 mm, and for pentane is 3.2 mm (Ref.: equation 1-2). To ensure the PHP can operate with any of these liquids, an inner capillary diameter of 3.2 mm or less was chosen. Additionally, literature data suggested that a PHPs flow circulation increase when the inner capillary diameter is 2 mm or less. To meet this requirement as well, an inner capillary diameter of 1.1 mm was selected, as it satisfies both the critical diameter condition and the operational flexibility. To complete the loop in the PHP, a capillary tube with an inner diameter of 2.3 mm, outer diameter of 3 mm, and a length of 99 mm was utilized. This configuration ensures the continuous flow of the heat carrier within the PHP system. Regarding the number of turns in the PHP, literature indicates that a PHP can function even in extreme conditions when the number of turns is greater than 5. However, to determine the critical factors affecting PHP performance in unfavorable orientations, it was necessary to investigate their influence on PHPs with a lower number of turns. Therefore, 5 turns were chosen as the boundary value between the "non-working" region and the "working" region in any operational condition.

2.1.2 Zones Length Selection

The length of the heating zone in a PHP is an important factor that can impact its performance. In this study, heating zone lengths of 10 mm, 30 mm, and 50 mm were selected to investigate their effects on PHP behavior. The choice of a 50 mm heating zone length aligns with practical applications of PHPs for electronics cooling, such as cooling modern CPUs, which typically have dimensions close to 47.5x47.5 mm. By utilizing a heating zone length that closely resembles the dimensions of such practical scenarios, the findings can be directly applicable to real-world cooling applications. To align with the overall height of modern CPU coolers based on conventional heat pipes, which typically range from 150-155 mm, the overall height of the PHP was set to 154 mm. This choice ensures compatibility and allows for easy integration with existing cooling systems. When the heating zone length is 50 mm (considering a fixed condensation zone length of 100 mm), the adiabatic zone is nearly absent. At a heating

zone length of 30 mm, the adiabatic zone measures 24 mm, and at a heating zone length of 10 mm, the adiabatic zone extends to 44 mm.

Furthermore, a trend towards decreasing the heating zone length was adopted based on literature data, which suggests that reducing the length leads to an increase in PHP performance. This trend allows for a systematic analysis of the relationship between heating zone length and PHP behavior. Additionally, investigations involving heating zone lengths less than 50 mm are warranted, as there is a lack of experimental data in this range. The main design parameters of the PHP under study are summarized as below in table (2.2) along with PHP experimental sample (see figure 2.1).

Table 2.2 – Main design parameters for the PHP

Sr. No	Parameter	Value
1	Inner/outer diameter	1.1/2.1 mm
2	Number of turns	5
3	Overall width	142 mm
4	Overall height	154 mm
5	Heating zone length	10, 30, 50 mm
6	Condensing zone length	100 mm

2.2 Experimental set up

The experimental samples of pulsating heat pipes (PHPs) used in this study were fabricated using copper capillary tubes with internal and outer diameters of 1.1 mm and 2.1 mm, respectively. The pulsating heat pipe along with cooler and heater is mounted on the aluminum plate with the help of screws. Insulating material is kept between cooler and plate to avoid heat leakages from cooler to the plate. To lower the thermal resistance between the PHP and cooler, a thermal grease with a thermal conductivity of 4.5 W/(m·K) is employed between their surface contacts. Subsequently, thermal insulation

made of basalt fibre is placed over the setup to stop heat leakages from PHP to environment. Figure 2.2 shows the experimental set up and thermocouple placement. The PHPs consisted of five turns and were designed with different heating zone lengths of 10 mm, 30 mm, and 50 mm. The condensing zone length was kept constant at 100 mm, while the overall length of the PHP remained the same for all heating zone lengths. PHP is then filled with working fluid and the filling ratio (FR) was set at $50 \pm 0.5\%$.



Figure 2.1 – PHP sample for the experimental investigation

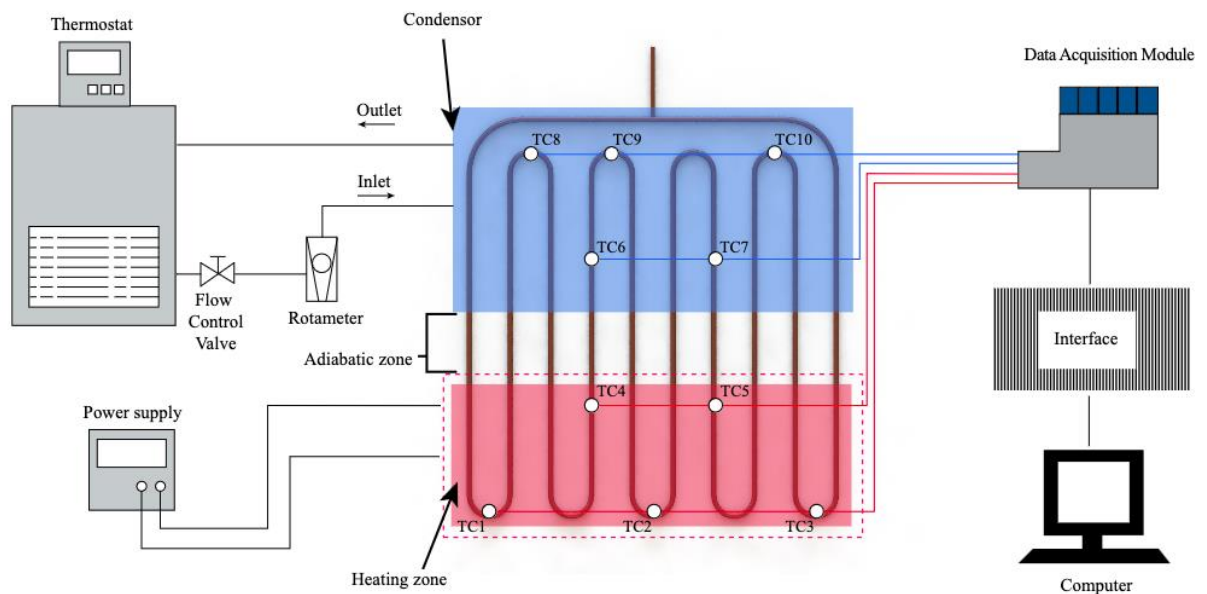


Figure 2.2 – Scheme of the experimental set up

To conduct the experiments, PHP was mounted on a metal plate along with an ohmic heater placed on the heating zone and a cooler positioned on the condensing zone. The metal plate was equipped with leveling screws to allow for the adjustment of the inclination angle. The investigation included five inclination angles: $+90^\circ$ (vertical position with bottom heating), $+45^\circ$, 0° (horizontal position), -45° , and -90° (vertical position with top heating) as shown in figure 2.3. This diagram also indicates the transitions between the heating zone (HZ) and cooling zone (CZ) at various orientations.

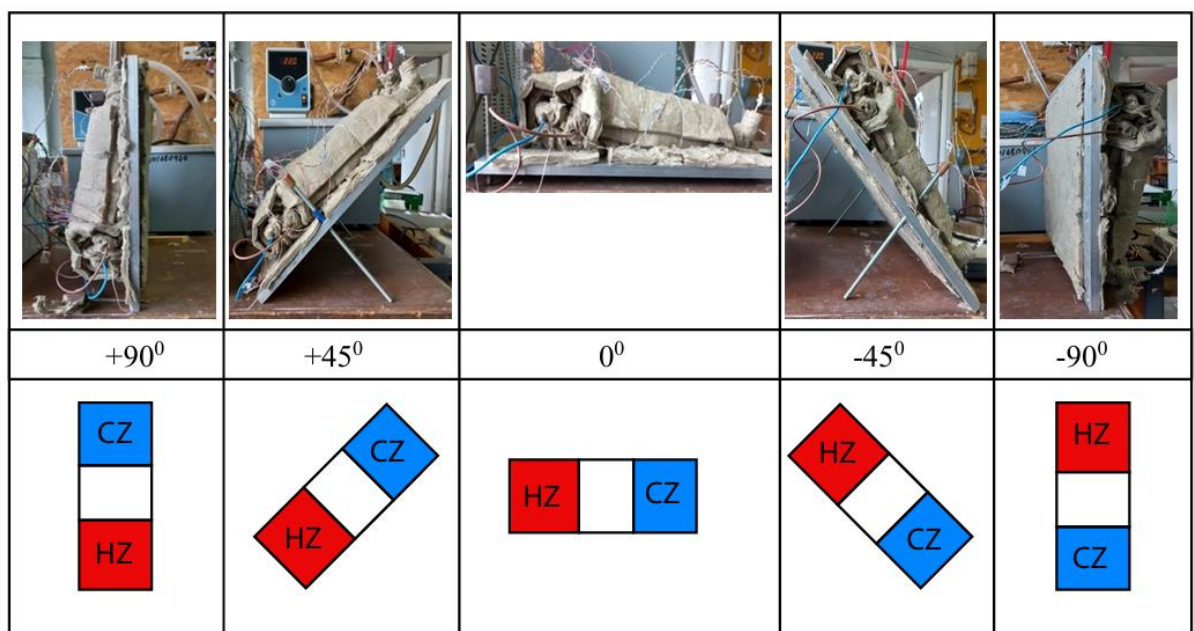


Figure 2.3 – PHP positions at different inclinations

The ohmic heater was powered by a DC power supply, and the electric power was controlled using a digital wattmeter. The cooler was connected to a thermostat, ensuring a constant temperature and flow rate of the cooling water, which was set to 22°C .

For temperature measurements along the PHP, ten T-type thermocouples were installed on the outer surface of the heat pipe (figure 2.4). Three thermocouples were placed in the heating zone, five in the condensing zone, and the remaining two thermocouples were positioned either in the heating zone (for a heating zone length of 50 mm) or in the adiabatic zone (for other heating zone lengths). The temperature data from

all thermocouples were collected using a multichannel data acquisition module, which was connected to a personal computer (PC) through an interface converter. A dedicated software installed on the PC enabled real-time monitoring of the thermocouple measurements and facilitated the storage of the data for subsequent analysis and processing.

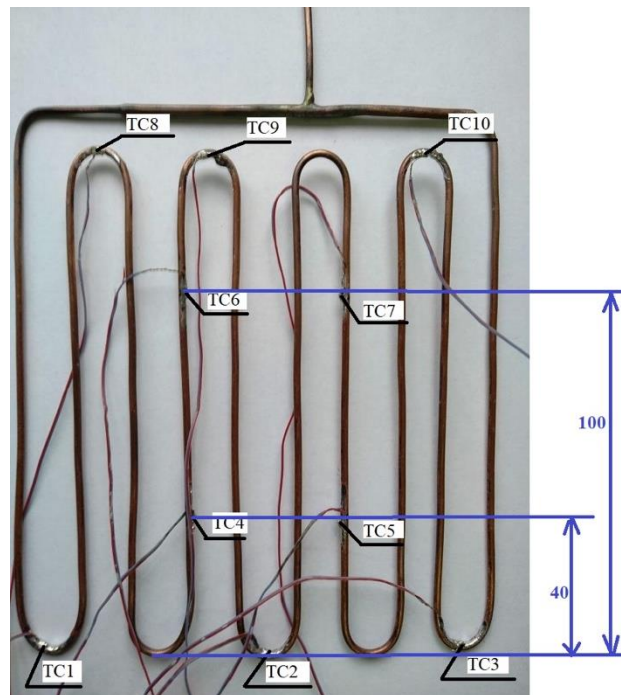


Figure 2.4 – Thermocouples placement

2.3 Experimental procedure

The experimental plan involved a systematic approach to evaluate the performance of the PHP under different conditions. Initially, the PHP was filled with water at a filling ratio of 50% to establish a consistent starting point for the experiments. Subsequently, the PHP was positioned vertically with bottom heating ($+90^\circ$), representing a challenging orientation that will test its capabilities. To assess the PHP's response to varying heat input levels over a different heat zone length, a series of experiments were conducted. The heat input began at a minimal value of 5 W, with an increment of 5 W steps until the onset of the pulsating mode. After the pulsating mode commenced, the step size was

increased to 10 W. The heat input was progressively increased until either local or full dry out in the heating zone was observed, as indicated by a significant rise in temperature on the thermocouples placed in that zone. After onset of the crisis the load was removed from the heater and the readings of the thermocouples and cooling water temperatures are stopped. The same experiment was then performed with different heating zone length of 10 mm, 30 mm, and 50 mm. By evaluating the PHP's behavior under different heat input levels, its thermal performance characteristics can be effectively analyzed. To comprehensively understand the PHP's orientation sensitivity, the previous steps were repeated for all inclination angles listed in table (2.1), including -90° , -45° , 0° , $+45^\circ$, and $+90^\circ$. This comprehensive assessment provided valuable insights into how the PHP performs under varying orientation conditions, enabling a thorough understanding of its orientation-dependent behavior through operational stability of PHP. Furthermore, the PHP then refilled with other pure liquids, namely methanol and pentane, at a filling ratio of 50%. The previous experimental steps were repeated for each of these liquids to investigate their respective impacts on PHP performance. This comparative analysis offered valuable insights into the influence of different heat carriers on the PHP's thermal behavior.

2.4 Methodology of data processing

This section focuses on the methodology for processing experimental data to define several critical parameters in pulsating heat pipe (PHP) operation. These parameters include the average start-up temperature (t_{start}), the start-up density of heat flux (q_{start}), the density of heat flux at the onset of the pulsation mode (q_{puls}), the average temperature of the heating zone ($\overline{t_h}$) and cooling zone $\overline{t_c}$, the PHP temperature difference (Δt), the PHP thermal resistance (R), the maximum transferred heat flux (Q_{max}), and the thermal resistance ratio (R/R_{vb}). In this context, R refers to the PHP thermal resistance in all spatial orientations except for the vertical bottom heating mode, while R_{vb} denotes the thermal resistance specifically in the vertical bottom heating mode. The precise

determination of these parameters is essential for understanding the thermal performance and efficiency of PHPs across different operational orientations.

Average start-up temperature was defined as

$$\overline{t_{start}} = \frac{\sum_{i=1}^k t_i}{k}, \quad (2.1)$$

where $\overline{t_{start}}$ – average start up temperature, °C;

k – quantity of thermocouples placed in the heating zone;

t_i – measurement of each thermocouple placed in the heating zone at start-up moment, °C.

Startup moment is defined by a graph of dependence between thermocouples measurements and time (see figure 2.5). Measurements of thermocouples placed in the heating zone corresponding to this moment of time was found in the experimental data and put into the equation (2.1) to define average startup temperature.

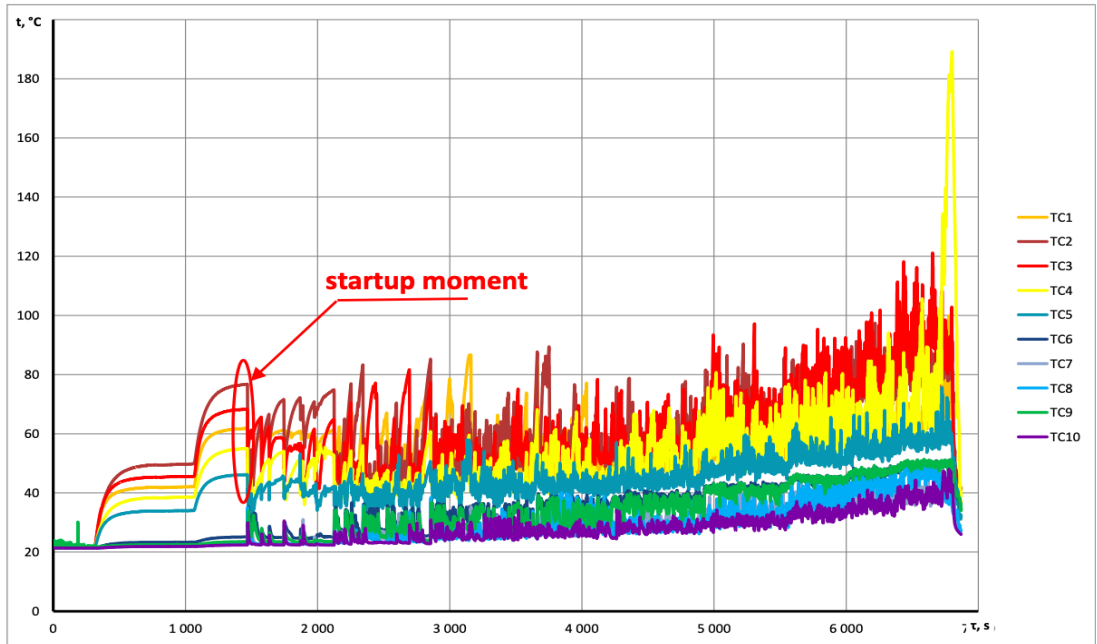


Figure 2.3 – Thermocouples measurements vs time

Transferred start up heat flux density (q_{start}) corresponding to the start-up moment i.e. in thermosyphone mode of operation is calculated using equation (2.2) as below

$$q_{start} = \frac{Q_{start}^{transf}}{F_h}, \quad (2.2)$$

where Q_{start}^{transf} – transferred heat flux corresponding to the start-up moment, W;

F_h – heat transfer area in the heating zone, m².

This transferred heat flux is calculated by the equation of thermal balance as below:

$$Q_{transf} = G \cdot C_p \Delta t_{cool}, \quad (2.3)$$

where G – mass flow rate of the cooling water, kg/s;

C_p – isobaric heat capacity of the cooling water, J/(kg·K);

Δt_{cool} – temperature difference of cooling water, °C.

Mass flow (G) was calculated by the equation obtained as a result of calibration of flowmeter:

$$G = 0.000131 \cdot x^{0.8664}, \quad (2.4)$$

where x – the number of divisions on the scale of flowmeter measured during experiment.

The isobaric heat capacity of the cooling water was obtained using reference data, based on the average temperature of the cooling water which is calculated as:

$$\overline{t_{cool}} = t_{therm} + \frac{\Delta t_{cool}}{2}, \quad (2.5)$$

where t_{therm} – thermostat temperature, °C.

Temperature difference of cooling water was measured during the experiment. Value of this difference which is used in equation (2.3) is defined as an average value during steady state mode.

Heat transfer area in the heating zone was calculated as:

$$F_h = \pi \cdot d_{in} \cdot n \cdot (2 \cdot (L_h - r_b - d_{out}) + \pi(r_b + d_{out}/2)), \quad (2.6)$$

where d_{in} , d_{out} – inner and outer diameter of PHP capillary tube respectively, m (for current PHP, $d_{in} = 0.0011$ m, $d_{out} = 0.0021$ m);

n – number of turns (for current study, $n=5$);

L_h – length of the heating zone, m;

r_b – bending radius, m (for current study $r_b = 0.006$ m).

Density of heat flux which corresponds to beginning of pulsation mode of PHP operation q_{pulse} was defined in the same way as q_{start} but Q_{transf} was taken corresponding to transition from thermosyphone to pulsation mode of PHP operation and was calculated the same way as equation (2.2).

Average temperature of the heating zone was ($\overline{t_h}$) defined as:

$$\overline{t_h} = \frac{\sum_{i=1}^k t_i}{k}, \quad (2.7)$$

where $\overline{t_i}$ – average measurement of each thermocouple placed in the heating zone during steady state mode, °C

Similarly, average temperature in cooling zone ($\overline{t_c}$) was defined as:

$$\overline{t_c} = \frac{\sum_{i=1}^k t_i}{k}, \quad (2.8)$$

where $\overline{t_i}$ - average measurement of each thermocouple placed in the cooling zone during steady state mode, °C

Average measurement of each thermocouple was defined by equation:

$$\overline{t_i} = \frac{\sum_{j=1}^m t_j}{m}, \quad (2.9)$$

where $\overline{t_j}$ – instantaneous value of thermocouple measurement during steady state mode, °C;

m – quantity of instantaneous thermocouple measurements during steady state mode.

PHP temperature difference is defined as:

$$\Delta t = \overline{t_h} - \overline{t_c}, \quad (2.10)$$

where $\overline{t_h}$ – average temperature of heating zone, °C;

$\overline{t_c}$ – average temperature of condensation zone, °C.

Finally, the PHP thermal resistance (R) was defined by equation (2.11)

$$R = \frac{\Delta t}{Q_{transf}}. \quad (2.11)$$

2.5 Assessment of measurement errors

The estimation of errors in the experiments was conducted using the method described in [116] with the use of Engineering Equation Solver (EES). which utilizes statistical and mathematical techniques to perform uncertainty calculations [117]. Three categories of errors are typically distinguished: random, gross, and systematic or instrumental errors. The reason for random errors in the calculations is that instantaneous values are utilized rather than the true values of the measured or averaged values. In this

work, averaged values of surface temperature of PHP wall and the temperature of cooling water are observed. In order to reduce the random errors multiple readings are recorded and then average values are calculated. Table 2.3 shows the instrumental errors of the measurement apparatus.

Table 2. 3– Measurement apparatus instrumental errors

Measurement	Range	Apparatus	Instrumental error
Temperature	0-200 ⁰ C	OMEGA T-type thermocouple	$\Delta t = 0.1^{\circ}\text{C}$
Cooling water mass flow rate, G	0.005-0.006 kg/s	Rotameter	*K _G = 2.5%
Temperature difference of cooling water, (Δt_{cool})	-	OMEGA T-type thermocouple	$\Delta(\Delta t_{cool}) = 0.05^{\circ}\text{C}$
Diameter, radius	-	Digital caliper	$\Delta d = \Delta r = 0.01\text{mm}$
Length	0-155mm	Ruler	$\Delta l = 0.5\text{ mm}$

*Instrumental error = $\Delta G = \frac{K_G \cdot G_{max}}{100} = 0.0001775$, where, $G_{max} = 0.0071$ kg/s (maximum mass flow rate which can be measured by rotameter).

In order to calculate relative errors involved in the calculation absolute uncertainties in the instruments measuring temperatures are initially evaluated. Absolute uncertainties are calculated by evaluating standard deviation of the set of data (equation 2.12) and then mean of standard deviation (equation 2.13) is calculated which is to be used as absolute uncertainty while calculating relative error [116].

$$\sigma_x = \sqrt{\frac{1}{N-1} \sum (x_i - \bar{x})^2}, \quad (2.12)$$

where σ_x – standard deviation;

x_i – set of measurements;

\bar{x} – average of the set of measurements.

Standard deviation was calculated as:

$$\sigma_{\bar{x}} = \sigma_x / \sqrt{N}, \quad (2.13)$$

where $\sigma_{\bar{x}}$ – standard deviation of the mean;

N – number of measurements.

For all other instruments like digital caliper and ruler, instrumental errors itself is used as an absolute uncertainty. The expression for determining the uncertainty in the single sample measurement is given by Kline and McClintock [118] and EES uses the same mathematics (equation 2.14) to determine it.

$$\delta_R = \left[\left(\frac{\partial R}{\partial x_1} \delta_1 \right)^2 + \left(\frac{\partial R}{\partial x_2} \delta_2 \right)^2 + \dots + \left(\frac{\partial R}{\partial x_n} \delta_n \right)^2 \right]^{1/2}, \quad (2.14)$$

where (δ_R) - the uncertainty of result (R).

All the equations described in methodology of data processing are used as input to the EES and its corresponding values of absolute uncertainty are also inputted. The uncertainty in the calculated parameters is evaluated based on these absolute uncertainties and instrumental errors. The maximum and minimum relative error calculating the main defining parameters such as total heat transferred (equation 2.3) and thermal resistance (equation 2.11) is observed to be less than 3.2% to 3.6%. The minimum and maximum relative errors for all other calculated parameters are presented in table 2.4.

Table 2.4 - Relative errors in determining key parameters during data processing

Sr. No.	Parameter	Minimum relative error	Maximum relative error
1	Mass flow rate (G, kg/s)	3.18%	3.25%
2	Average temperature of heating zone ($\overline{t_h}$, °C)	0.06%	0.49%
3	Average temperature of condensation zone ($\overline{t_c}$, °C)	0.07%	0.27%
4	Temperature difference of cooling water (Δt_{cool} , °C)	0.14%	0.80%
5	PHP temperature difference (Δt , °C)	0.09%	0.28%
6	Heat transfer area in the heating zone (F_h , m ²)	3.96%	3.96%
7	Transferred heat flux (Q_{transf} , W)	3.26%	3.27%
8	Transferred heat flux density (q_{transf} , W/m ²)	5.13%	5.13%
9	Thermal Resistance (R, K/W)	3.27%	3.57%

2.6 Conclusions

1. Experimental samples of copper Pulsating Heat Pipes (PHPs) with 5 turns, matching the overall height of modern CPU coolers, have been developed. Thermocouples are mounted at appropriate levels, and provisions have been made to vary the length of the heating zone. This design allows for the experimental investigation of the effect of heating zone length on start-up and transient characteristics of PHP.

2. An experimental setup has been developed to facilitate research at various orientations, including vertical bottom heating (90°), horizontal (0°), top heating (-90°), and inclined positions ($+45^\circ$ and -45°). The setup is equipped with the facilities to vary the heat input to the heating zone, maintain the cooling water at a constant temperature in the condenser and record observations through data acquisition system. This installation will make it possible to examine how different heat carriers, heat flux density, and heating zone length affect PHP performance.

3. The experimental methodology for the study and the data processing procedures have been clearly defined. Uncertainties in the measuring instruments and their propagation during data processing have been evaluated, with the relative error not exceeding 6% in any case.

Chapter 3 – Operational Modes of Pulsating Heat Pipe

3.1 Operational modes

Pulsating Heat Pipes (PHPs) are advanced thermal management systems that rely on the oscillatory motion of a working fluid to transfer heat efficiently between an evaporator and a condenser. Their operation is governed by a combination of: internal processes (phase change, phase interaction, acting of: pressure difference between HZ and CZ, capillary forces, friction forces) influence of external factors (heat input, inclination angle) and design parameters of PHPs. Understanding the operational behavior of PHPs under different heat inputs and inclination angles is crucial for optimizing their design and performance. Figure 3.1 demonstrates the transition of a PHP through various operational modes for PHP lengths ratio of 0.48 and water as a heat carrier at vertical bottom heating mode, highlighting the thermal and fluidic behavior at different heat input levels. The PHP length ratios for heat zone lengths of 10 mm, 30 mm, and 50 mm are 0.069, 0.242, and 0.481 respectively, and is defined as follows in equation 3.1:

$$PHP \text{ length ratio } (LR) = \frac{L_{HZ}}{(L_{AZ}+L_{CZ})}, \quad (3.1)$$

where L_{HZ} — length of heating zone, m;

L_{AZ} — length of adiabatic zone, m;

L_{CZ} — length of condensation zone, m.

A higher length ratio indicates that a larger portion of the pipe is exposed to the heating zone. Each mode—heat conductivity, thermosyphone, transition from thermosyphone to pulsating, pulsating, and dry-out—is discussed in detail below.

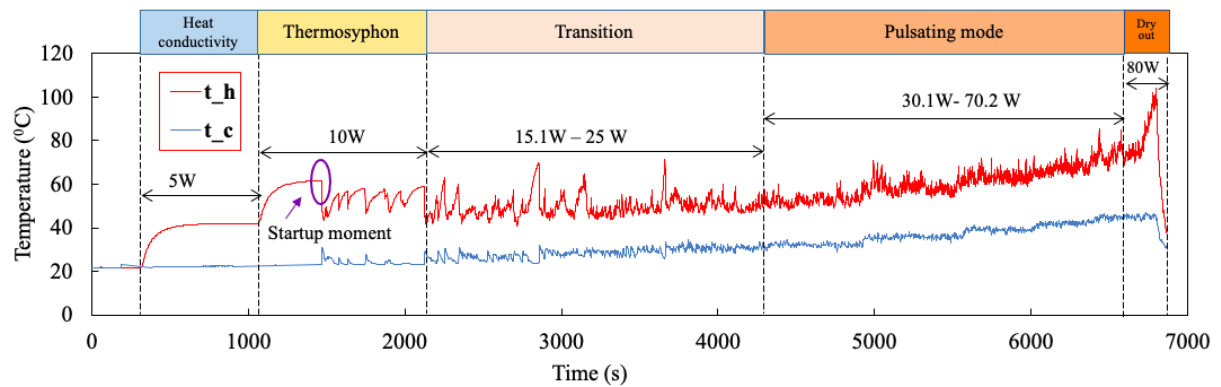


Figure 3.1– Operational modes of pulsating heat pipe (t_h , t_c : average temperatures of heating and condensing zone respectively)

3.1.1 Heat conductivity mode

In the initial phase, the system operates predominantly in the heat conductivity mode, as seen in the first segment of the graph (fig. 3.1). Here, the heat input to the system is minimal, around 5 W, which is insufficient to induce significant phase change in the working fluid. The average temperature at the evaporator (t_h) and condenser (t_c) exhibits a large difference. This large temperature gradient indicates that heat transfer is governed primarily by thermal conduction through the PHP casing. The fluid does not exhibit any noticeable motion, as the thermal energy supplied is not enough to initiate boiling process in HZ which is a driving force for pulsating heat carrier motion. However, occasional unstable single pulsations can be observed, but they did not last long. This mode reflects a thermally stable state where thermal conduction is the dominant mechanism, and no major thermal instabilities or fluid dynamics are observed.

3.1.2 Thermosyphone mode

Upon increasing the heat input to 10 W, the heating zone temperature continues to rise until both the PHP wall temperature and the boundary layer temperature reach overheating relative to the saturation temperature enough for activation of the first nucleation sites. Thus, boiling begins in HZ. When inertial forces, which take place during appearance and growing of vapor bubbles, become enough to overcome

gravitational, capillary and friction forces they initiate beginning of heat carrier movement inside PHP. This is the start-up moment of PHP. It can be detected on temperature-time dependence graph by the first drastically decreasing of HZ temperature with simultaneously drastically increasing of CZ temperature (fig. 3.1). This increasing is connected with arrival of the first portion of hot heat carrier to CZ from HZ. At the same time a portion of cold heat carrier comes to HZ from CZ causing the decreasing of HZ temperature because of which active nucleation sites stop their action. Then HZ temperature rises again until reaching overheating enough for beginning of boiling and the whole process repeats. That's why this operational mode is characterized with temperature fluctuations which have large amplitude and duration and low frequency. In this mode, each PHP channel acts separately from other channels and its acting is like that one of closed two-phase thermosyphone, hence this mode is called thermosyphone mode. It will be shown below that thermosyphone mode is not always present during PHP operation. Its presence depends on thermophysical properties of heat carrier.

3.1.3 Transition from thermosyphone to pulsating mode

As the heat input increases to the range of 15–25 W (fig. 3.1), the system begins transitioning from thermosyphone behavior to the pulsating mode. This transition is marked by the emergence of small temperature fluctuations in all PHP zones. At this stage, number of active nucleation sites increases because of increasing in input heat flux. This initiates appearance of small temperature pulsations during “rest periods” in between large temperature fluctuation typical for thermosyphone mode. The last ones remain present in PHP temperature profile and the character of heat carrier movement also remains the same as for thermosyphone mode. However, as the heat input continues to rise, the intensity of vapor generation increases, pushing the system closer to a pulsating regime. This transitional phase highlights the system's response to increasing thermal energy, where heat and mass transfer become more dynamic due to intensification of boiling process and oscillatory flow.

3.1.4 Pulsating mode

In this phase, the system fully enters the pulsating mode, which represents the optimal operating condition of the pulsating heat pipe. With heat inputs in the range of 30–70 W (fig. 3.1), temperature pulsations in all PHP zones become stable, their frequency increases and amplitude decreases. This can be explained by further increasing of active nucleation sites number with rising of input heat flux. The number of active nucleation sites becomes enough to create driving force, which appears on each site during grooving and departure of vapor bubble, sufficient for initiating and maintaining of stable pulsating heat carrier movement between heating and condensation zones. This pulsating motion enhances heat transfer efficiency significantly, as the combined effects of heat transfer during phase change and convective transport dominate the heat transfer mechanism. This mode is characterized by high thermal performance and efficient energy transfer, showcasing the strength of pulsating heat pipes in managing moderate to high heat loads.

3.1.5 Dry-out mode

The final phase, observed at heat inputs of 80 W and higher (fig. 3.1), corresponds to the dry-out mode. In this region, the evaporator temperature (t_h) rises sharply, exceeding 120°C, while the condenser temperature (t_c) remains relatively low. This sharp increase in t_h signals a failure in the fluid dynamics and heat transfer mechanisms. Excessive thermal energy causes the complete vaporization of the working fluid within the evaporator. This can be caused by two reasons: appearance of imbalance between vapor generation and condensation in heating and condensation zones respectively or by transferring from bubble to film boiling mode in heating zone (boiling heat transfer crisis of the first kind). Without liquid to oscillate and carry heat to the condenser, the PHP loses its ability to effectively transfer thermal energy. This mode is characterized by a dramatic reduction in heat transfer efficiency and a significant rise in thermal resistance. The dry-out condition represents a critical failure mode of the PHP,

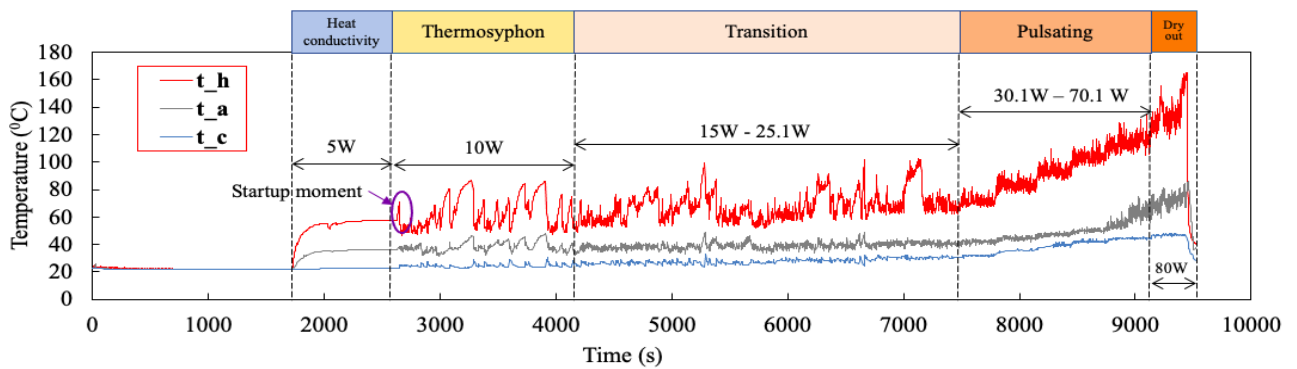
emphasizing the importance of maintaining a balance between heat input and the system's capacity to sustain oscillatory fluid motion.

It should be noted that values of input heat flux corresponding to borders of operating modes were stated above only as an example. In fact, they depend on physical, geometrical, and operating factors which will be discussed below.

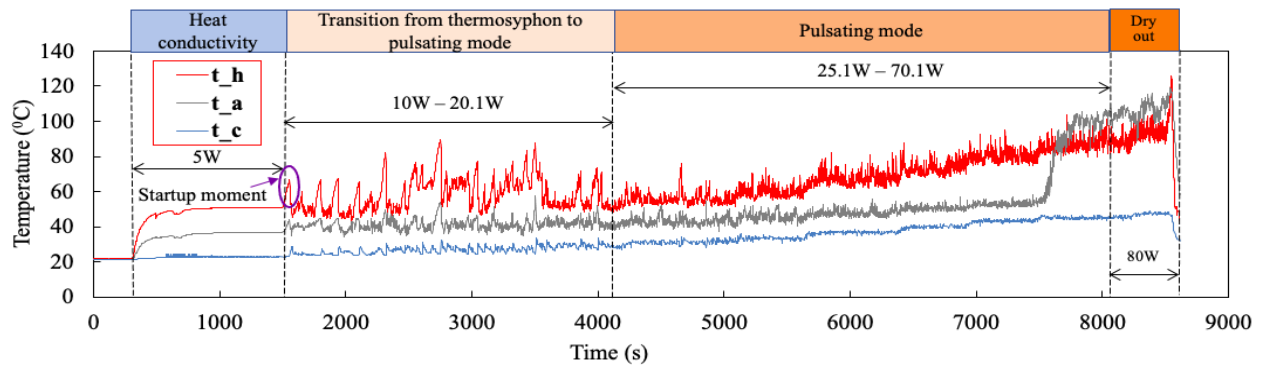
3.2 Effect of heat carriers, PHP length ratio, and inclination angles on PHP behaviour

The operational characteristics of pulsating heat pipes (PHPs) are highly sensitive to a range of design and operational parameters, including the type of heat carrier, PHP lengths ratio, and the inclination angle. These parameters influence the system's ability to transition between operational modes, the amplitude and stability of pulsations, and the thermal performance of the PHP. By analyzing temperature-time dependence graphs for each combination of heat carrier, PHP lengths ratio, and inclination angle, a comprehensive understanding of their effects on the PHP's behavior can be developed.

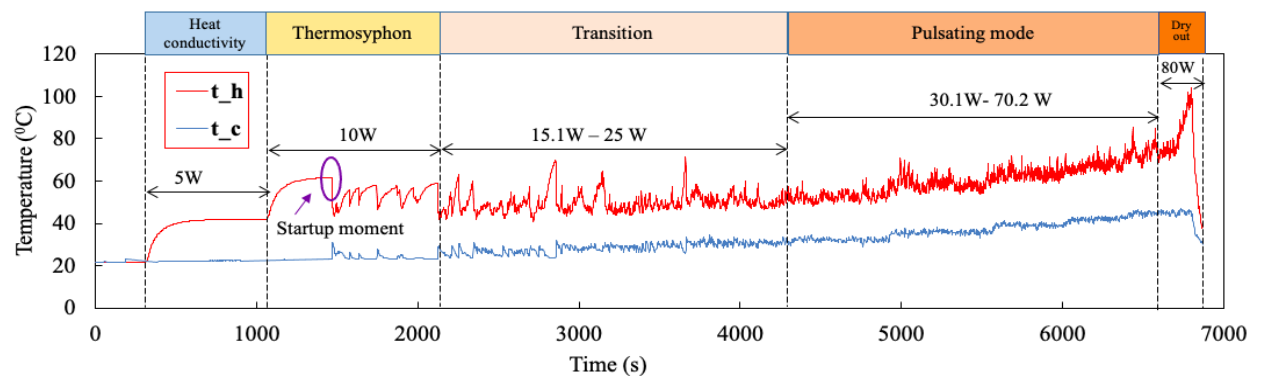
Case 1: heat carrier – water; 90° orientation of PHP (vertical bottom heating mode) (fig. 3.2)



(a)



(b)



(c)

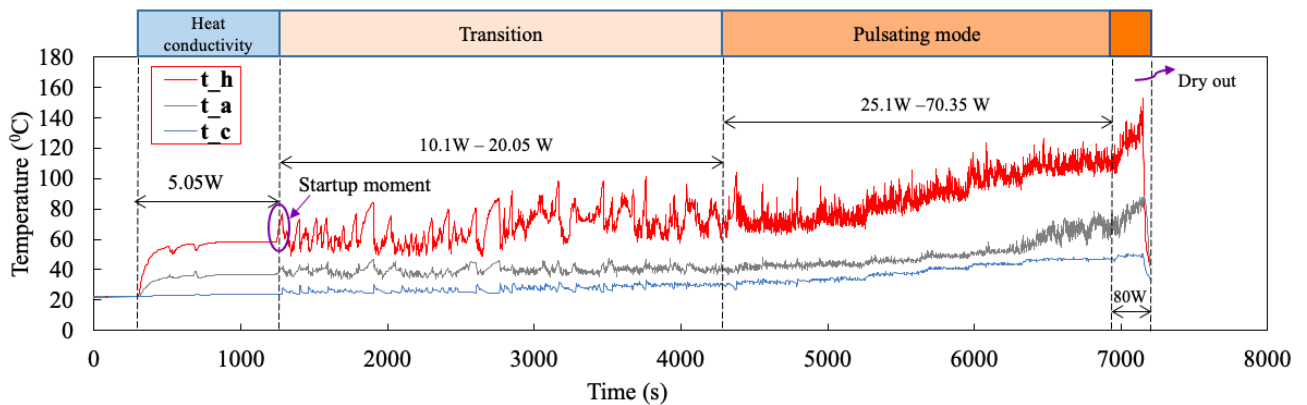
Figure 3.2– Variation of temperature with time for water at 90° inclination for PHP length ratios (a) 0.069 (b) 0.242 (c) 0.481 (t_h , t_a , t_c : average temperatures of heating, adiabatic and condensing zone respectively)

As it can be seen from fig. 3.2, PHP started at input power of 10 W for all length ratios. It must be noted that different start-up densities of heat flux correspond to this input power because of difference in heat transfer area for different length ratios. At the same time, the PHP with length ratio of 0.069 (fig. 3.2a) and 0.242 (fig. 3.2b) took less time to start compared to the PHP with a length ratio of 0.481 (fig. 3.2c). This can be attributed to two factors. First, the PHP with a length ratio of 0.481 exhibits the lowest heat flux density among all the length ratios. Second, it has the largest heat zone (HZ) volume, resulting in a greater amount of liquid in the HZ, which requires more time to heat up to the saturation temperature and initiate the boiling process.

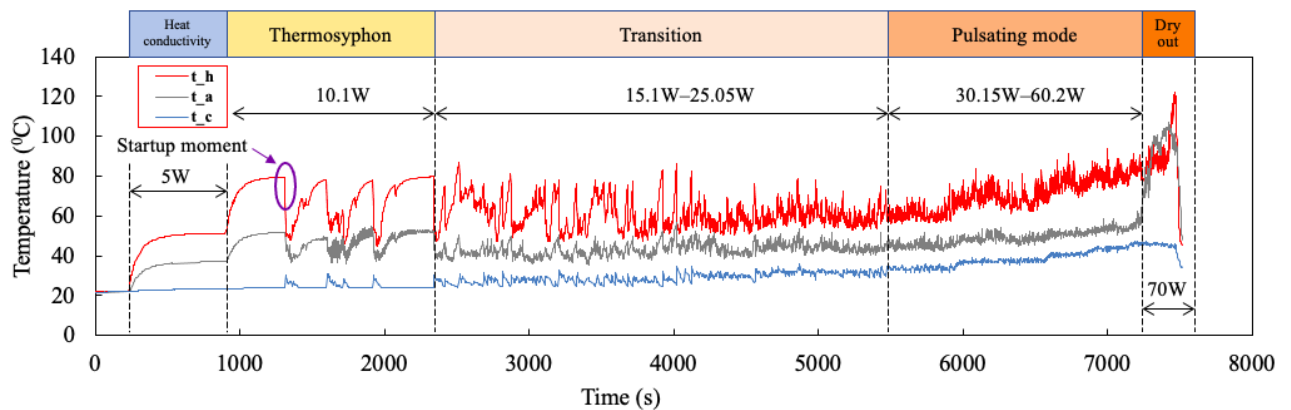
The primary distinction between the tested PHP length ratios was the absence of a thermosyphon mode at a length ratio of 0.242. At this ratio, the PHP began operating in a transient mode between thermosyphon and pulsating modes. In contrast, thermosyphon mode was the initial operational mode following startup for length ratios of 0.069 and 0.481. The length ratio of the PHP did not affect the pulsating mode boundaries, which consistently initiated at an input power of 25–30 W and terminated with a local crisis at 80 W input power across all tested length ratios.

The lowest heating zone temperature was observed at a length ratio of 0.481. Given that the cooling zone temperature remained nearly constant for all length ratios, this indicates a reduced temperature difference and consequently, lower thermal resistance for the PHP with a length ratio of 0.481. This is evidence of more efficient heat transfer compared to the other tested length ratios.

Case 2: heat carrier – water; 45° orientation of PHP (fig. 3.3).



(a)



(b)

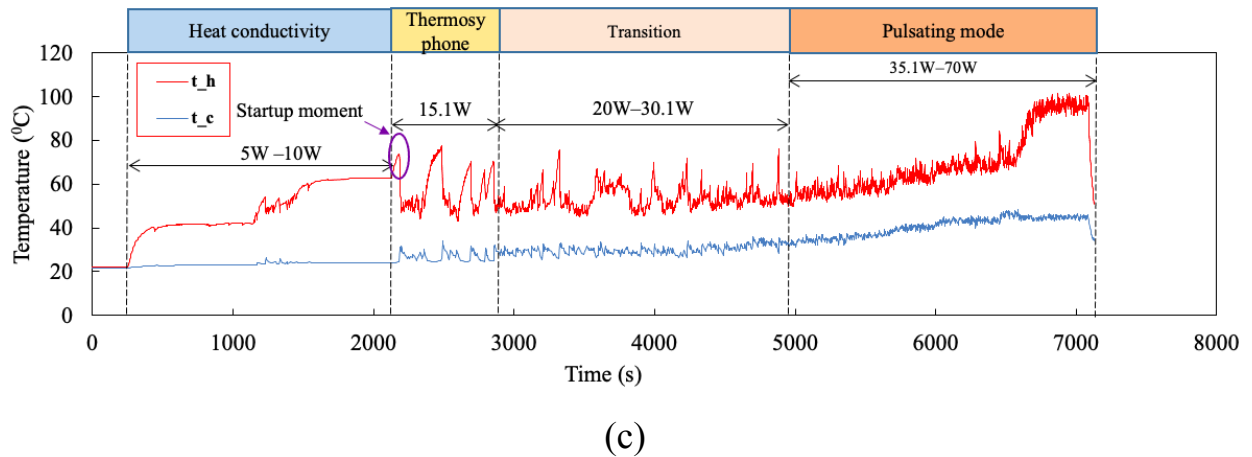


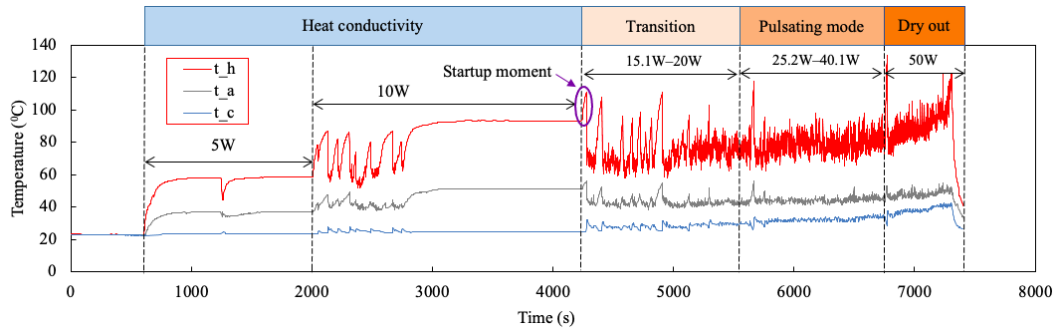
Figure 3.3 – Variation of temperature with time for water at 45° inclination for PHP length ratios (a) 0.069 (b) 0.242 (c) 0.481 (t_h , t_a , t_c : average temperatures of heating, adiabatic and condensing zone respectively)

The observations reveal that PHPs with different length ratios exhibit distinct startup and operational behaviors due to variations in heat flux density and heat zone liquid volume. The PHPs with length ratios of 0.069 (fig. 3.3a) and 0.242 (fig. 3.3b) started at lower input heat flux compared to the PHP with a length ratio of 0.481 (fig.3.3c). Heat conductivity mode was the first operational mode for PHP with all length ratios. A notable characteristic of the PHP with a length ratio of 0.069 is its absence of thermosyphone mode, as it started to work in transition mode instantly. This is attributed to the high heat flux density associated with the smaller heat zone volume of the shorter PHP. In contrast, the PHP with a length ratio of 0.242 and 0.481 operated in thermosyphone mode initially, with a gradual temperature rise and unstable fluctuations. But for PHP with LR of 0.242 beginning of thermosyphone mode was at 10 W of input heat flux and for PHP with LR of 0.481 – at 15 W. Increasing of LR leads to shifting of borders of all operation modes toward higher values of input heat flux. For the PHP with a length ratio of 0.481, local thermal crisis was not observed. Instead, the experiment was terminated due to elevated temperatures in one of the thermocouples inside the heating zone. This highlights the ability of higher-length-ratio PHPs to handle larger liquid volumes, resulting in delayed dry-out and enhanced thermal stability under high heat

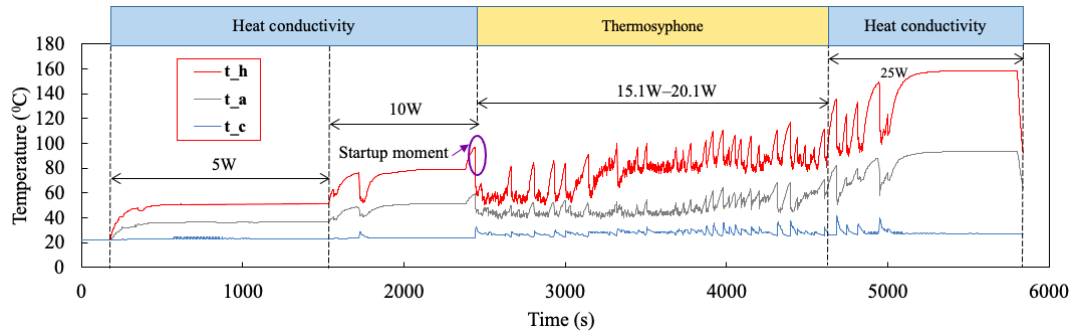
inputs. The PHP with a length ratio of 0.481 exhibited the most stable pulsations among all configurations, reflecting its capacity to maintain a balanced two-phase flow regime. This stability is attributed to its larger heat zone volume, which distributes the heat input more effectively and delays the onset of dry-out.

At inclination angle 90° (fig. 3.2) PHP was almost insensitive to LR changing in terms of start-up heat flux and borders of operational modes. In contrast, at inclination angle 45° (fig. 3.3) increasing of LR leads to shifting of both start-up heat flux and borders of all operation modes toward higher values of input heat flux. It must be noted that pulsations stability was higher at 90° , with lower heating zone temperatures for higher length ratios (0.481) (fig. 3.2c).

Case 3: heat carrier – water; 0° orientation of PHP (horizontal operation) (fig. 3.4).



(a)



(b)

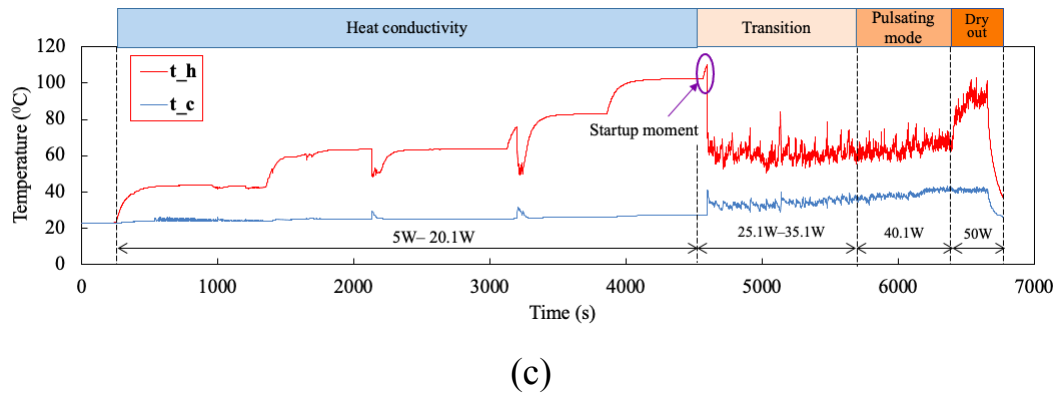


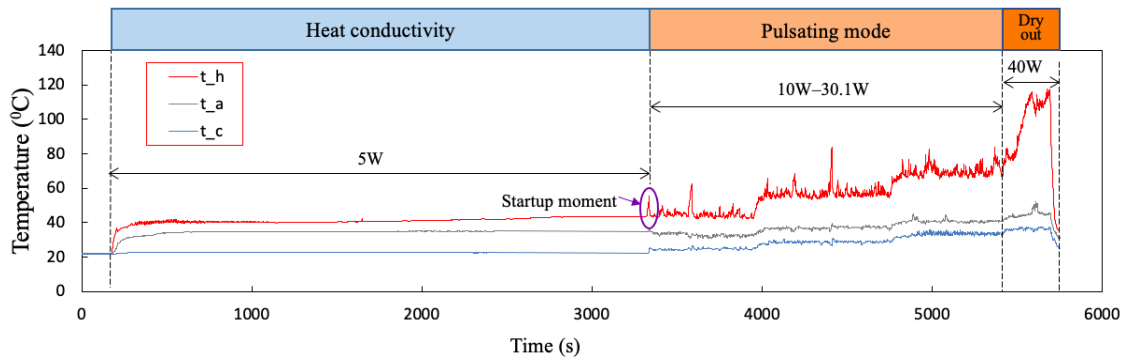
Figure 3.4 – Variation of temperature with time for water at 0° inclination for PHP length ratios (a) 0.069 (b) 0.242 (c) 0.481 (t_h , t_a , t_c : average temperatures of heating, adiabatic and condensing zone respectively)

For all PHP length ratios in the horizontal orientation the startup temperature was higher, requiring a higher heat input to initiate the system (fig. 3.4). When comparing the PHP with a length ratio of 0.069 (Fig. 3.4a) to the PHP with a length ratio of 0.242 (Fig. 3.4b) it can be noted that both start at heat input flux of 15 W. But significant differences arise when considering further operation. The 0.242 configuration enters a distinct thermosyphon mode which terminates at input heat flux of 25 W and PHP returns to heat conductivity mode. This is because all HZ is occupied with long vapor plugs at this heat flux and capillary force is insufficient to overcome pressure force inside these plugs and return liquid to HZ. However, PHP with length ratio 0.069 transitions more directly into pulsating mode after a brief transitional phase between 15 W and 20 W. In pulsating mode, the 0.069 PHP exhibits more unstable oscillations than 0.481 PHP and ultimately experiences dry-out at heat input of 50 W. However, the start-up moment for the 0.481 PHP was observed at 25 W, which is higher than for the 0.069 and 0.242 configurations. In the same way as the 0.069 PHP, which bypasses the thermosyphone mode, the 0.481 PHP transitions smoothly into pulsating mode through a broad transitional phase between 25.1 W and 35.1 W. But for the 0.481 PHP pulsating mode was observed only at 40 W heat input while for the 0.069 PHP it lasted between 25 and 40 W. Once in pulsating mode, the 0.481 PHP demonstrates the most stable behaviour, with minimal

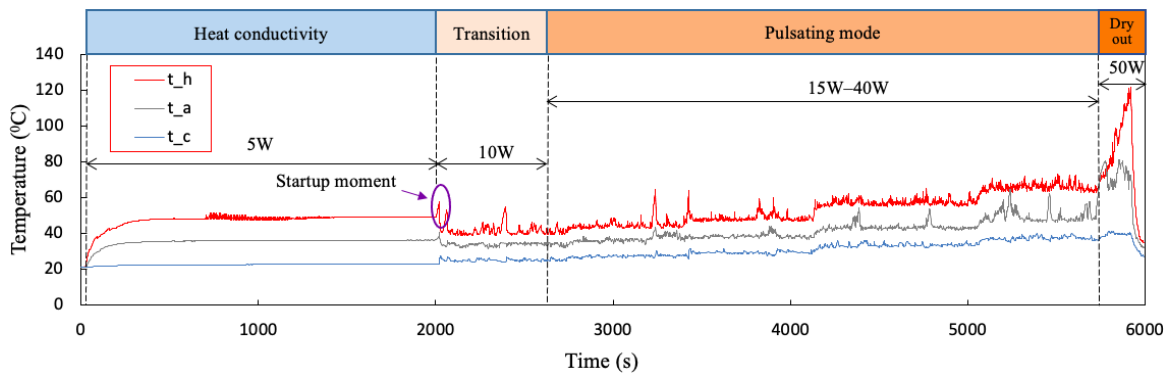
pulsations amplitude. It handles heat and mass transfer most consistently due to its larger heat zone volume, which provides sufficient liquid for stable phase change. Dry-out occurs at 50 W in the same way as for the 0.069 PHP. This comparison highlights that the 0.481 PHP offers the best stability and reliability under horizontal orientation, while the 0.069 PHP provides start-up at the least input heat flux and maintains pulsating mode of operation in the widest range of input power.

The inclination angle significantly influences the start-up behavior, operational modes, and thermal stability of the PHP. In horizontal orientation (0°), PHPs experienced the highest start-up input heat fluxes and temperatures. Moreover, there is possibility of termination of heat carrier movement and returning of PHP to heat conductivity mode in this position as it was observed for PHP with LR of 0.242. These findings confirm that 90° inclination provides the most favorable conditions for stable pulsating motion, whereas horizontal orientation poses the greatest challenges, leading to delayed activation, unstable oscillations, and increased thermal resistance.

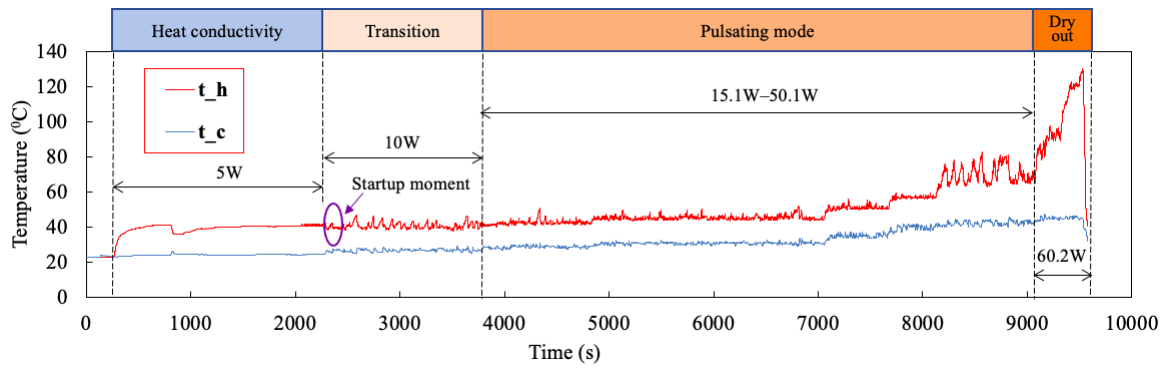
Case 4: heat carrier – methanol; 90° orientation of PHP (fig. 3.5).



(a)



(b)



(c)

Figure 3.5 –Variation of temperature with time for methanol at 90° inclination for PHP length ratios (a) 0.069 (b) 0.242 (c) 0.481 (t_h , t_a , t_c : average temperatures of heating, adiabatic and condensing zone respectively)

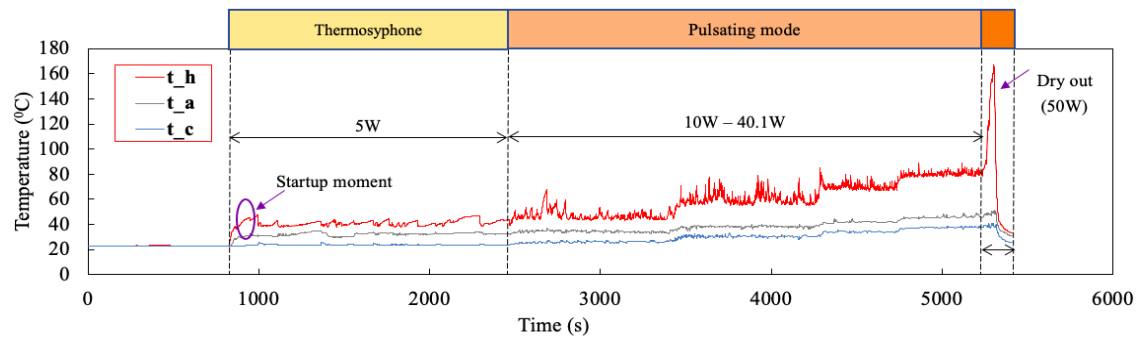
In this case PHP with all tested length ratio started at input power 10 W (fig. 3.5), but PHP with lowest length ratio 0.069 immediately begin to work in pulsating mode (fig. 3.5a) while PHP with other length ratio started from transition mode. For PHPs with length ratio 0.242 and 0.481, beginning of pulsating mode was observed at 15 W of input power (fig. 3.5b, c). Input power corresponding to dry-out phenomena increased from 40 to 60 W with increasing of length ratio from 0.069 to 0.481. Thus, length ratio doesn't affect the start-up input power but its increasing leads to appearance of transition mode between heat conductivity and pulsating and to shifting of beginning of pulsating mode and dry-out phenomena toward higher input power. This is attributed to increasing of heat flux density in HZ with decreasing of length ratio.

PHP with highest length ratio 0.481 had the most stable pulsations with the lowest amplitude and, as a consequence, the lowest average HZ temperature and the lowest temperature difference between HZ and CZ which is evidence of the most effective heat and mass transfer when compared to PHP with other length ratios.

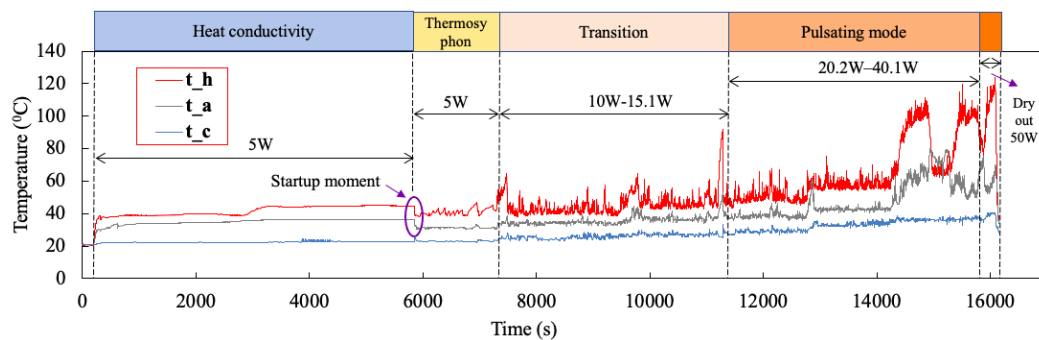
Start-up input power is similar for PHP with both heat carriers methanol and water at 90° inclination angle (fig. 3.2 and 3.5 respectively) and equals to 10 W. Unlike PHP with water, thermosyphon mode of operation wasn't observed for methanol filled PHP. Also,

PHP with methanol has lower input power corresponding to beginning of pulsating mode of operation (10-15 W for methanol and 25-30 W for water), lower amplitude of pulsations and provides lower average HZ temperature than PHP with water. This can be explained by combined action of three factors: lower heat of vaporization, lower saturation temperature and lower critical radius of nucleation sites for methanol than these of water. Lower heat of vaporization means that less energy is necessary for starting of active boiling in HZ. Lower saturation temperature provides lower average HZ temperature. Critical radius of nucleation sites for methanol is approximately 13 times lower than of water (at input power 15 W, 90° inclination angle and length ratio 0.481) which means that quantity of active nucleation sites for methanol is much higher than for water at the same heating area. This provokes more active bubble nucleation in HZ and, as a consequence, more intense heat carrier movement with pulsations of lower amplitude. Thus, methanol can be more suitable as heat carrier of PHP for electronics cooling because of low average HZ temperature and low pulsations amplitude. But from the other hand, it has lower dry-out input power than that of water.

Case 5: heat carrier – methanol; 45° orientation of PHP (fig. 3.6).



(a)



(b)

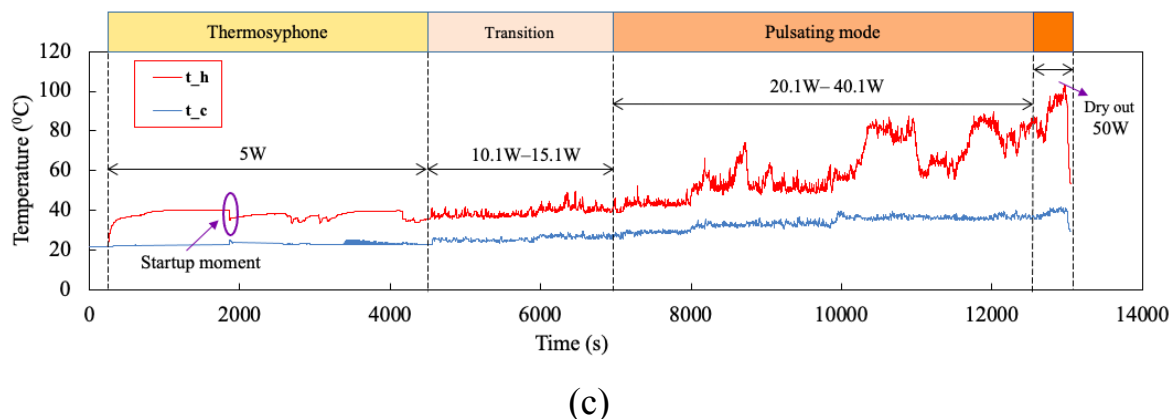


Figure 3.6– Variation of temperature with time for methanol at 45° inclination for PHP length ratios (a) 0.069 (b) 0.242 (c) 0.481 (t_h , t_a , t_c : average temperatures of heating, adiabatic and condensing zone respectively)

The PHP with a length ratio of 0.069 (fig. 3.6a) transitions quickly from thermosyphon mode to pulsating mode at 10 W, with pulsations stabilizing between 10 W and 40.1 W. It has the most stable oscillations with the smallest amplitude when compare it to methanol filled PHP with other LRs at the same inclination angle (fig. 3.6b-c). Dry-out occurs at 50 W. In contrast, the PHP with a length ratio of 0.242 (fig. 3.6b) exhibits a more gradual transition, starting with thermal conductivity and thermosyphon mode at 5 W and transitioning (10.1W-15.1 W) into pulsating mode which takes place at 20.1-40.1 W. Although it still experiences dry-out at 50 W and few localized temperature jumps.

The PHP with a length ratio of 0.481 (fig. 3.6c) operates in thermosyphon mode at low heat input (5W). As the heat input increases to 10.1W - 15.1W, the system enters a transition phase, where localized bubble nucleation and intermittent vapor-liquid slug movement begin, causing small temperature fluctuations due to partial oscillatory behavior. At 20W - 40W, the PHP operates into pulsating mode, where continuous vapor-liquid slug oscillations enhance heat and mass transfer efficiency. Pulsations are more stable compared to PHP with LR of 0.242 but less stable compared to PHP with LR of 0.069. However, at 50 W the system experiences dry-out, where excessive vapor

generation suppresses liquid return, leading to an abrupt temperature rise in the heating section.

Thus, in this case, LR doesn't influence on the value of start-up input heat load but its increasing shifts lower border of pulsating mode from 10 W at LR 0.069 to 20 W at LR 0.242 and 0.481. The same picture was observed for methanol PHP at inclination angle 90° (fig. 3.5) but in terms of values, start-up occurs at higher input heat power (10 W) at all LR and pulsating mode begins at slightly lower input heat power (15 W) at LR of 0.242 and 0.481 than that at inclination angle 45° (fig. 3.6). At inclination angle 45° , LR doesn't influence on dry-out input heat load when at 90° inclination angle it increases with increasing of LR. Also, decreasing of inclination angle from 90° to 45° leads to appearance of thermosyphone mode of operation. When comparing with water PHP at the same inclination angle (fig. 3.3) it can be said that methanol provides: lowering of start-up input heat power and borders of all operational modes, narrowing of heat power range in which transition mode takes place, lowering of pulsations amplitude in pulsations amplitude in pulsating mode but pulsations stability is better for water.

Case 6: heat carrier – methanol; 0° orientation of PHP (fig. 3.7).

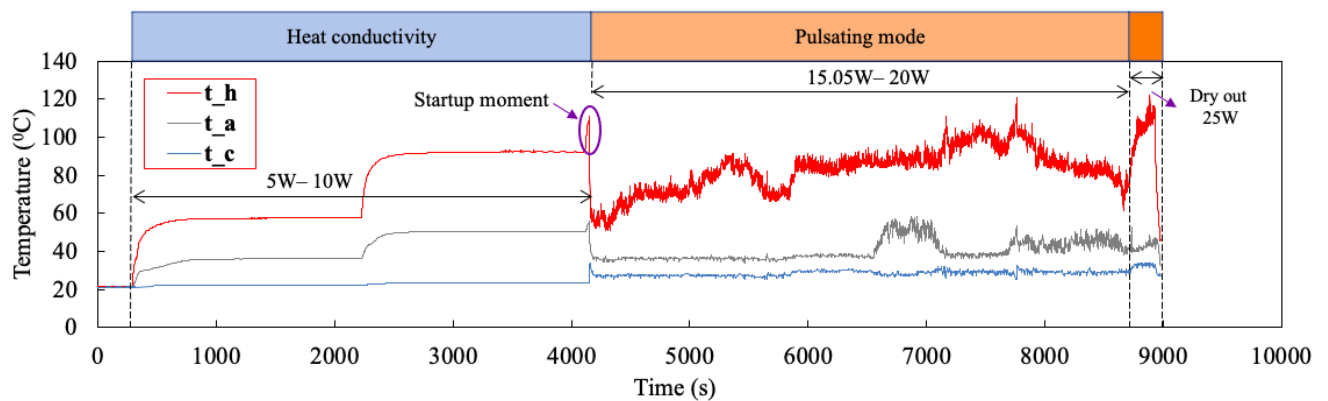
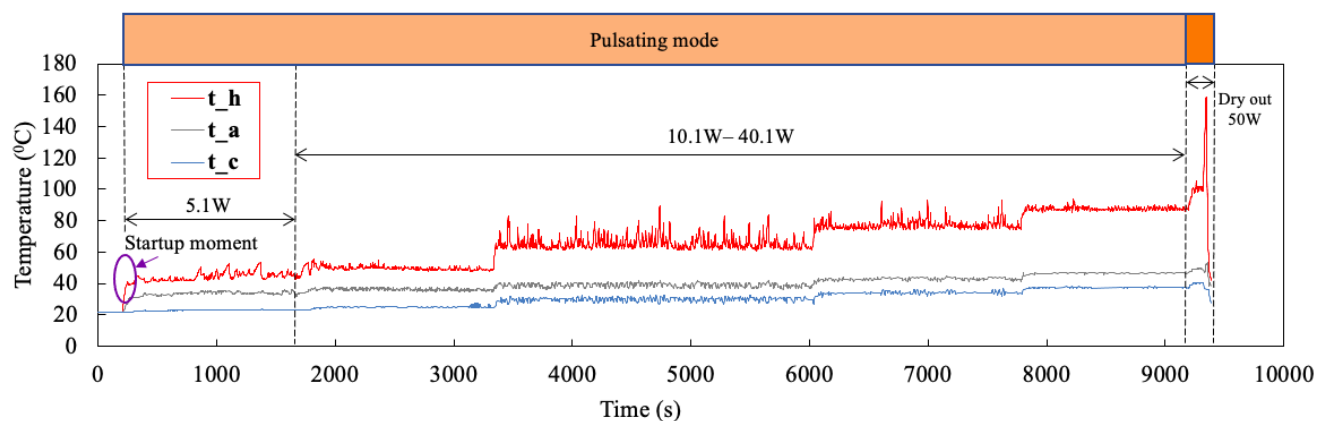


Figure 3.7– Variation of temperature with time for methanol at 0° inclination for PHP length ratio 0.069 (t_h , t_a , t_c : average temperatures of heating, adiabatic and condensing zone respectively)

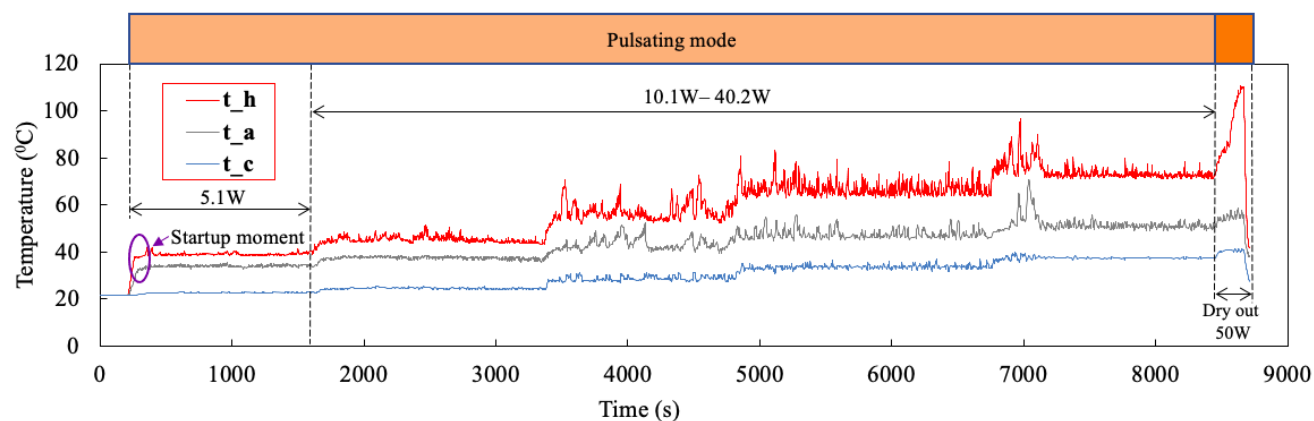
For the methanol-based pulsating heat pipe (PHP) with a length ratio of 0.069 (fig. 3.7) at a 0° inclination, the system exhibits unique behavior influenced by the horizontal orientation. Initially, the PHP operates in the heat conductivity mode from 5 W to 10 W, with a steady increase in t_h , reflecting conduction-dominated heat transfer. However, even during the heat conductivity mode, t_h remains significantly high, indicating limited heat dissipation efficiency due to full absence of heat carrier movement. The startup moment occurs at 15 W, marking the transition into pulsating mode. Pulsations are observed between 15.05 W and 20 W. The heating zone temperature t_h drastically decreases at start-up moment with simultaneously increasing of CZ temperature indicating enhancing of heat transfer. But during further operating in pulsating mode HZ temperature remains elevated and very unstable when CZ temperature remains at almost constant level which is only slightly higher than in heat conductivity mode, suggesting that the heat and mass transfer process is not highly effective in horizontal operation. Eventually, dry-out occurs at 30 W, as evidenced by a sharp rise in t_h . The elevated temperatures and earlier dry-out are attributed to the smaller heat zone volume and the challenges posed by horizontal orientation.

As it can be seen, in horizontal position, PHP has the highest value of start-up input heat flux among described above inclination angles for methanol (fig. 3.5-3.6) but it begins to work in pulsating mode directly after start-up. This can be explained by occupation of the whole HZ with vapor before the start-up moment which leads to high overheating of HZ wall. This overheating is so high that when liquid returns to HZ because of capillary force acting, it boils instantly with simultaneous activating of large amount of nucleation sites which provides pulsating movement of heat carrier. But from the other hand, pulsations and HZ temperature are unstable and the latter is also high when CZ temperature remains low which indicates the worst efficiency of heat transfer. When compare it to PHP with water at the same position and with the same LR (fig. 3.4a), both PHPs starts at the same heat input but PHP with water has transition mode between heat conductivity and pulsating modes. PHP with methanol has wors stability of pulsations and HZ temperature and worse heat transfer efficiency than PHP with water.

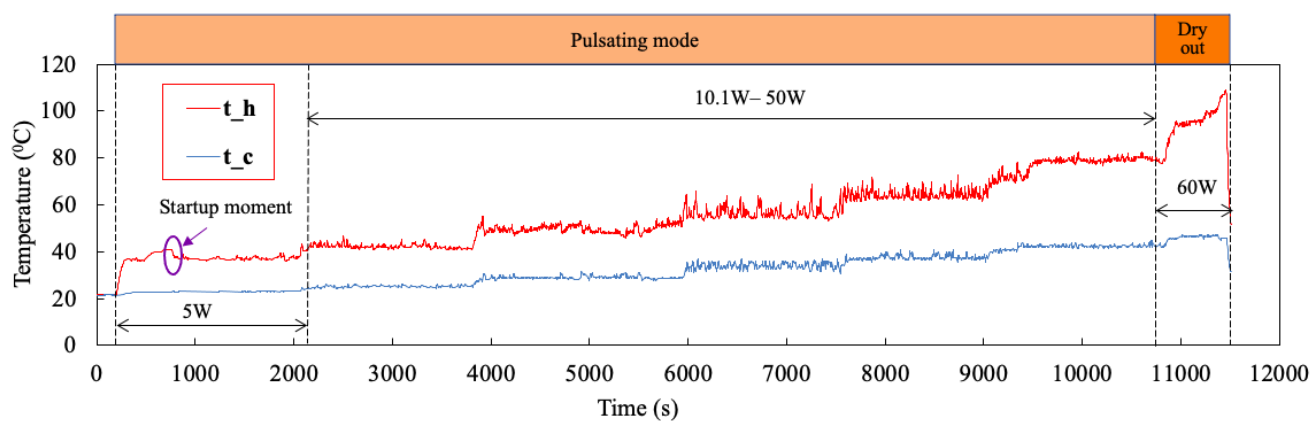
Case 7: heat carrier – pentane; 90^0 orientation of PHP (fig. 3.8).



(a)



(b)



(c)

Figure 3.8– Variation of temperature with time for pentane at 90^0 inclination for PHP length ratios (a) 0.069 (b) 0.242 (c) 0.481 (t_h , t_a , t_c : average temperatures of heating, adiabatic and condensing zone respectively)

From Fig. 3.8, it is evident that all three PHP configurations, with length ratios of 0.069 (Fig. 3.8a), 0.242 (Fig. 3.8b), and 0.481 (Fig. 3.8c), starts at 5 W input power. This behavior is attributed to pentane's lowest boiling point, lowest heat of vaporization, and smallest critical nucleation radius among the tested heat carriers. Since pentane has the lowest heat of vaporization, it requires minimal energy to initiate active boiling. Additionally, its critical nucleation site radius is approximately 34.6 times smaller than that of water and 2.6 times smaller than that of methanol (at 5 W input power, 90° inclination angle, and length ratio 0.481), resulting in a significantly higher density of active nucleation sites on the heating surface. This promotes intense bubble formation in the heating zone (HZ), enabling a rapid transition to pulsating mode.

The primary distinction among the three configurations lies in the amplitude of pulsations. The PHP with length ratio 0.481 exhibits the lowest pulsation amplitude due to its almost negligible adiabatic zone (AZ), measuring only 4 mm. This minimal AZ allows the working fluid to transfer almost directly from the HZ to the cooling zone (CZ) with minimal energy loss. Conversely, the PHP with length ratio 0.242 has an AZ six times longer than that of the 0.481 configuration, introducing higher hydraulic resistance. As a result, the working fluid requires greater energy and driving force to overcome energy losses during movement from HZ to CZ, leading to a higher pulsation amplitude.

Although the PHP with length ratio 0.069 has an AZ 1.8 times longer than that of the 0.242 configuration, it exhibits a lower pulsation amplitude. This is due to the highest heat flux density among all tested PHPs at the same input power, which intensifies bubble nucleation in the HZ and generates a stronger driving force. This force helps to overcome hydraulic resistance but remains insufficient to equalize or reduce the pulsation amplitude compared to the 0.481 configuration. Consequently, in terms of pulsation amplitude, the PHP with length ratio 0.069 falls between the 0.481 and 0.242 configurations.

Summarizing, it can be said, that for this configuration LR influences only on pulsations amplitude and slightly influences dry-out input heat flux. When compare it to PHP with methanol at the same inclination angle (fig. 3.5), it can be seen, that

functioning of these two configurations is quite similar with only one difference in presence of heat conductivity and transition modes for PHP with methanol. In contrast, PHP with water at the same position (fig. 3.2) works in all operational modes and has less stable pulsations with significantly higher amplitude.

Case 8: heat carrier – pentane; 45° orientation of PHP (fig. 3.9).

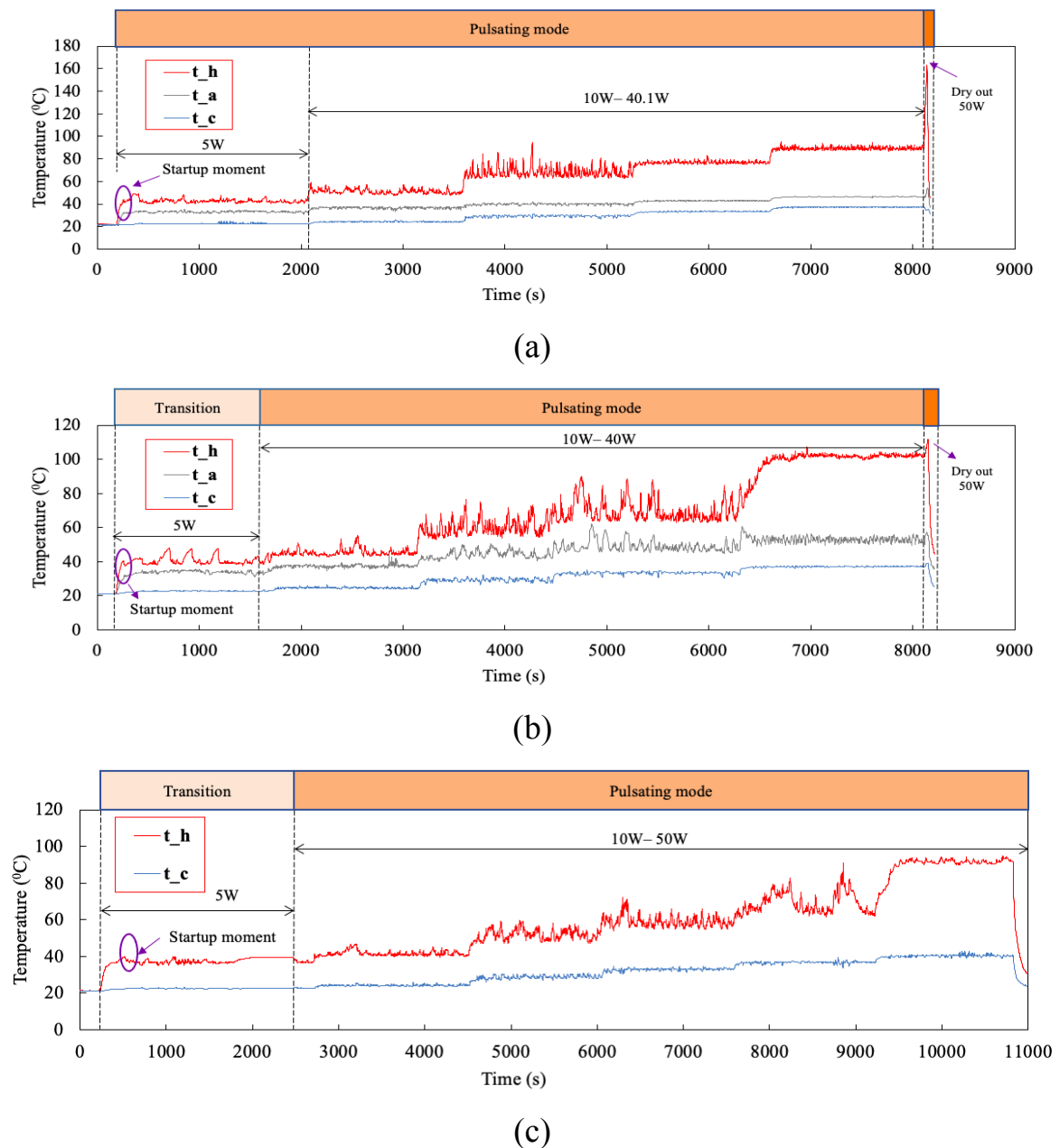


Figure 3.9– Variation of temperature with time for pentane at 45° inclination for PHP length ratios (a) 0.069 (b) 0.242 (c) 0.481 (t_h , t_a , t_c : average temperatures of heating, adiabatic and condensing zone respectively)

It is evident from Fig. 3.9 that pentane at a 45° inclination exhibited behavior similar to the vertical bottom heating mode, with some key differences. Notably, sustaining stable pulsations was more challenging, leading to a higher average heating zone temperature compared to the vertical bottom heating configuration. Unlike the vertical bottom heating mode, where all configurations directly entered pulsating mode, at 45° inclination, PHPs with length ratios of 0.242 (Fig. 3.9b) and 0.481 (Fig. 3.9c) experienced a transition mode before reaching pulsating mode. This indicates that at an inclined position, the buoyancy force does not align with the PHP channel axis, weakening the piston-like pushing action of vapor bubbles and requiring additional energy input to establish sustained pulsations.

For the PHP with a length ratio 0.069 and 0.242, dry-out occurred at the same input power 50 W. PHP with LR 0.069 has the most stable pulsations with the least amplitude. In contrast, PHP with LR 0.242 demonstrates the less stable pulsations with highest amplitude and PHP with LR 0.481 – in between them. For the PHP with a length ratio of 0.481, pulsations also began after a brief transitional phase and were sustained up to 50 W. However, dry-out was not observed during the test. Instead, the experiment was terminated at 50 W due to two critical reasons: first, the maximum temperature in the heating zone was close to the melting point of the soldering material, risking the detachment of thermocouples from the PHP wall; second, the temperature reached approximately 180°C , which is too close to pentane's critical temperature (196.6°C).

Thus, functioning of PHP with pentane at inclination angle 45° is quite similar to function in vertical bottom heating position (fig. 3.8). The only differences are: presence of transitional mode as first mode of operation for PHP with LR 0.242 and 0.481 and less stable pulsations with higher amplitude. Unlike PHP with pentane, PHP with methanol demonstrates presence of thermosyphone mode of operation at the same inclination angle (fig. 3.6). Both PHPs have the same values of start-up and dry-out input heat fluxes at all tested LR. But for methanol PHP, increasing of LR leads to increasing of transient input heat flux from 10 to 20 W when for pentane PHP it remains constant and equal to 10 W. Pentane provides more stable pulsations with less amplitude than methanol. PHP with

water (fig. 3.3) works in all operational modes, has higher start-up and dry-out values of input heat flux and higher amplitude of pulsations than PHP with pentane at inclination angle 45° .

Case 9: heat carrier – pentane; 0° orientation of PHP (fig. 3.10).

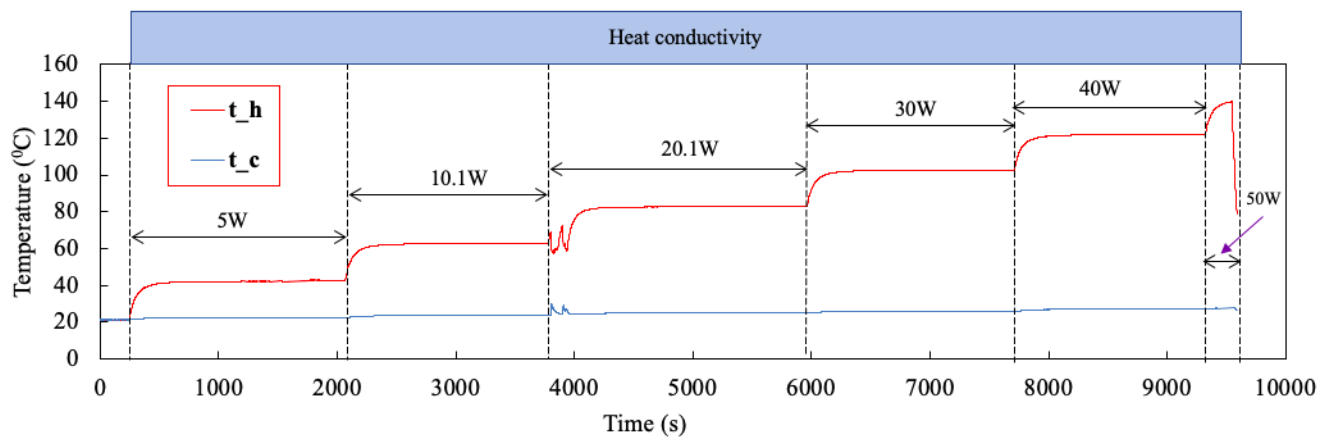


Figure 3.10– Variation of temperature with time for pentane at 0° inclination with PHP length ratio 0.481 (t_h , t_c : average temperatures of heating, condensing zone respectively)

PHP did not start in the horizontal mode of operation (fig. 3.10). The experiment proceeds with stepwise increases in heat input, starting from 5W and progressing through 10.1W, 20W, 30W, 40W, and 50W. Throughout the experiment, the system operates in heat conduction mode, as indicated by the stable temperature profile in the condensing zone and the steady, stepwise rise in the heating zone temperature without significant oscillations. The experiment was terminated at 50 W because of high local HZ temperature.

Unlike PHP with water (fig. 3.4) and methanol (fig. 3.7), PHP with pentane did not start to operate at 0° inclination angle. Pentane has the least surface tension among all tested heat carriers. This means that capillary force acting on liquid inside PHP is also the least and it is insufficient to return liquid to HZ without gravity force assistance.

Case 10: PHP at top heating mode; -90° orientation of PHP (fig. 3.11).

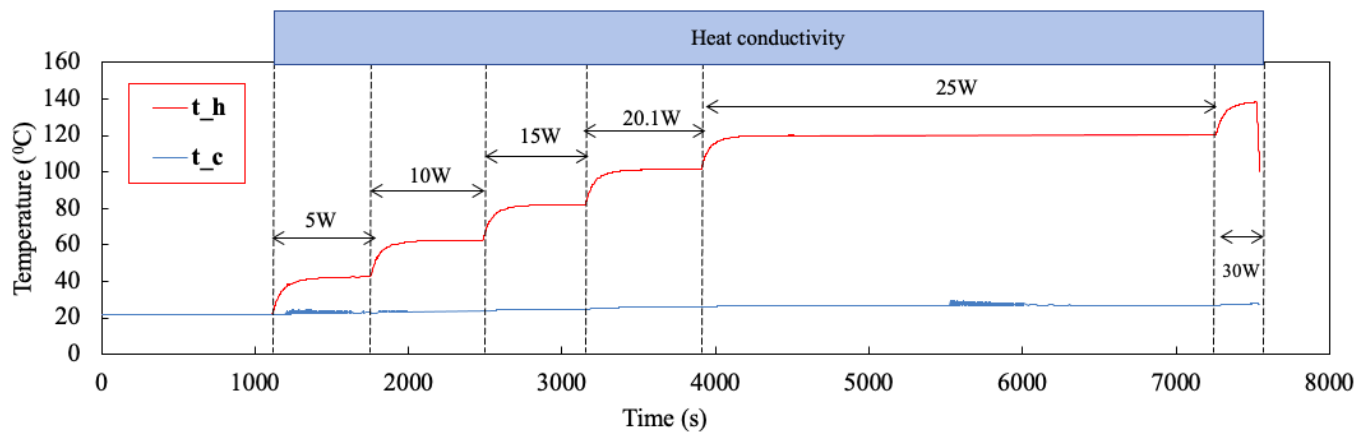


Figure 3.11– Variation of temperature with time for water at -90° inclination with PHP length ratio 0.481 (t_h , t_c : average temperatures of heating, condensing zone respectively)

It was observed throughout the experimental procedure that none of the tested PHP configurations can start in top heating mode. For example, behavior of PHP with water and length ratio 0.481 at top heating mode is shown in fig. 3.11. Throughout the experiment, the system remains in heat conduction mode, as indicated by the stable temperature in the condensing zone and the stepwise rise in the heating zone temperature without significant oscillations, confirming the absence of pulsations (fig. 3.11). In the top-heating mode, the fundamental working mechanism of the PHP is disrupted. PHP operation relies on the continuous motion of vapor bubbles and liquid slugs driven by inertial forces taking place during growth and departure of vapor bubbles, pushing piston-like action of vapor bubbles and plugs and pressure difference between HZ and CZ. However, when the heating zone is at the top, the vapor bubbles, which are naturally buoyant, remain in the upper section of the pipe rather than moving downward to the condensing zone. They merge into large vapor plugs which push out liquid from HZ when expanding and occupy whole HZ. Liquid must return to HZ for starting of pulsation movement. But the only force able to return liquid to HZ at this position is capillary force. It is insufficient to overcome gravity force which moves liquid in the

opposite way, i.e. toward CZ, and pressure inside vapor plugs which occupy HZ. Thus, pulsating motion of heat carrier inside PHP doesn't start and it remains in heat conductivity mode of operation.

3.3 Conclusions

The operational behavior of pulsating heat pipes (PHPs) is highly dependent on heat input, PHP length ratio, inclination angle and heat carrier properties as listed below.

1. PHPs follow distinct operational modes: heat conductivity, thermosyphone, transition, and pulsating. These modes differ from each other by hydrodynamic peculiarities, heat and mass transfer mechanisms and heat transfer efficiency. The least efficient mode is heat conductivity mode when heat is transferred only by heat conductivity of PHP casing because of absence of heat carrier movement inside PHP. It takes place at low heat inputs before the start-up moment. Pulsating mode demonstrates the highest heat transfer efficiency due to stable pulsating movement of heat carrier between HZ and CZ which provides two-phase heat transfer. Presence of thermosyphone and transient modes, values of start-up and dry-out input heat flux and borders of all operational modes are strongly dependent on LR, inclination angle and heat carrier properties.

2. PHP with pentane starts at the least input heat flux of 5 W. PHP with methanol requires 5-10 W (up to 15 W in horizontal position) to start and PHP with water – 10-15 W (up to 25 W in horizontal position). The same trend is observed for transient input heat flux (beginning of pulsating mode): for pentane it is 5-10 W, for methanol – 10-20 W and the highest one is for water – 25-40 W. PHP with pentane starts directly in pulsating mode or has transient mode of operation at 5 W of input power depending on inclination angle. PHP with methanol and water work in all operational modes but water provides the widest heat input range for transient mode with significantly unstable pulsations. In pulsating mode, pentane filled PHP demonstrates the most stable pulsations with the least amplitude. PHP with water also have good pulsations stability but with the highest amplitude. PHP with methanol is in between them in terms of

amplitude but it has the worst stability of pulsations. Despite number of advantages (low start-up and transient input heat flux, low pulsations amplitude with high stability) of pentane as heat carrier of PHP for electronics cooling it has serious disadvantage – low dry-out input heat flux which in this investigation was equal to 50-60 W. In contrast, water provides much higher value up to 80 W. Methanol is close to pentane with dry-out at 40-60 W.

3. PHP with pentane is the most independent from LR influence, because start-up, transient, dry-out input heat flux and borders of operational modes remain constant with changing of LR. But LR increasing leads to appearance of transient mode of operation with LR increasing at inclination angle 45° . Also, LR influences on stability and amplitude of pulsations of pentane filled PHP. PHP with LR of 0.481 and 0.069 has the most stable pulsations with the least amplitude at inclination angles 90° and 45° correspondingly and PHP with LR of 0.242 demonstrates the worst pulsations stability and the highest amplitude at both inclination angles. Influence of LR on start-up input heat flux of methanol filled PHP is also absent. But LR increasing leads to: appearance of transitional mode before pulsating, shifting of lower border of pulsating mode toward higher values of input heat flux and increasing of dry-out input heat flux. It has to be noted, that only LR 0.069 provides functioning of PHP with methanol in horizontal position. Influence of LR on stability and amplitude of pulsations in pulsating mode is the same as for PHP with pentane. LR has the most explicit influence on PHP with water. Increasing of LR leads to: increasing of start-up and dry-out input heat flux, shifting of borders of all operational modes toward higher values of input heat flux, improving of pulsations stability and decreasing of their amplitude.

4. The only influence of inclination angle on operating of PHP with pentane is appearance of transitional mode when inclination angle was decreased from 90° to 45° . At 0° PHP with pentane didn't start working. Decreasing of inclination angle from 90° to 45° leads to decreasing of start-up input heat flux from 10 W to 5 W for methanol PHP with further increasing to 15 W when angle was decreased to 0° . Also, thermosyphone mode appears for PHP with methanol with decreasing of inclination angle from 90° to

45°. Start-up input heat flux of PHP with water increases with decreasing of inclination angle from 90° to 0°. The same decreasing of inclination angle leads to shifting of transient input heat flux toward higher values and decreasing of dry-out input heat flux for PHP with water and methanol. For PHP with all tested heat carriers, stability of pulsations become worse, and their amplitude increases with decreasing of inclination angle.

Chapter 4 – Influence of Heat Carrier Physical Properties on Start-up and Transient Characteristics of Pulsating Heat Pipe

The performance of pulsating heat pipes (PHPs) is critically influenced by the choice of working fluid, as its thermophysical properties govern the phase change dynamics, heat transfer efficiency, and thermal stability of the system. Thermophysical properties of all three working fluids at standard operating conditions are mentioned in the table 4.1 below. Water, with its high boiling point, specific heat capacity and heat of vaporization, is ideal for high thermal loads but disadvantage of water is high start-up input power and high start-up temperature. Methanol and pentane have much lower start-up input power and temperature than water due to lower boiling point and heat of vaporization but dry-out also occurs at lower input power and hence they can't withstand to high heat loads. Understanding the interplay between these fluids' physical properties and operational parameters, such as PHP length ratio and inclination angle, is essential for optimizing PHP performance.

Table 4.1 – Physical Properties of Water, Methanol, and Pentane at 20°C and atmospheric pressure

Property	Water	Methanol	Pentane
Boiling point (°C)	100	64.7	36.1
Density (kg/m ³)	998	790	626
Heat of vaporization (kJ/kg·K)	2453	1176	370
Specific heat capacity (J/kg·K)	4184	2504	2294
Thermal conductivity (W/m·K)	0.60	0.20	0.11
Dynamic viscosity (Pa·s)	$1.0 \cdot 10^{-3}$	$5.8 \cdot 10^{-4}$	$2.3 \cdot 10^{-4}$
Surface tension (N/m)	0.072	0.023	0.016

This chapter explores the dependencies between start-up and transient PHP parameters (q_{start} , $\overline{t_{start}}$, and q_{pulse}) and physical properties of the working fluids.

4.1 Influence of physical properties on start-up characteristics of pulsating heat pipe

4.1.1 Start-up heat flux density

Influence of vapor density on start-up heat flux density is depicted in fig. 4.1.

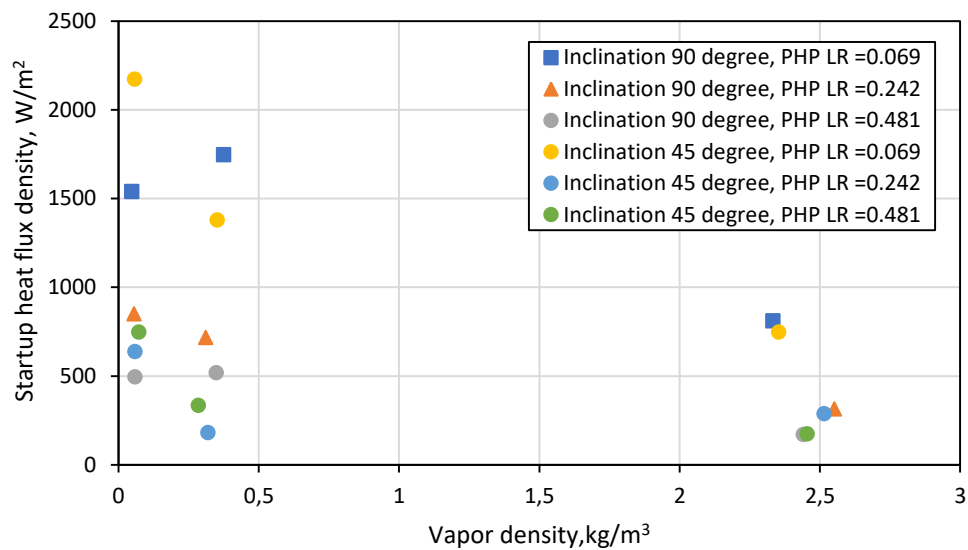


Figure 4.1– Variation of start-up heat flux density with vapor density at different PHP length ratio and inclination

Start-up heat flux density shows an inverse relationship with vapor density (fig. 4.1): increasing of vapor density from 0.05 to 2.5 kg/m³ leads to reducing start-up heat flux density by approximately 2 times. This is because the higher vapor density the less work is necessary to form vapor bubble with critical (minimal) radius, hence less energy is necessary to initiate boiling which means lower start-up heat flux density.

Influence of liquid physical properties on start-up heat flux density is depicted on fig. 4.2.

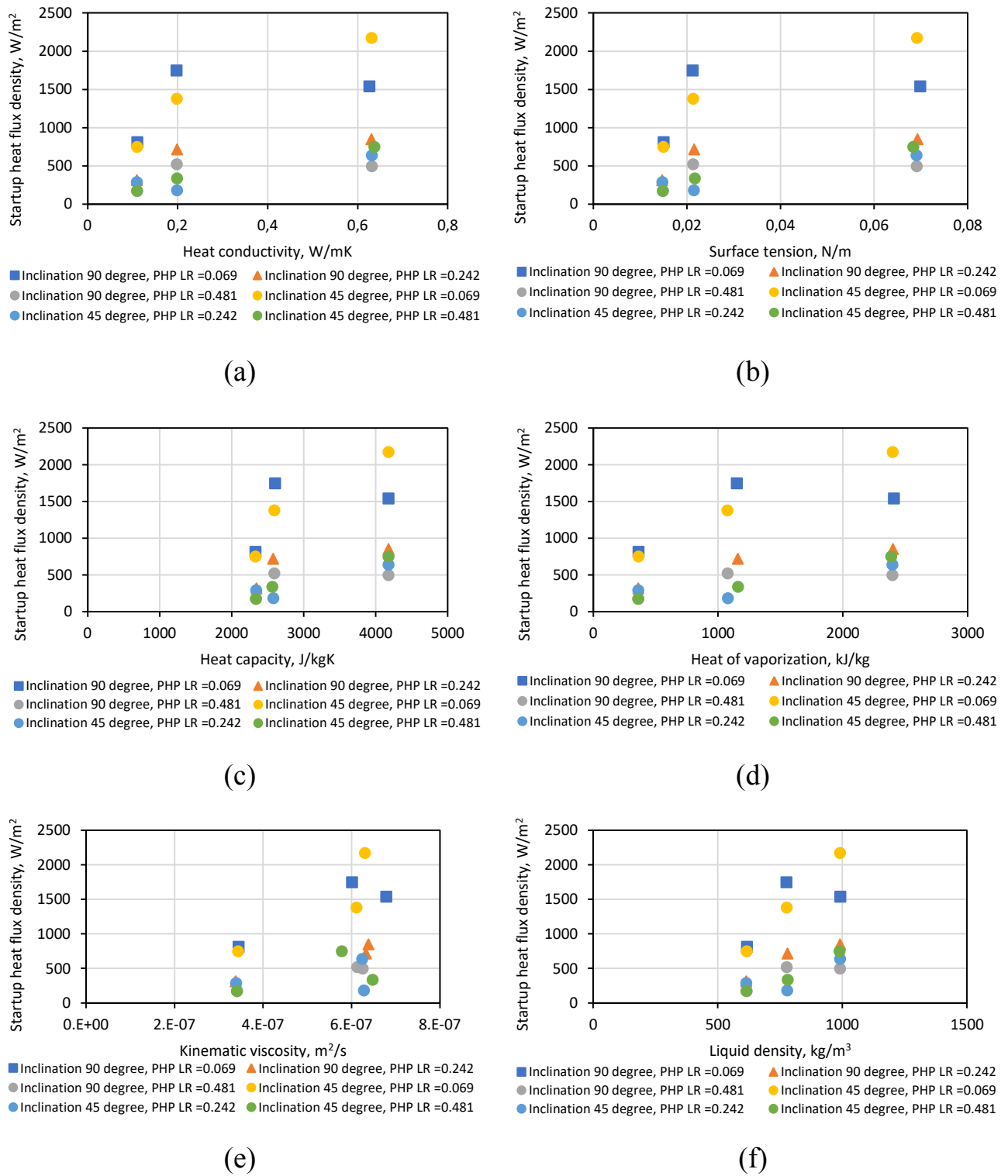


Figure 4.2– Influence of various physical properties of liquid on startup heat flux density at different PHP length ratio and inclination angle.

All liquid physical properties show the same trend: increasing of their values leads to increasing of start-up heat flux density (fig. 4.2). Higher thermal conductivity increases the startup heat flux density (Fig. 4.2a) because greater conductivity enhances heat dissipation within the liquid bulk, leading to more efficient heat removal from the heat transfer surface, specifically the PHP wall. As a result, more energy must be supplied to the PHP wall to sufficiently overheat the wall-liquid boundary layer and initiate boiling. Higher surface tension supports bubble formation but requires a higher startup heat flux density because it increases the energy needed to initiate both vapor bubble formation and the movement of the heat carrier (Fig. 4.2b). These two stages are inherently linked, as the successful formation of a vapor bubble directly influences the ability of the heat carrier to start moving. In the first stage, when a vapor bubble forms, the internal pressure within the bubble must exceed the external forces acting on it. One of the dominant opposing forces is surface tension, which is proportional to the surface tension coefficient. A higher surface tension coefficient results in a stronger force holding the liquid together, making it more difficult for a bubble to grow. Consequently, more energy must be supplied to overcome this resistance and allow the vapor bubble to expand. Once the vapor bubble reaches a sufficient size, the second stage begins, where the bubble's inertial forces push against the surrounding liquid plug, attempting to initiate movement. However, this movement is resisted by capillary forces, which act to maintain the meniscus shape of the liquid due to molecular interactions caused by viscosity. Since capillary forces are also proportional to surface tension, a higher surface tension coefficient strengthens this resistance, requiring additional energy to deform the meniscus and allow the liquid plug to move. Thus, a higher surface tension first demands more energy for bubble nucleation, and then further increases the resistance against the movement of the heat carrier. This combined effect explains why higher surface tension leads to a greater startup heat flux density in a pulsating heat pipe.

Fluids with higher heat capacity (Fig. 4.2c) and higher heat of vaporization (Fig. 4.2d) require a higher startup heat flux density because more energy is needed, first to raise the liquid temperature to its saturation point, and then to provide the additional

energy required for evaporation. Startup heat flux density exhibits a direct correlation with kinematic viscosity (fig. 4.2e), where higher viscosities result in greater resistance to fluid motion, because of higher molecular interaction. It means higher driving force is necessary to overcome this resistance. Inertial force taking place during vapor bubble growing and pushing action of vapor bubbles are one main driving forces in PHP. Active boiling with large quantity of active nucleation sites, low departing diameter of vapor bubbles and high frequency of vapor bubble departure is necessary to increase these forces. Initiating of such active boiling needs input of heat flux with high density.

The influence of liquid density on startup heat flux density (Fig. 4.2f) is like that of kinematic viscosity, but the underlying mechanism differs. For a vapor bubble to form, the internal pressure must overcome two external forces: the surface tension force and the pressure exerted by the surrounding liquid. The latter force is directly proportional to the liquid's density, meaning that as liquid density increases, a greater energy input is required to overcome this resistance and initiate bubble formation. Consequently, higher liquid density results in a higher startup heat flux density.

4.1.2 Start-up temperature

Influence of vapor density on start-up temperature is depicted on fig. 4.3. As shown in fig. 4.3, a 50-fold increase in vapor density results in a decrease in startup temperature by approximately 1.5 to 1.8 times. The startup moment of the PHP marks the initiation of heat carrier movement, which is directly linked to the onset of boiling in the heating zone. As previously mentioned, the heat transfer surface requires a certain level of overheating to trigger boiling. This overheating is defined as the difference between the surface temperature and the saturation temperature. In this case, the PHP wall in the heating zone acts as the heat transfer surface, and the average heating zone temperature at the startup moment, referred to as the startup temperature, represents the surface temperature.

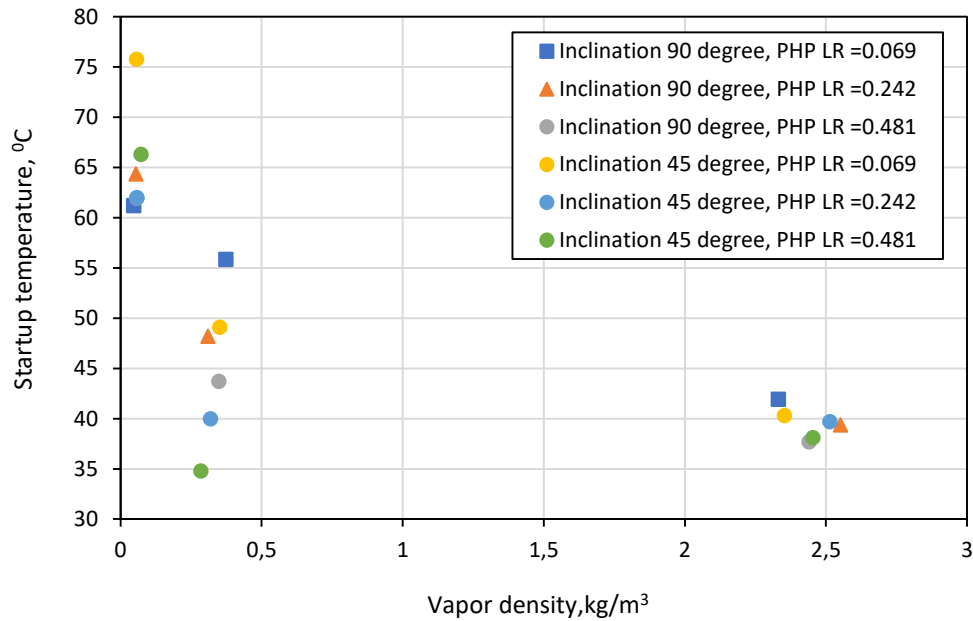
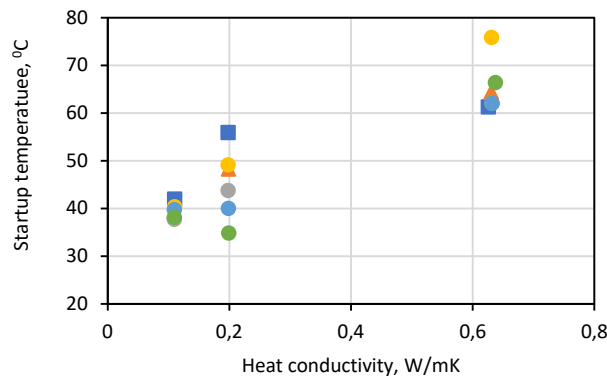


Figure 4.3– Variation of start-up temperature with vapor density at different PHP length ratio and inclination

It is important to note that lower startup temperatures correspond to lower saturation temperatures, meaning that an increase in vapor density reduces the required overheating of the PHP wall. Overheating is one of the key parameters influencing the onset of boiling, but its precise analytical determination is highly complex due to the stochastic nature of the boiling process and the multitude of influencing factors. For the same reasons, experimental data on overheating often exhibit significant variability. Despite these challenges, several studies, such as [119-122], have attempted to analytically determine overheating, with most findings indicating that overheating is inversely proportional to vapor density. In other words, as vapor density increases, the required overheating decreases.

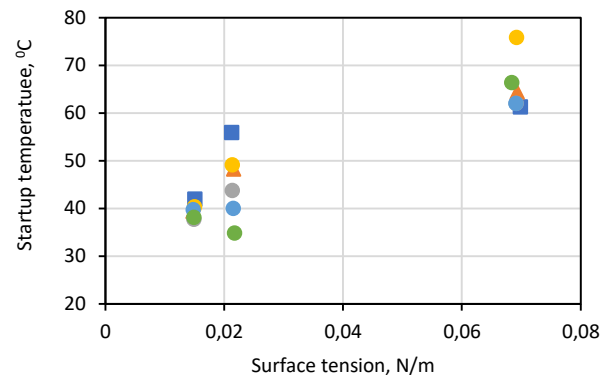
Fig. 4.4 describes the relationship between physical properties of heat carrier and PHP start-up temperature under varying length ratios and inclinations. As it can be seen on fig. 4.4, the same trend is observed for all liquid properties and all PHP configurations: increasing of properties values leads to rising of start-up temperature. This trend is similar to liquid physical properties influence on start-up heat flux density

(fig. 4.2). As it was shown before, increasing in liquid physical properties needs more heat energy to be supplied to PHP heating zone for initiating of boiling process and heat carrier motion. Increasing of supplied quantity of heat energy leads to intensifying of molecular oscillations inside a structure of PHP wall and, as a consequence, to increasing of wall temperature.



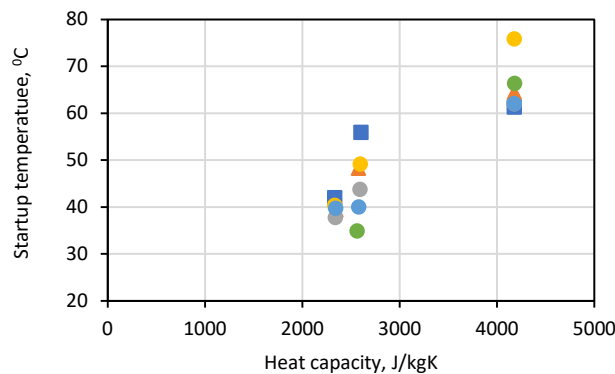
■ Inclination 90 degree, PHP LR =0.069 ▲ Inclination 90 degree, PHP LR =0.242
 ● Inclination 90 degree, PHP LR =0.481 ● Inclination 45 degree, PHP LR =0.069
 ● Inclination 45 degree, PHP LR =0.242 ● Inclination 45 degree, PHP LR =0.481

(a)



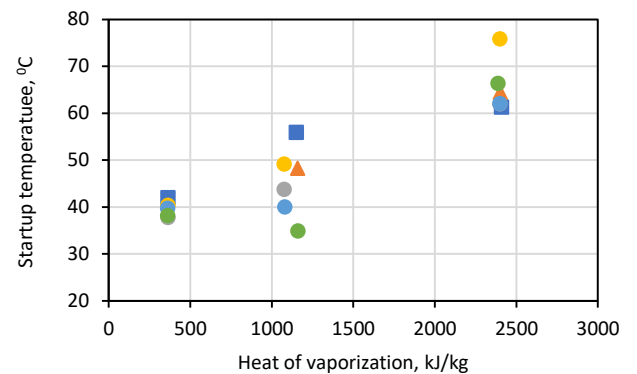
■ Inclination 90 degree, PHP LR =0.069 ▲ Inclination 90 degree, PHP LR =0.242
 ● Inclination 90 degree, PHP LR =0.481 ● Inclination 45 degree, PHP LR =0.069
 ● Inclination 45 degree, PHP LR =0.242 ● Inclination 45 degree, PHP LR =0.481

(b)



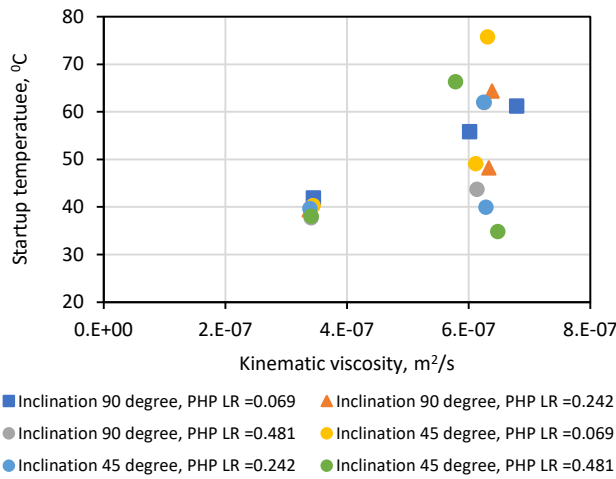
■ Inclination 90 degree, PHP LR =0.069 ▲ Inclination 90 degree, PHP LR =0.242
 ● Inclination 90 degree, PHP LR =0.481 ● Inclination 45 degree, PHP LR =0.069
 ● Inclination 45 degree, PHP LR =0.242 ● Inclination 45 degree, PHP LR =0.481

(c)

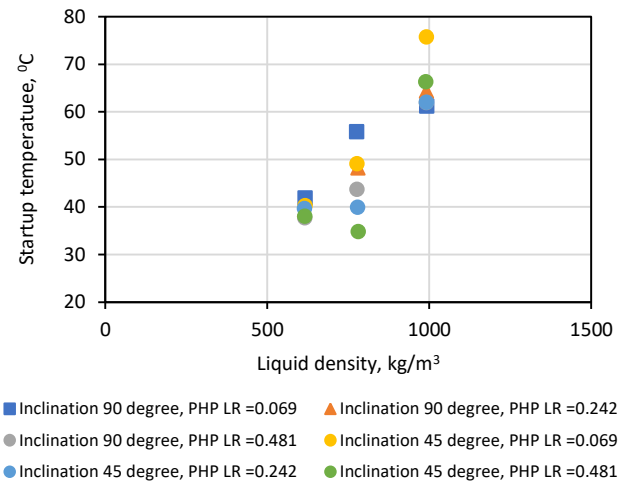


■ Inclination 90 degree, PHP LR =0.069 ▲ Inclination 90 degree, PHP LR =0.242
 ● Inclination 90 degree, PHP LR =0.481 ● Inclination 45 degree, PHP LR =0.069
 ● Inclination 45 degree, PHP LR =0.242 ● Inclination 45 degree, PHP LR =0.481

(d)



(e)



(f)

Figure 4.4– Influence of various physical properties of liquid on start-up temperature at different PHP length ratio and inclination angle

Coefficient of surface tension (fig. 4.4b) also has direct impact on beginning of boiling via surface tension force which is proportional to this coefficient and plays one of major roles in vapor bubble formation and growth. Heat transfer surface, which is PHP wall in our case, needs initial overheating for boiling beginning. According to analytical models of this process [119-122] overheating is proportional to surface tension coefficient which means increasing of overheating value with increasing of surface tension. In our investigation higher overheating corresponds to higher start-up temperature.

4.2 Influence of Physical Properties on transient Heat Flux Density

Influence of vapor density on transient heat flux density is depicted in fig. 4.5. It is evident from fig. 4.5 that increase in vapor density leads to a reduction in transient heat flux density.

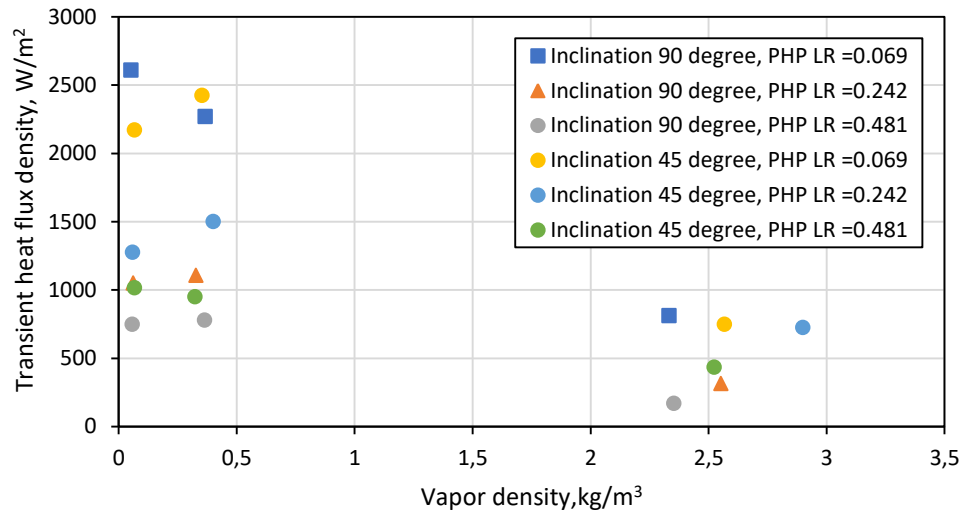
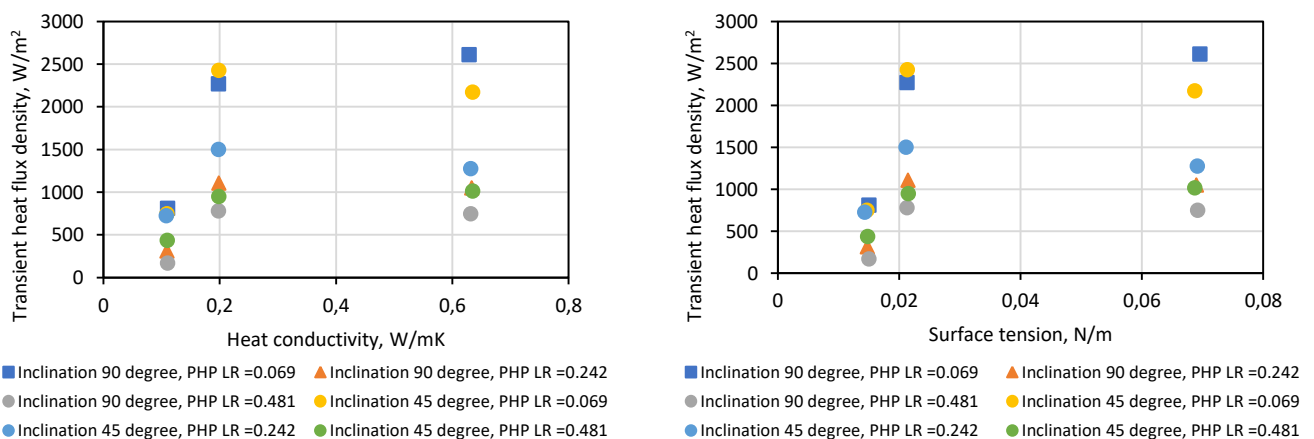


Figure 4.5– Variation of transient heat flux density with vapor density at different PHP length ratio and inclination

This influence is similar to that on start-up heat flux density (fig. 4.1) and the reason is similar too. Increasing of vapor density leads to decreasing of work necessary to form vapor bubble with minimal radius. This means that there are more active nucleation sites, and more vapor bubbles are generated at lower heat flux densities which, in its turn, leads to beginning of stable pulsating movement of heat carrier inside PHP. Such behaviour makes high-vapor-density fluids particularly suitable for applications where initiating pulsations at lower heat flux levels is desirable.

Influence of liquid physical properties on transient heat flux density is depicted on fig. 4.6.



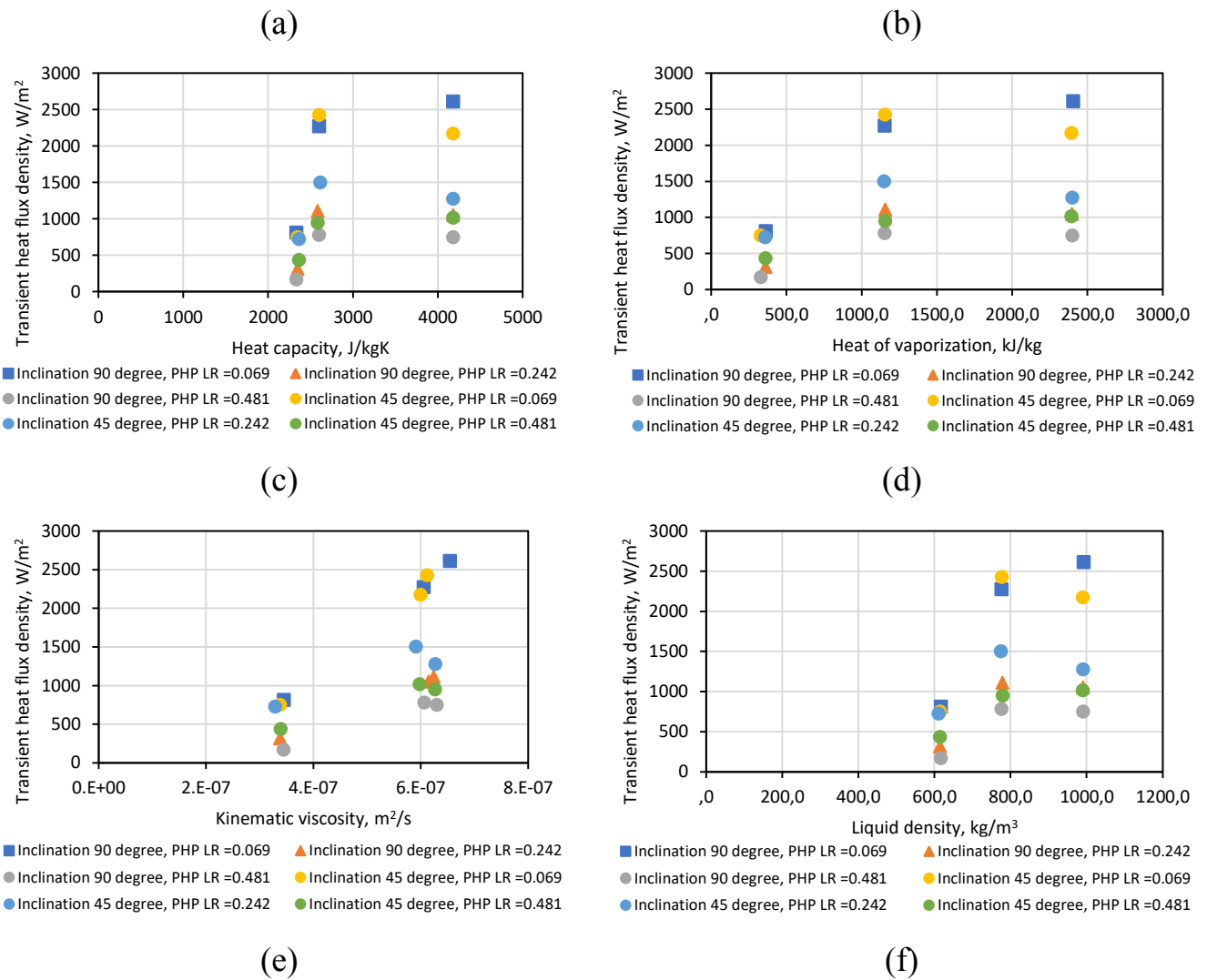


Figure 4.6– Influence of various physical properties of liquid on transient heat flux density at different PHP length ratio and inclination angle.

All liquid physical properties exhibit a similar influence on transient heat flux density as they do on start-up heat flux density. However, while start-up heat flux density determines the conditions required to initiate heat carrier movement inside PHP, which is directly connected with activation of the first nucleation sites and boiling beginning in HZ, transient heat flux density governs moment when boiling become stable and active, i.e. when number of active nucleation sites become enough for initiating and maintaining of stable pulsating movement of heat carrier.

Higher thermal conductivity leads to an increased transient heat flux density (fig. 4.6a), as it enhances heat dissipation throughout the liquid bulk. The difference between thermal conductivity influence on start-up and transient heat flux density is that in the first case it is necessary to initiate boiling and in the second – stabilize and make it more active. Portions of cold (relatively to saturation point) liquid, which arrive to HZ from CZ during PHP working in thermosyphone or transient mode, suppress action of nucleation sites. It is necessary to terminate this suppression and activate large number of nucleation sites simultaneously for transferring to pulsating operational mode. This requires high PHP wall overheating, even higher than for starting of boiling. The higher thermal conductivity of liquid, the higher heat dissipation throughout the liquid bulk is which provokes necessity of higher heat flux to provide this overheating.

Similarly, surface tension continues to play a dual role by increasing both energy necessary for vapor bubble formation and energy needed for the sustained pulsating motion of the heat carrier (fig. 4.6b). Fluids with higher heat capacity and heat of vaporization also demand higher transient heat flux densities (fig. 4.6c, fig.4.6d), because liquid in HZ should be overheated to begin and maintain active boiling and sustainable pulsating motion of heat carrier. Thus, increasing of heat capacity and heat of vaporization requires more energy for overheating and evaporating of liquid.

Kinematic viscosity (fig. 4.6e) directly affects the internal resistance to fluid motion. Even after pulsations are initiated, higher viscosity results in stronger molecular interactions that resist phase change-driven movement, requiring a greater heat flux density to counteract these effects. Similarly, liquid density continues to influence transient heat flux density (fig. 4.6f) in the same way as it does during start-up, as higher density increases the pressure resistance against vapor bubble expansion and fluid motion, necessitating sustained higher energy input to overcome these forces.

4.3 Conclusions

By analyzing the effects of thermophysical properties of different working fluids on start-up and transient characteristics of PHP such conclusions can be made:

1. An increase in vapor density reduces the start-up heat flux density and start-up temperature. Higher vapor density decreases the energy and overheating required for vapor bubble nucleation, leading to easier initiation of pulsations. A 50-fold increase in vapor density results in a 1.5 to 1.8 times decrease in start-up temperature, and 2 times decrease in start-up heat flux density is lower for fluids with higher vapor density, making them more efficient for initiating and maintaining pulsations at lower heat flux levels.

2. Higher values of liquid physical properties lead to an increase in both start-up heat flux density and start-up temperature. Fluids with higher thermal conductivity dissipate heat more efficiently, requiring greater heat input to reach the necessary overheating for boiling initiation. Increased surface tension strengthens resistance to vapor bubble formation and liquid movement, raising the required energy for PHP activation. Similarly, higher heat capacity and heat of vaporization demand greater energy input to reach the boiling point and evaporate liquid. Liquid density also contributes to this effect by increasing the resistance against vapor bubble formation.

3. Vapor density increasing leads to a reduction in transient heat flux density due to decreasing of work necessary to form vapor bubble with minimal radius. This increases number of active nucleation sites tends to begin stable pulsation movement of heat carrier inside PHP by generating more vapor bubbles at lower heat flux density. Such behaviour makes high-vapor-density fluids particularly suitable for applications where initiating pulsations at lower heat flux levels is desirable.

4. In the same way as for start-up heat flux density, increasing of thermophysical properties values leads to increasing of transient heat flux density. Higher thermal conductivity enhances heat energy rejecting from PHP wall; thus, it requires more energy to provide its overheating enough for simultaneously activating of large number of

nucleation sites necessary for initiating of sustainable pulsating heat carrier movement. Increasing of surface tension and liquid density tends to increase energy necessary for maintaining of stable formation and growth of large number of vapor bubbles which drive sustainable pulsations in PHP. These properties together with viscosity also introduce resistance to fluid movement, necessitating greater energy input to overcome it and maintain sustainable oscillations. Fluids with higher heat capacity and heat of vaporization need higher heat input to maintain phase change.

Chapter 5 - Influence of Geometrical and Operating Parameters on Start-up and Transient Characteristics of Pulsating Heat Pipe

5.1 Influence on startup and transient characteristics

The combined influence of inclination angle and PHP length ratio on start-up heat flux density (q_{start}) is shown in fig. 5.1.

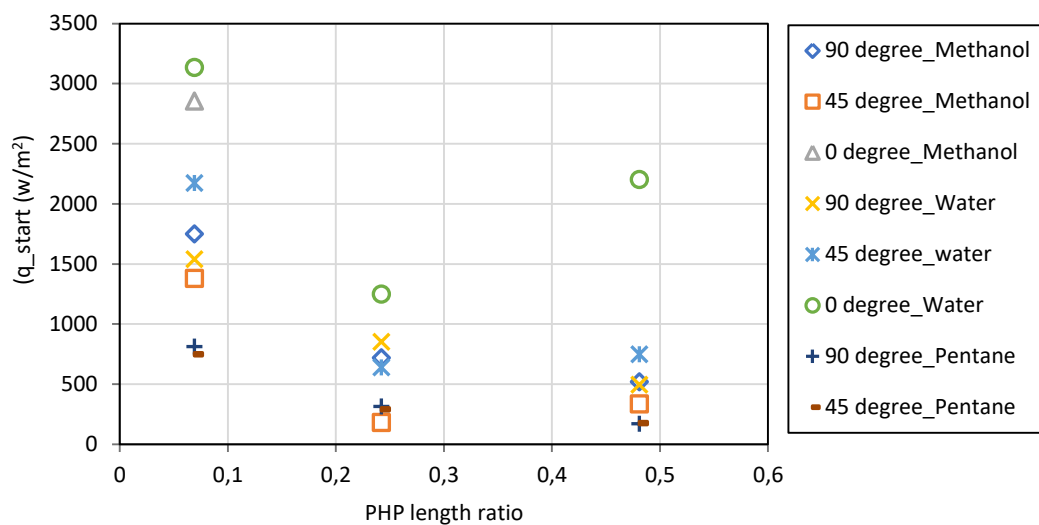


Figure 5.1– Effect of PHP length ratio and inclination angle on start-up heat flux density

At horizontal orientation (inclination angle 0°), water shows the highest values of start-up heat flux density indicating more energy needed to initiate PHP operation. PHP with methanol started only at $LR = 0.069$. Although PHP with pentane did not start working at all in the horizontal orientation, however, it consistently required lower starting heat flux at all other orientation potentially making pentane more efficient for PHP operation at non-horizontal orientations, for example, pentane required only 500 W/m^2 at $+90^\circ$ compared to 1000 W/m^2 for methanol.

In order to explain such PHP behavior at horizontal orientation, first of all, in should be noted, that despite direct connection between beginnings of heat carrier motion inside PHP and boiling, absence of the first doesn't mean absence of the latter. Boiling occurs independent of PHP orientation when overheating of PHP wall and liquid border

layer becomes enough for starting of the process. Difficulties with PHP start-up at horizontal position relate to direction of vapor formations (bubbles or plugs) movement and absence of gravity action.

After filling of PHP with heat carrier, liquid slugs are formed under capillary force action. Thus, heat carrier exists inside PHP in form of chain which consists of alternating liquid slugs and vapor plugs. When heat input to HZ and heat removal from CZ are absent this system is in a state of mechanical equilibrium. It is necessary to upset this equilibrium for starting of heat carrier motion inside PHP. If PHP is oriented vertically with bottom heating ($+90^\circ$ inclination angle) and heat is inputted to HZ vapor formations (bubbles or plugs) move upward along PHP axis pushing heat carrier toward CZ. This pushing action upsets the equilibrium. When vapor reaches CZ, it condenses, and new portion of liquid appears. This portion joins nearest liquid slug, thus, increasing its mass. When mass of the slug becomes enough for gravity force to overcome pushing action of vapor plug, liquid slug begins to move downward to HZ under action of gravity force (capillary force may also assist this movement). Thus, gravity force assists to upset the equilibrium, but it should be noted, that before vapor reaches CZ gravity force counteracts pushing action of vapor plug.

The other picture can be observed when PHP is oriented horizontally. There can be two cases when boiling takes place in one PHP turn in HZ fully filled with liquid: detachment diameter of vapor bubble is larger than inner diameter of PHP capillary tube and it is smaller than inner diameter. In the first case, when bubble diameter equalizes to inner diameter of capillary tube it begins to transform into vapor plug. In the second case, bubble detaches PHP wall and moves upward under buoyancy force action. Considering horizontal position of PHP, direction of this movement is perpendicular to PHP axis in contrast with inclination angle $+90^\circ$ where it coincides with the axis which allows bubble to leave HZ. Thus, in horizontal position bubble stays in HZ and transforms into vapor plug merging with other bubbles. This vapor plug expands and occupies whole volume of HZ. Expanding is caused by two reasons: supplying of heat energy to HZ and evaporation from phase interface. The latter takes place because liquid

in HZ is overheated due to small capillary diameter and uniform heat input on the whole perimeter of HZ cross section.

Taking into account that initial distribution of liquid slugs and vapor plugs inside PHP is random, another two cases of heat carrier presence in HZ at initial moment are possible: the turn is fully filled with vapor plug and both liquid slugs and vapor plugs are present in the turn. In the first case vapor plug begins to expand when heat is applied to HZ. In the second one vapor plug forms because of merging of new vapor bubbles with already existing vapor plugs. Thus, in any case, large expanding vapor plug occupies HZ when PHP is oriented horizontally.

Vapor plug pushes neighbor liquid slugs toward AZ while expanding. Coming out of these plugs from HZ leads to termination of evaporation from their meniscus to vapor plug because of decreasing of liquid temperature to saturation temperature due to heat transfer to PHP wall. From this moment vapor quantity in the vapor plug remains constant and it expands only due to increasing in heat input. When liquid slugs have fully pushed out from AZ to CZ, vapor plug reaches CZ and vapor condensation begins. Decreasing of vapor quantity in the plug because of condensation leads to decreasing of pressure inside the plug. Further increasing in input power leads only to arriving of new portions of vapor to CZ and their condensation. Thus, vapor quantity in the vapor plug decreases with increasing in input power. This leads to decreasing of pressure inside the vapor plug. When this pressure becomes lower than capillary pressure in liquid slugs it makes possible returning of liquid to HZ. If liquid reaches HZ instant explosive boiling occurs because of high overheating of PHP wall in this zone. This process provokes start of pulsating heat carrier movement inside PHP.

Taking into account mechanics of interaction between vapor plugs and liquid slugs described above, it can be summarized that PHP orientation influences on forces balance in the system of vapor plugs-liquid slugs and, thus, on PHP start-up. From the other hand forces acting in this system connected with such processes as: evaporation, boiling, capillary effect, etc. This means they depend on physical properties of heat carrier. That's why influence of inclination angle on start-up heat flux density differs for

different heat carriers (fig. 5.1). For water, increasing of inclination angle from 0° to $+90^\circ$ leads to decreasing of start-up heat flux density. This means that increasing of inclination angle simplifies vapor coming out from HZ, intensifies pushing action of vapor formations and gravity influence on forces balance. Methanol has the lowest values of start-up heat flux density at inclination angle $+45^\circ$ and the highest one – at 0° . This means that optimal forces ratio for start-up was achieved at $+45^\circ$. PHP with pentane didn't start in horizontal orientation at any of tested LR. In contrast, PHP with water started-up at all tested LR. This is because surface tension of water approximately 4.7 times higher than that of pentane which means that capillary force of water is enough to return liquid to HZ as opposed to pentane.

As it was mentioned in the Chapter 3, any of tested PHP configurations didn't start at inclination angles -45° and -90° . This is because mechanics of interaction between vapor plug and liquid slugs is the same as for horizontal position, but gravity force become present again in balance of forces. When mass of liquid slugs increases because of vapor condensation gravity force is assisting them to move down toward CZ, thus, counteracting to capillary force which tends to transfer them to HZ. Capillary force of tested heat carriers was not enough to overcome gravity force, that's why PHP didn't start.

Influence of PHP length ratio on start-up heat flux density depends on inclination angle and heat carrier (fig. 5.1). For all tested heat carriers and inclination angle $+90^\circ$, increasing of PHP length ratio leads to a decrease in start-up heat flux density, for example, for methanol at $+90^\circ$, it reduced from 1747 W/m^2 at $\text{LR} = 0.069$ to 519 W/m^2 at $\text{LR} = 0.481$. This is because AZ length decreasing with increasing of LR. The less AZ length, the less its hydraulic resistance, the less driving force is necessary to overcome it for PHP starting, the less heat flux density is required to generate this driving force.

The other picture is observed at inclination angle $+45^\circ$ for water and methanol: the highest values of start-up heat flux density correspond to the lowest $\text{LR} = 0.069$, the lowest ones – to $\text{LR} = 0.242$ and values for $\text{LR} = 0.481$ are between previous two but slightly closer to these ones at $\text{LR} = 0.282$ (fig. 5.1). For example, for methanol $q_{\text{start}} =$

1378 W/m² at LR = 0.069, it decreases to 181 W/m² at LR = 0.282 and then increases to 335 W/m² for LR = 0.481. Water has similar trend at 0° inclination angle. Decreasing of inclination angle makes it more complicated for vapor to come out from HZ, thus, making interaction between vapor plugs and liquid slugs at +45° closer to that one at 0°. In this case, it is necessary to supply to HZ energy enough for transferring vapor to CZ and starting instant active boiling when liquid returns to HZ. It is obviously, that the highest amount of energy is necessary for these processes in PHP with the longest AZ, i.e. the lowest LR. AZ is almost absent at LR = 0.481 which means vapor can reach CZ at low heat flux densities. But from the other hand, this flux is too low for providing instant active boiling, that's why PHP with LR = 0.481 needs higher start-up heat flux density than at LR = 0.242. As for the latter, it needs the lowest start-up heat flux density because it provides some optimal balance between two previous cases. In contrast to water and methanol, pentane demonstrates other trend at +45° inclination angle: decreasing of start-up heat flux density with increasing of LR, which is similar to that one at +90°. This is because pentane has the lowest kinematic viscosity among all tested heat carriers which allows buoyancy force to act at +45° inclination with approximately the same efficiency as at +90° making PHP start-up almost similar. This is confirmed by very close values of start-up heat flux density for both inclination angles at the same LR.

PHP with methanol started at horizontal position only at LR = 0.069 (fig. 5.1). It means, that capillary force was enough to transfer liquid to HZ and heat flux density was enough to start instant active boiling at this LR. This also means that capillary force was also enough to transfer liquid to HZ at higher LR, i.e., shorter AZ, but PHP didn't start to work. This because overheating of PHP wall in HZ was not enough for beginning of instant active boiling.

Influence of LR and inclination angle on start-up temperature for different heat carriers is depicted on fig. 5.2.

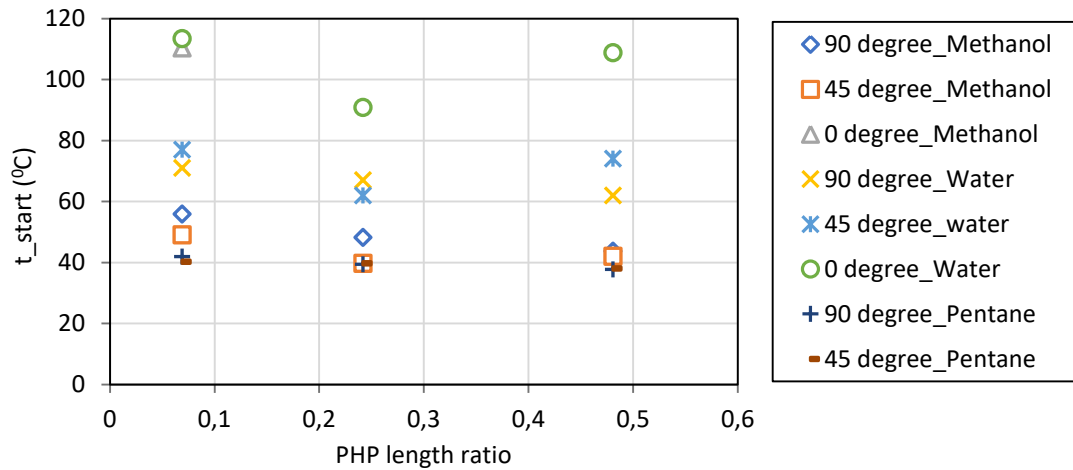


Figure 5.2– Effect of PHP length ratio and inclination angle on start-up temperature

In general, influence of LR and inclination angle on start-up temperature (fig. 5.2) is similar to that one on start-up heat flux density (fig. 5.1). This is because temperature depends on heat flux density: the higher heat flux density is supplied to HZ, the higher PHP wall temperature in this zone.

Influence of PHP length ration and inclination angle on transient heat flux density for different heat carriers is shown on fig. 5.3.

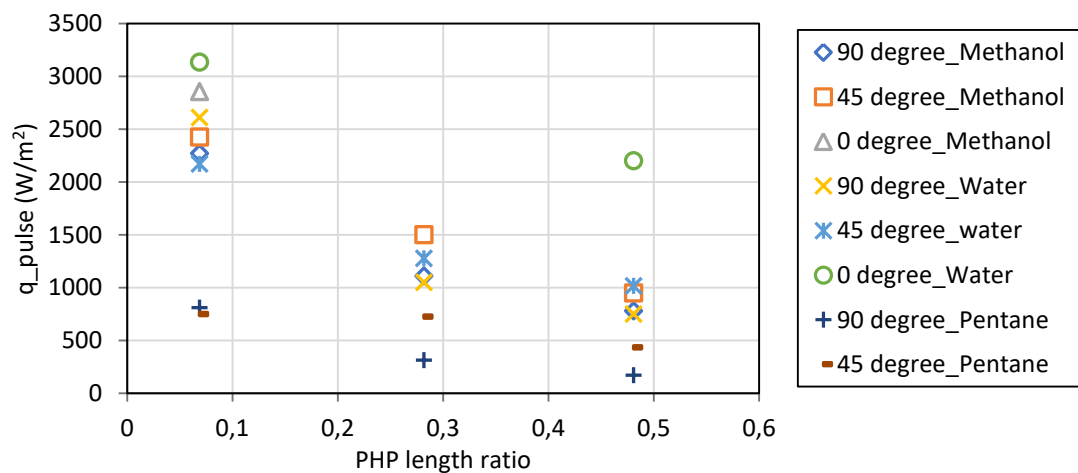


Figure 5.3– Effect of PHP length ratio and inclination angle on transient heat flux density

It was observed, that increasing of both length ratio and inclination angle leads to decreasing of the heat flux density corresponding to beginning of pulsation mode, which

is defined as transient heat flux density q_{pulse} , for all tested heat carriers (fig. 5.3). Among all working fluids, pentane exhibited the lowest of q_{pulse} value, reaching 169.4 W/m² at a length ratio of 0.481. This suggests that pentane is well-suited for applications where PHP operation requires a transition to pulsation mode at low heat flux densities.

Well-developed boiling with large number of active nucleation sites is necessary to begin and maintain sustainable pulsating movement of heat carrier inside PHP, i.e. for PHP transition to pulsating mode of operation and its working in this mode. Increasing of LR leads to increasing of heat transfer area in HZ which, in its turn, leads to increasing of number of potential nucleation sites. The more this number, the lower heat flux density is necessary to activate these sites. As for the inclination angle influence, its decreasing makes it more difficulty for vapor to come out from HZ. It is necessary to activate large number of nucleation sites simultaneously to avoid occupation of HZ with vapor and to begin sustainable pulsating heat carrier movement inside PHP. Such activation needs high heat flux densities because only these nucleation sites can be activated which sizes less than critical radius and the latter decreases with increasing of heat flux density.

5.2 Generalization of experimental data

In order to have possibility of calculation of start-up and transient heat flux density based on geometrical parameters of PHP, heat carrier physical properties and operational parameters obtained experimental data were generalized. For this purpose, heat flux density in HZ was considered as a function of such parameters:

$$q = f(L_{HZ}, L_{AZ}+L_{CZ}, l_{cap}, g, v, r, \lambda, c_p), \quad (5.1)$$

where q – HZ heat flux density (depending on purpose of calculation it can be start-up (q_{start}) or transient (q_{pulse}) heat flux density), W/m²;

L_{HZ} , L_{AZ} , L_{CZ} – length of heating, adiabatic and condensation zone correspondingly, m;

l_{cap} – capillary constant, m;

g – acceleration of gravity, $g = 9.81 \text{ m/s}^2$;

ν – saturated liquid kinematic viscosity, m^2/s ;

r – heat of vaporization, J/kg;

λ – saturated liquid thermal conductivity, $\text{W}/(\text{m}\cdot\text{K})$;

c_p – saturated liquid isobaric heat capacity, $\text{J}/(\text{kg}\cdot\text{K})$.

Capillary constant in (5.1) is calculated as:

$$l_{cap} = \sqrt{\frac{\sigma}{g(\rho - \rho_v)}}, \quad (5.2)$$

where σ – saturated liquid surface tension, N/m;

ρ , ρ_v – saturated liquid and saturated vapor density correspondingly, kg/m^3 .

All physical properties of liquid and vapor in (5.1) and (5.2) are defined by saturation temperature. For PHP, saturation temperature can be assumed as average AZ temperature or as mean of average HZ and CZ temperatures when AZ is absent.

Experimental data were generalized with using of Buckingham pi-theorem. Dimensions of length [L], mass [M], time [T] and temperature [θ] were used as basic dimensions. As a result, correlation between dimensionless complexes was obtained:

$$\frac{qc_p}{g\lambda} = C \left(\frac{L_{HZ}}{L_{AZ} + L_{CZ}} \right)^b Bo_*^m Ga^k \left(\frac{L_{HZ}^3 r}{\nu^2} \right)^f, \quad (5.3)$$

where C – coefficient;

Bo_* – modified Bond number;

Ga – Galileo number;

b, m, k, f – degrees.

Modified Bond number in (5.3) is calculated as:

$$Bo_* = \frac{L_{HZ}}{l_{cap}}. \quad (5.4)$$

Diameter or radius is used in classical Bond number as linear size but in our case, this is HZ length. That's why number is called "modified". It represents ratio between HZ length and capillary constant.

Galileo number in (5.3) is calculated as:

$$Ga = \frac{L_{HZ}^3 g}{\nu^2}. \quad (5.5)$$

Galileo number represents ratio between gravity force and molecular friction force in heat carrier stream.

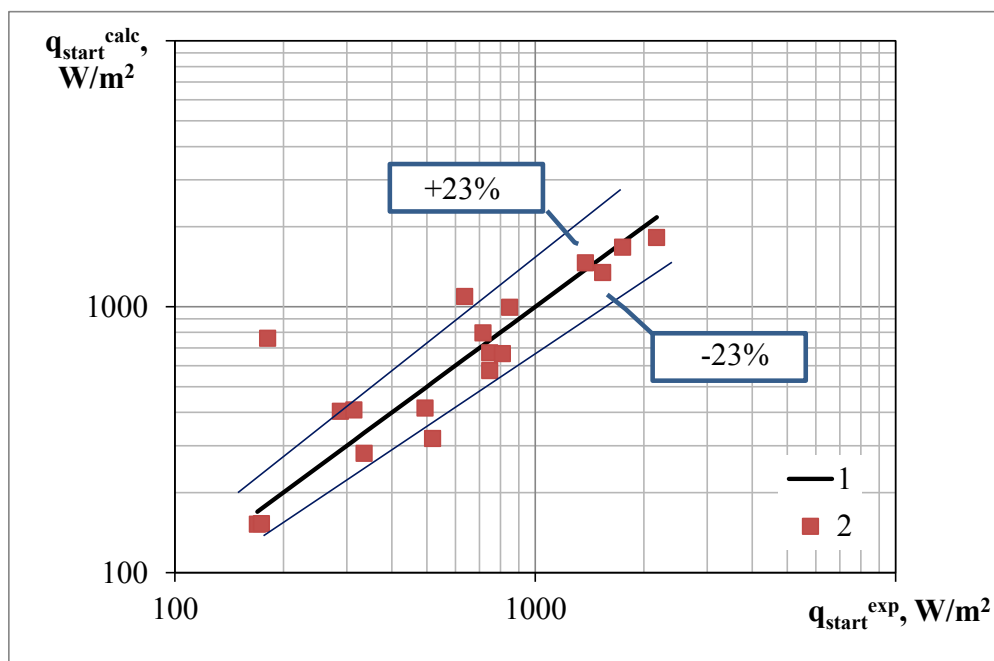
Least square method was used to find values of coefficient C and degrees b, m, k, f . Value of coefficient C depends on calculated heat flux density (start-up or transient), heat carrier type and inclination angle. This coefficient values are presented in table 5.1.

Table 5.1 – Values of coefficient C

Heat carrier type	q_{start}		q_{pulse}	
	Inclination angle		Inclination angle	
	90°	45°	90°	45°
Water	$2.1 \cdot 10^{-23}$		$3.5 \cdot 10^{-23}$	$2.3 \cdot 10^{-23}$
Alcohols	$4.5 \cdot 10^{-23}$		$7.5 \cdot 10^{-23}$	
Organic fluids	$1 \cdot 10^{-23}$		$9.5 \cdot 10^{-24}$	$1.3 \cdot 10^{-23}$

Values of degrees are independent from mentioned above factors and equal to: $b = -6.57$; $m = 0.93$; $k = 0.94$; $f = 1.07$.

In order to check accuracy of obtained equation (5.3) results of start-up heat flux density calculation were compared with experimental results as depicted in fig. 5.4.



1 – experimental data; 2 – calculation on (5.3)

Figure 5.4 – Comparison of calculated and experimental values of start-up heat flux density

As it can be seen from fig. 5.4, equation (5.3) generalizes 72% of experimental data with accuracy $\pm 23\%$ which is quite sufficient for engineering calculations. Results of calculation by equation (5.3) were also compared with values of start-up heat flux density obtained from experimental data presented by Patel et al. [106] (table 5.2).

Table 5.2 – Comparison of calculation results for start-up heat flux density with data from literature

Heat carrier	$q_{\text{start}}, \text{ W/m}^2$		$\delta, \%$
	Data [106]	Calculation on (5.3)	
Methanol	4201.9	5154.5	22.7
Acetone	4201.9	4762.6	13.3

As it can be seen from table 5.2, results of calculation on equation (5.3) are in good correlation not only with experimental data obtained in current investigation but also with data of other authors. It must be noted that design of PHP investigated in [106] differs from that in current investigation: it has inner diameter 2 mm, number of turns was equal to 9 and acetone was used as organic heat carrier. Length of HZ, AZ and CZ were also different but value of LR was in the range investigated in this study. Despite these differences deviation of calculated results from data [106] was not more than approximately 23% which in the range of equation (5.3) accuracy. Thus, equation (5.3) can be used for calculation of PHP start-up heat flux density for water, alcohols, and organic fluids as heat carriers in such conditions: the range of heat flux density from 150 to 4200 W/m², PHP inner diameter 1-2 mm, LR range from 0.069 to 0.481, inclination angle from +45° to +90°.

Results of transient heat flux density calculation on equation (5.3) were compared with experimental values as shown on fig. 5.5.

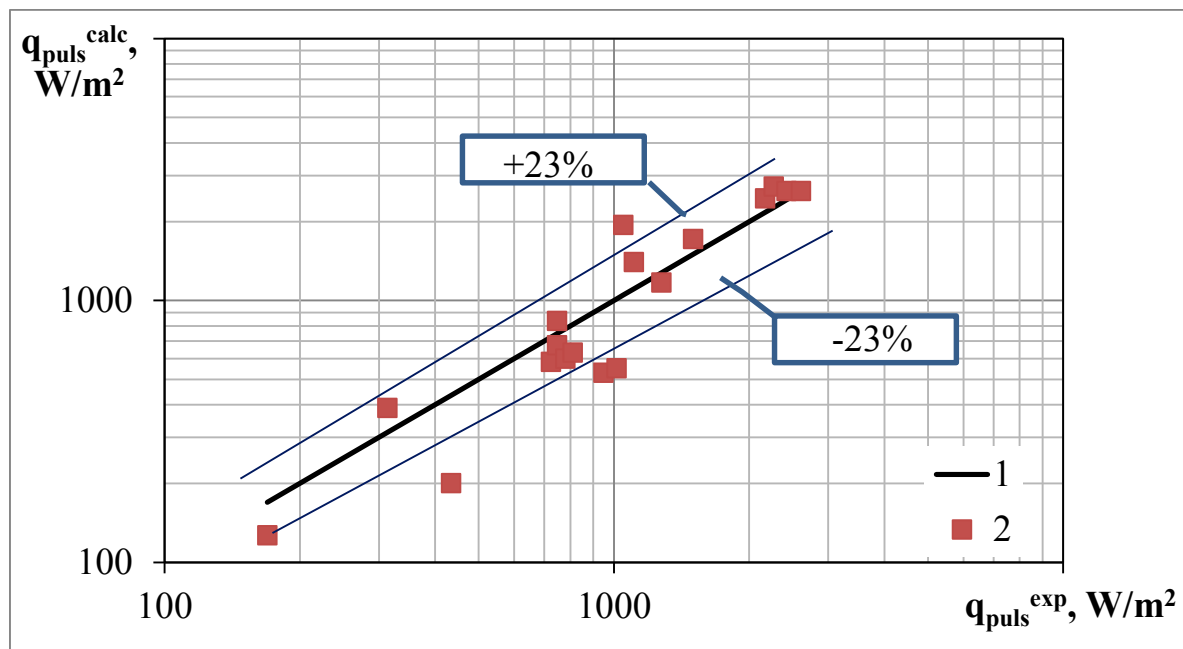


Figure 5.5 – Comparison of calculated and experimental values of transient heat flux density

Equation (5.3) generalizes 72% of experimental data with accuracy $\pm 23\%$ (fig. 5.5) which is quite sufficient for engineering calculations. This equation can be used for calculation of transient heat flux density for the same heat carriers and in the same conditions as for calculation of start-up heat flux density.

5.3 Conclusions

The above findings examine how inclination angle and PHP length ratio affect the start-up and transient behavior of a pulsating heat pipe. The key findings are summarized as follows.

1. The inclination angle significantly affects PHP start-up behavior by influencing the balance of forces acting on liquid slugs and vapor plugs. Horizontal orientation (0°) provides unfavorable conditions for vapor to come out of HZ which makes PHP start-up difficult, requiring the highest start-up heat flux density. The only force which can return liquid to HZ at this orientation is capillary force. Water, due to capillary force provided by its high surface tension, successfully starts at all tested length ratios (LR), whereas pentane fails to start at 0° for any LR. For water and methanol, increasing of inclination angle from 0° to $+90^\circ$ leads to decreasing of start-up heat flux density because it makes easier for vapor to come out of HZ, increases piston-like action of vapor bubbles and plugs on liquid slugs and gravity assists returning liquid to HZ. Start-up heat flux density for PHP with pentane is almost the same at inclinations $+90^\circ$ and $+45^\circ$ because pentane has the least kinematic viscosity which allows buoyancy force to act with approximately the same efficiency at both angles.

2. The impact of LR on start-up heat flux density varies with inclination angle and heat carrier properties. At $+90^\circ$ inclination, increasing LR reduces start-up heat flux density for all fluids due to the shortened adiabatic zone (AZ), which lowers hydraulic resistance and allows easier vapor transport to the condensation zone (CZ). For example, methanol's start-up heat flux density drops from 1747 W/m^2 at $\text{LR} = 0.069$ to 519 W/m^2 at $\text{LR} = 0.481$. At $+45^\circ$ inclination, water and methanol (and water also at 0°) exhibit a non-monotonic trend, where the least start-up heat flux density is observed at $\text{LR} =$

0.242. This occurs because such LR provides well balanced conditions for both returning of liquid to HZ by capillary force and immediate active boiling for initiating of heat carrier pulsating movement. Pentane follows the same trend at $+45^\circ$ as at $+90^\circ$.

3. PHP fails to start at -45° and -90° inclinations for all tested configurations. This happens because HZ is occupied by long vapor plugs and gravity counteracts capillary forces, preventing liquid slugs from returning to the heating zone (HZ). Since the capillary force of the tested heat carriers is not strong enough to overcome gravity at negative inclinations, PHP start-up is impossible in these orientations.

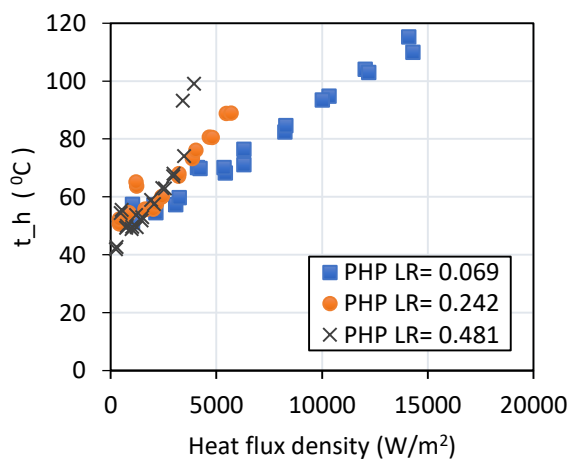
4. The transition to pulsation mode is easier at higher inclination angles and longer length ratios (LR). Increasing LR reduces transient heat flux density (q_{pulse}), as larger heat transfer areas in the HZ contains more large-size nucleation sites, requiring lower heat flux density for activation and, thus, lower heat flux density to initiate sustainable pulsating heat carrier movement. Decreasing inclination angles (approaching 0°) hinders vapor movement, requiring a larger number of active nucleation sites to provoke immediate explosive boiling for starting of pulsating movement. This necessitates higher heat flux densities. Among the tested fluids, pentane exhibits the lowest q_{pulse} (169.4 W/m² at LR = 0.481).

5. A generalized dimensionless correlation is developed for predicting start-up and transient heat flux density in PHPs. The proposed equation was validated through comparison with both experimental data and literature, exhibiting an accuracy of $\pm 23\%$. It can be used for water, alcohols, and organic fluids as heat carriers in the range of heat flux density from 150 to 4200 W/m², PHP inner diameter 1-2 mm, LR range from 0.069 to 0.481, inclination angle from $+45^\circ$ to $+90^\circ$.

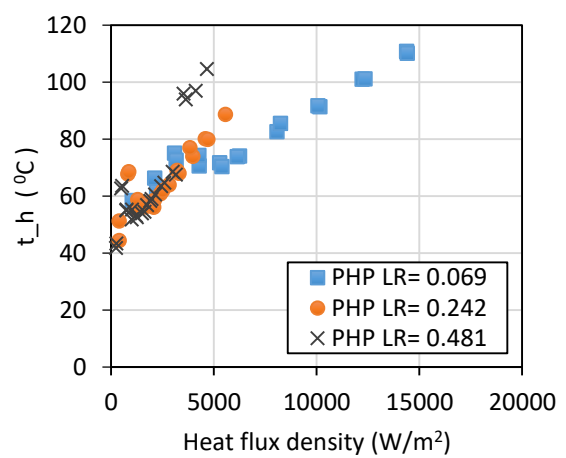
Chapter 6 - Heat Transfer Characteristics of Pulsating Heat Pipe

6.1 Average temperature of heating zone

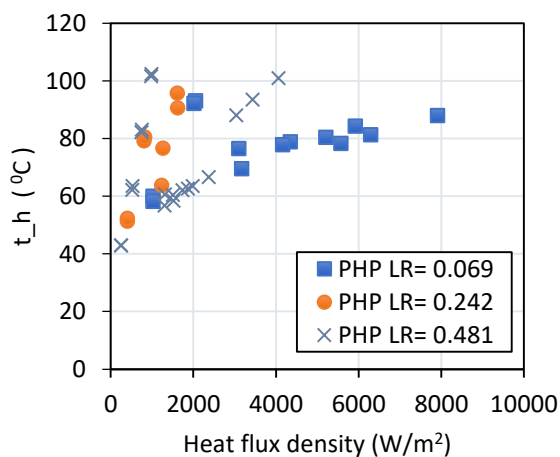
It is important to know the average heating zone temperature (t_h) of PHP intended for electronics cooling because temperature of cooled electronic element is connected with it. Dependence of average HZ temperature on heat flux density, PHP LR, orientations, and working fluids is presented on fig. 6.3.



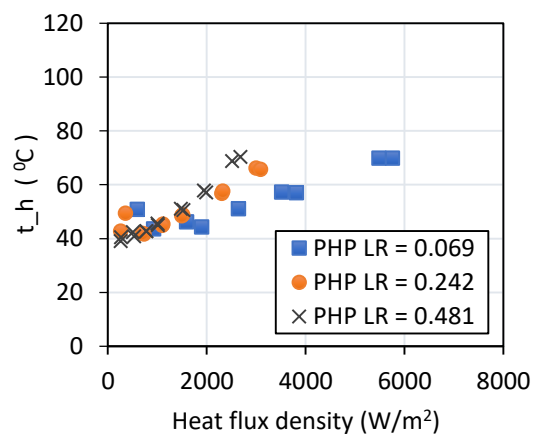
(a) Water – orientation 90°



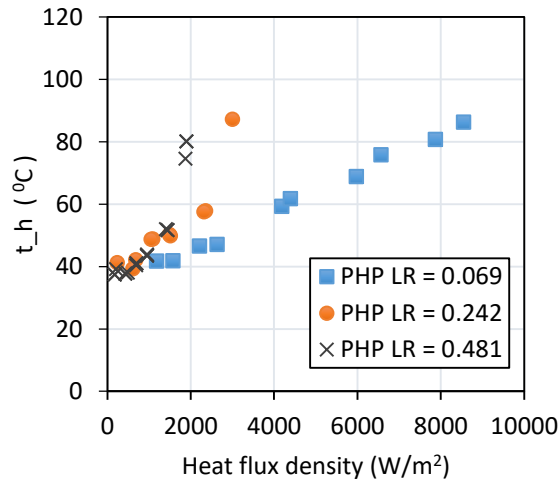
(b) Water – orientation 45°



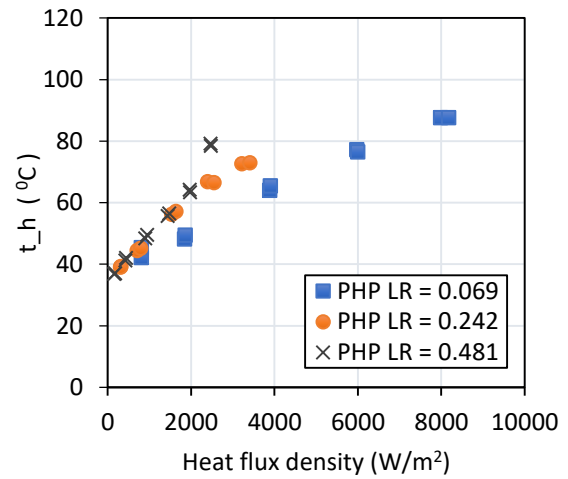
(c) Water – orientation 0°



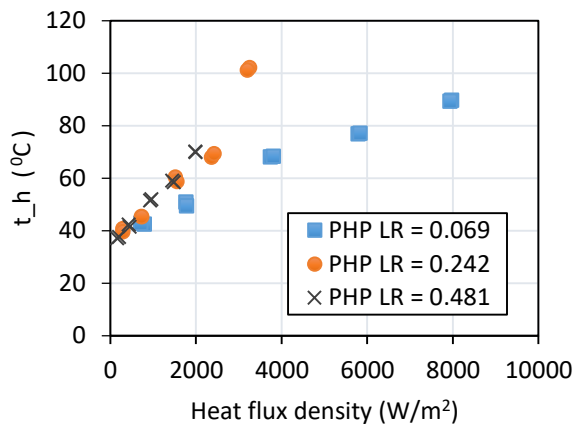
(d) Methanol – orientation 90°



(e) Methanol- orientation 45°



(f) Pentane -orientation 90°



(g) Pentane -orientation 45°

Figure 6.1– Analysis of average temperature of heating zone at various PHP length ratio and inclinations

As it can be seen from fig. 6.1, average HZ temperature is equal for LR 0.242 and 0.481 and higher than that for LR 0.069 in all cases, except PHP with water in horizontal orientation (fig. 6.1c). Analysis of obtained experimental data has shown that increasing of LR leads not only to increasing of average HZ temperature but to increasing of average CZ temperature also. This means that overall temperature level of PHP increases and, as a consequence, increases pressure inside PHP. It leads to increasing of saturation temperature which provokes increasing of average HZ temperature.

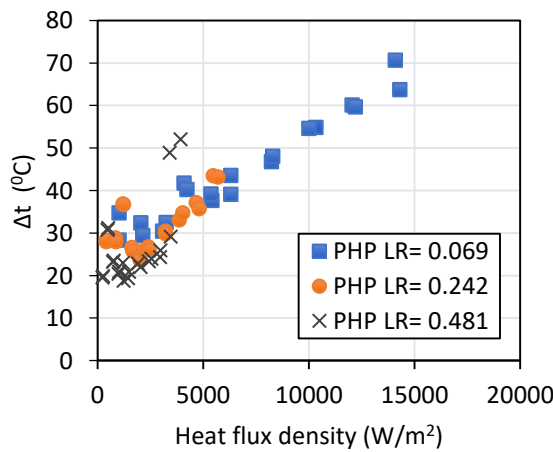
The other picture is observed for PHP with water at 0° inclination angle (fig. 6.1c). Average HZ temperature for LR 0.481 is lower than for LR 0.069 in the range of heat flux density from 1300 to 3000 W/m^2 and vice versa when heat flux density is higher than 3000 W/m^2 . PHP with LR 0.242 has the highest average HZ temperature. Such behavior of average HZ temperature for LR 0.069 and 0.481 can be explained by that fact that PHP with LR 0.481 works in pulsating mode of operation when PHP with LR 0.069 only starts to operate, at heat flux density range 1300-3000 W/m^2 . At higher heat flux densities both PHP configurations operates in pulsating mode and difference between their average HZ temperature is caused by by precrisis behavior of PHP with LR of 0.481 which makes its average HZ temperature higher than for LR 0.069. PHP with LR 0.242 demonstrates the highest average HZ temperature because of its unstable operation (it returned to heat conductivity mode after working in thermosyphone mode).

There are some differences between values of average HZ temperature in last points, which correspond to the highest heat flux densities, for LR 0.242 and 0.481 in almost all cases. This is because of beginning of dry-out process in these points. Decreasing of inclination angle leads to increasing of average HZ temperature (fig. 6.1) due to the complication of conditions for vapor to come out form HZ and decreasing of gravity influence on heat carrier movement. This deteriorates heat transfer from HZ wall to heat carrier and, as a consequence, increases its temperature.

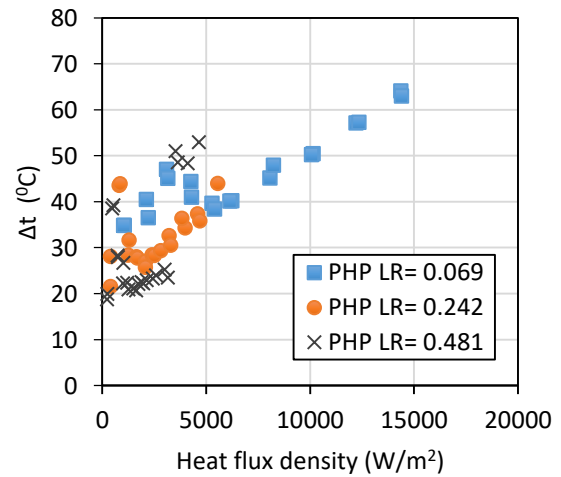
PHP with methanol has the least average HZ temperature, PHP with pentane – the highest and PHP with water – in between them. This is because critical radius of nucleation sites for methanol is much smaller than for water. It means that in HZ of PHP with methanol acts more nucleation sites than in PHP with water at the same heat flux density. This leads to intensification of heat transfer between HZ wall and heat carrier which provokes decreasing of HZ temperature. Critical radius of nucleation sites for pentane is lower than for methanol but this together with low heat of vaporization lead to generation of big amount of vapor in HZ and not all of this vapor condensates in CZ. Thus, large parts of PHP can be occupied by vapor which deteriorates heat transfer in PHP and leads to increasing of average HZ temperature.

6.2 Temperature difference

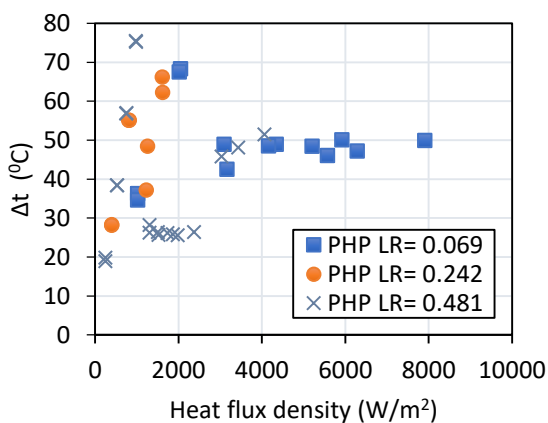
Temperature difference (Δt) between the heating and cooling zones provides important insights into the thermal behaviour of pulsating heat pipes (PHP), namely, it allows to estimate efficiency of PHP operation. As for the practical applications, such as electronics cooling, PHP temperature difference makes the largest contribution in overall temperature difference between cooled electronic component and cooling medium when PHP is used as a main heat transfer device of a system. The variation of PHP temperature difference against heat flux density under different operating conditions, including working fluid types, PHP length ratio (LR), and orientations is shown on fig. 6.2



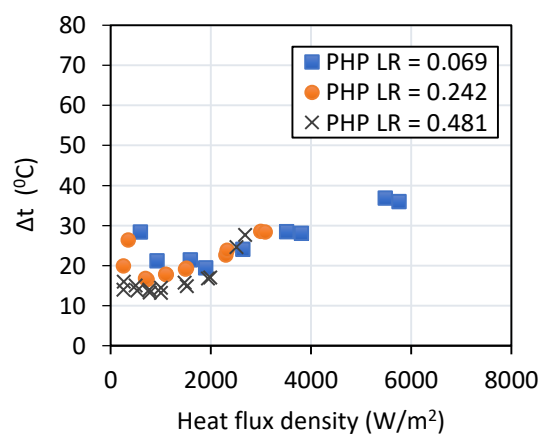
(a) Water – orientation 90°



(b) Water – orientation 45°



(c) Water – orientation 0°



(d) Methanol – orientation 90°

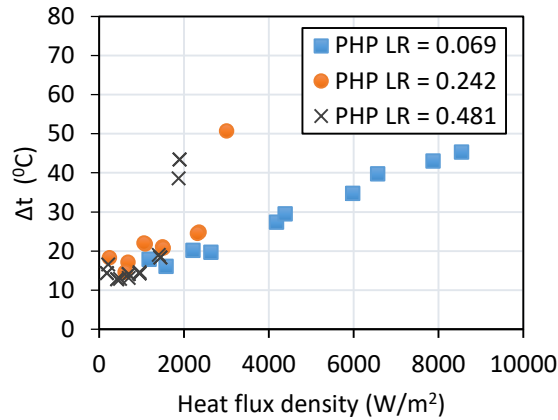
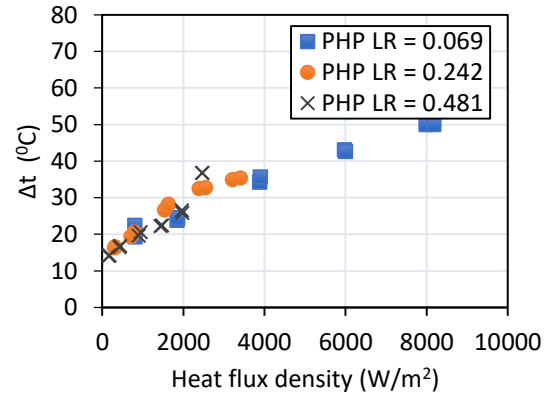
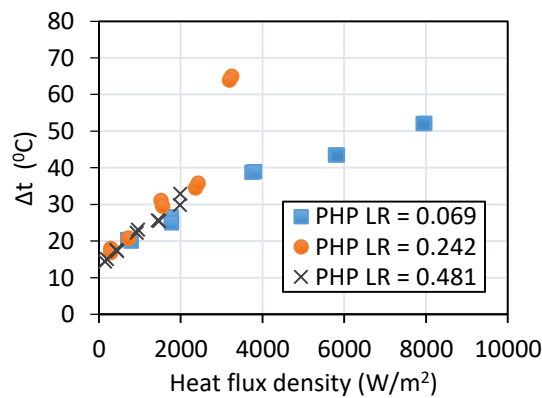
(e) Methanol- orientation 45^0 (f) Pentane -orientation 90^0 (g) Pentane -orientation 45^0

Figure 6.2 – Effect of heat flux density on temperature difference at various PHP length ratio and inclination angles

The variation of PHP temperature difference with heat flux density slightly differs for different heat carriers. For water, temperature difference drastically rises at low heat flux densities, then it decreases and rises again at higher heat flux densities. This trend is similar for all inclination angles (fig. 6.2a-c). It indicates the start-up moment of PHP. At low heat flux densities heat is transferred along PHP by heat conductivity (heat conductivity mode of operation) which provokes drastically increasing of temperature difference with increasing of heat flux density. This increasing lasts until start-up moment when boiling starts in HZ initiating heat carrier movement and two-phase heat transfer. Beginning from this moment temperature difference decreases because two-

phase heat transfer is much more effective than heat conductivity. This decreasing corresponds to thermosyphone, transient and beginning of pulsating mode of PHP operation. The last part of the dependence $\Delta t = f(q_{HZ})$, where temperature difference increases again, corresponds to pulsating mode of operation and increasing of temperature difference is a consequence of heat flux density increasing. The last points with the highest temperature difference correspond to dry-out moment. Slightly different picture is observed for methanol (fig. 6.2d-e) where temperature difference decreases at low heat flux densities and increases at higher heat flux densities. This is because PHP with methanol starts at 1.5-2 times lower input heat flux than PHP with water, thus, duration of working in heat conductivity mode for PHP with methanol is much shorter than for PHP with water and this operational mode is presented on each graph for methanol only by the first point. So, in fact, graphs for methanol depict thermosyphone, transient and pulsating mode of operation and have the same form as for water at the same operating modes. For PHP with pentane, temperature difference increases with increasing of heat flux density (fig. 6.2f-g). This is because PHP with pentane begin to operate in pulsating mode instantly (only at inclination angle $+45^\circ$ it has very short transient period) and such temperature difference behaviour corresponds to this mode of operation.

For water and methanol, increasing of LR leads to decreasing of PHP temperature difference. It can be explained by decreasing of start-up and transient heat flux density with increasing of LR. This means, that PHP with the largest LR can operate in pulsating mode and has, correspondingly, the least temperature difference, PHP with the least LR – in heat conductivity mode and has the highest temperature difference and PHP with middle LR – in thermosyphone or transient mode and its temperature difference is between two previous at the same heat flux density. Temperature difference of PHP with pentane is almost independent from LR (fig. 6.2f-g). Let us consider average HZ temperature to explain such behavior (fig. 6.3f-g). This temperature rises with increasing of LR. This means that average CZ temperature should also rise to maintain temperature difference at almost constant level for different LR at the same heat flux density in HZ.

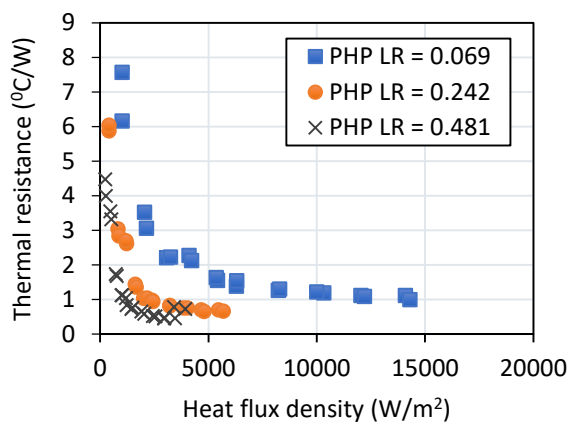
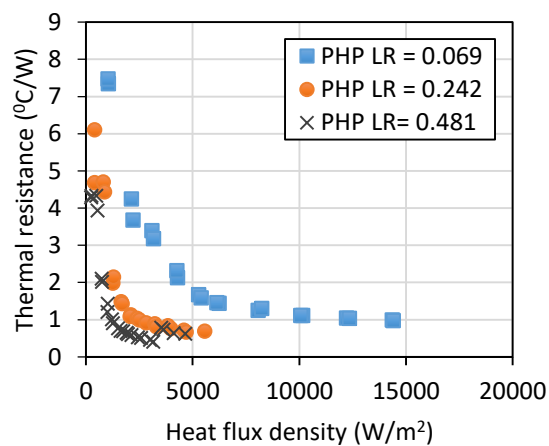
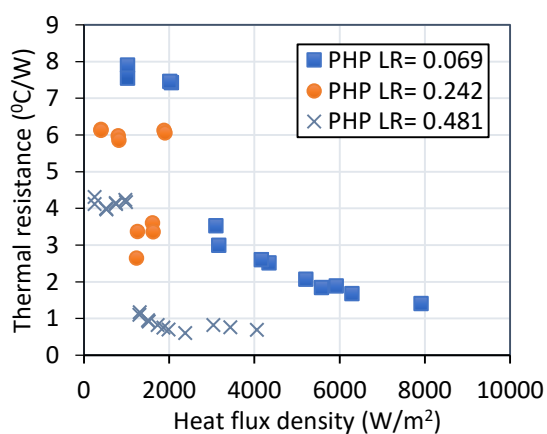
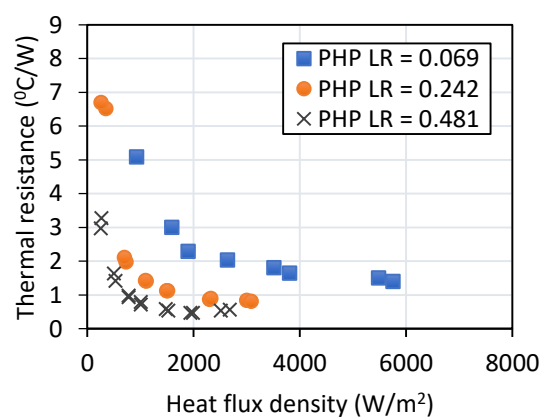
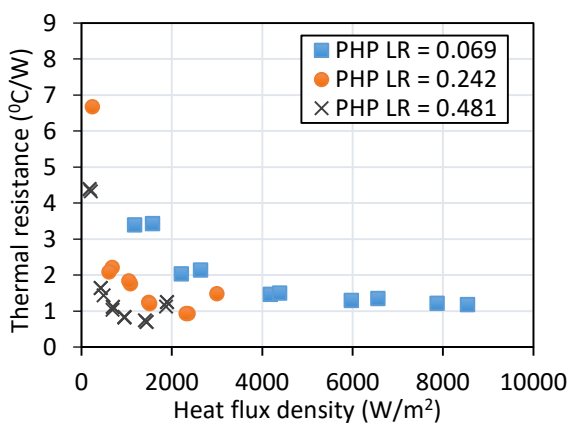
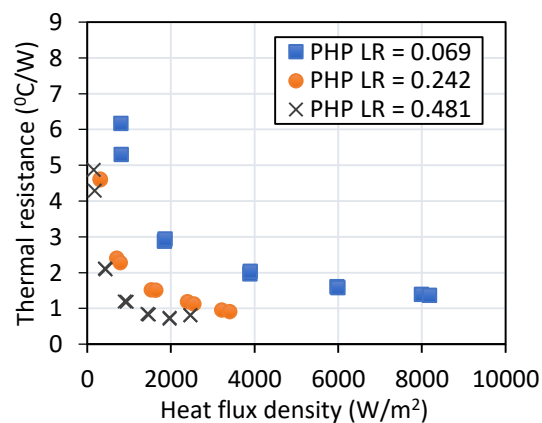
Obtained experimental data confirm increasing of average CZ temperature with increasing of LR at such conditions. It means that increasing of LR intensifies heat and mass transfer between HZ and CZ. This intensification takes place because increasing of LR leads to increasing of heat transfer area which, in its turn, increases number of active nucleation sites in HZ at the same heat flux density.

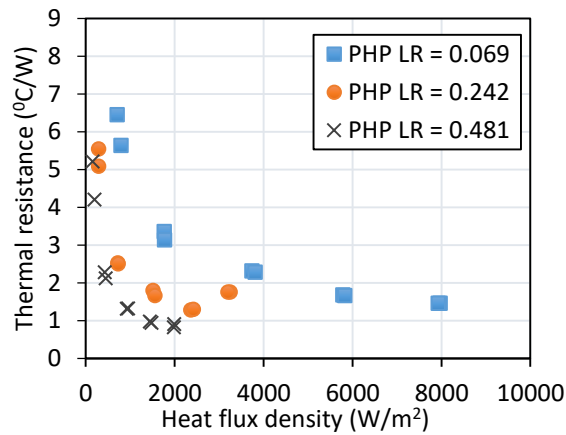
Decreasing of inclination angle leads to increasing of PHP temperature difference for all tested heat carriers (fig. 6.2). This is because of deterioration of conditions for vapor to come out from HZ and decreasing of gravity influence on heat carrier movement with decreasing of inclination angle.

Methanol provides the least PHP temperature difference, pentane – the highest one and water – in between them. Critical radius of nucleation sites for methanol is much lower than for water, thus there more active nucleation sites in HZ of PHP with methanol than with water at other equal conditions. This means more active heat carrier movement and heat and mass transfer between HZ and CZ which decreases temperature difference. Critical radius of nucleation sites for pentane even lower than for methanol but high number of active nucleation sites together with the least heat of vaporization among all tested heat carriers provides generation of big amount of vapor. Not all vapor condensates in CZ which leads to occupation of large parts of PHP with vapor. This deteriorates heat and mass transfer between HZ and CZ and increases temperature difference.

6.3 Thermal resistance

The thermal performance of a pulsating heat pipe (PHP) is evaluated through the overall thermal resistance, which shows the efficiency of heat transfer. The fig. 6.3 illustrate how thermal resistance varies with HZ heat flux density for different working fluids, PHP length ratio, and inclination angles.

(a) Water – orientation 90° (b) Water – orientation 45° (c) Water – orientation 0° (d) Methanol – orientation 90° (e) Methanol- orientation 45° (f) Pentane -orientation 90°



(g) Pentane -orientation 45°

Figure 6.3– Effect of heat flux density on thermal resistance at various PHP length ratio and inclination angles

Thermal resistance consistently decreases as heat flux density increases (fig. 6.3). This decrease is primarily due to enhanced fluid circulation within the PHP, facilitating more effective heat and mass transfer. Increasing the PHP length ratio contributes to reduced thermal resistance because of three reasons: decreasing of start-up and transient heat flux density, increasing of number of potential nucleation sites, and minimizing the adiabatic zone (AZ) length. As it was shown and explained in previous Chapter, increasing of LR leads to decreasing of start-up and transient heat flux density, which means PHP begins to work and transfers to pulsating mode at lower heat flux density. When heat flux density in HZ is lower than start-up level ($q_{HZ} < q_{start}$) PHP has the highest thermal resistance because two-phase heat transfer has not started yet and heat is transferred only by heat conductivity of PHP casing. The least thermal resistance corresponds to pulsating mode of operation which takes place at $q_{HZ} \geq q_{pulse}$ because pulsating movement of heat carrier is stable in this operational mode, and it provides effective two-phase heat transfer between HZ and CZ. PHP thermal resistance in thermosyphon and transient modes ($q_{start} \leq q_{HZ} < q_{pulse}$) is in between two previous but still too high for most practical applications because pulsating motion of heat carrier, which has already started, is unstable. For example, thermal resistance of PHP with water

at $+90^\circ$ inclination angle and heat flux density approximately 1000 W/m^2 is equal to $1.13 \text{ }^\circ\text{C/W}$ for $\text{LR} = 0.482$, $2.73 \text{ }^\circ\text{C/W}$ – for $\text{LR} = 0.242$ and $6.16 \text{ }^\circ\text{C/W}$ – for $\text{LR} = 0.069$ (fig. 6.3a). This is because PHP with the highest LR works in pulsating mode of operation at this heat flux density, PHP with the least one has not started yet and PHP with $\text{LR} = 0.242$ works in thermosyphone or transient mode.

Analysing graphs on fig. 6.3 one can see, that tendency on decreasing of thermal resistance with increasing of LR still remains true even when all PHP configurations work in pulsating mode. This can be explained by increasing of number of potential nucleation sites with increasing of LR. The latter leads to increasing of heat transfer area. The larger heat transfer area the more potential nucleation sites are placed on it. More potential nucleation sites mean more active nucleation sites when boiling occurs. Action of larger number of nucleation sites provoke more active pulsating heat carrier movement inside PHP which provides more effective heat and mass transfer and leads to decreasing of thermal resistance. Additionally, with a higher PHP length ratio, the working fluid transfers heat directly from the heating zone to the condensation zone with minimal energy losses, avoiding energy dissipation on AZ hydraulic resistance. For instance, when the PHP length ratio reaches 0.481, the AZ is nearly eliminated, enabling a direct and efficient energy transfer from HZ to CZ. Conversely, shorter length ratio increases AZ hydraulic resistance, necessitating additional energy to overcome it, thereby increasing the temperature difference along the PHP and raising its thermal resistance.

Among the tested working fluids, PHP with water and methanol exhibits the least thermal resistance and PHP with pentane – the highest one. For example, the least thermal resistance values, which were achieved at $\text{LR} = 0.481$ and vertical bottom heating orientation ($+90^\circ$), are: $0.45 \text{ }^\circ\text{C/W}$ for water, $0.47 \text{ }^\circ\text{C/W}$ for methanol and $0.72 \text{ }^\circ\text{C/W}$ for pentane (fig. 6.3a, d, f respectively). Despite that fact, that lowest values of thermal resistance for water and methanol are very close to each other, they were obtained at different heat flux densities: 2954 W/m^2 for water and 1990 W/m^2 for methanol. Such trend, when PHP with methanol has lower thermal resistance than PHP

with water at the same values of heat flux density, is true in the whole range of working heat flux densities for both positive inclination angles ($+45^\circ$ and $+90^\circ$) at all tested length ratios. This is because critical radius of nucleation sites for methanol is approximately 12-13 times lower than for water at other equal conditions. Taking into account, that only these nucleation site activates whose dimensions are larger than critical radius, there are much more active nucleation sites in HZ of PHP with methanol than PHP with water at the same heat flux density. This provides more active pulsating heat carrier movement in PHP with methanol and, thus, intensifies heat and mass transfer decreasing thermal resistance. From this point of view, PHP with pentane should have the least thermal resistance among all tested heat carriers because critical radius of nucleation site for pentane is approximately 2.5-2.6 times lower than for methanol, but, in fact the situation with thermal resistance is vice versa. This is because the highest number of active nucleation sites and the lowest heat of vaporization provides generation of large amount of vapour in HZ. For example, mass flow rate vapor at inclination angle $+90^\circ$ and $LR = 0.481$ during start-up moment for PHP with water is $1.9 \cdot 10^{-6}$ kg/s and for PHP with pentane – $9.3 \cdot 10^{-6}$ kg/s, i.e., vapor mass flow rate for PHP with pentane is approximately 4.9 times higher than for PHP with water. In means, that it takes only for 62 s to evaporate all pentane filled to PHP at full absence of condensation. Taking into account, that amount of vapour phase tends to increase during PHP operation, such intensive pentane evaporation leads to occupying of large parts of PHP with vapour which decreases intensity of pulsating heat carrier movement and, as a consequent, decreases intensity of heat and mass transfer and increases thermal resistance. At heat flux densities more than approximately 2000 W/m^2 , both methanol and pentane display a slight increase in thermal resistance (fig. 6.3e-g) due to the onset of the dry-out phenomenon, where the liquid film within the heating zone evaporates completely, thereby hindering heat and mass transfer. Unlike these two heat carriers, PHP with water continues operating with decreasing thermal resistance up to approximately $5500\text{-}14000 \text{ W/m}^2$ which makes it more suitable for applications with high heat load.

Inclination angle plays a significant role in the thermal resistance behaviour of PHPs. Generally, decreasing of inclination angle from $+90^\circ$ to 0° leads to increasing of thermal resistance, but there are some peculiarities connected with PHP operational modes, heat flux density and heat carriers. Inclination angle influence is more pronounced when PHP has not reached pulsating mode of operation yet. This is attributed to effect of inclination angle on start-up heat flux density and borders of operational modes which was described and explained in previous Chapters. At pulsating mode of operation difference between values of thermal resistance for angles $+90^\circ$ and $+45^\circ$ decreases with increasing of heat flux density, but thermal resistance at angle 0° remains the highest one. This can be explained by difficulties for vapor to come out from HZ and decreasing of gravity influence on heat carrier movement at horizontal position. Thermal resistance of PHP with pentane demonstrates the least sensitivity to inclination angle among all tested heat carriers.

In summary, $LR=0.481$ provides the least PHP thermal resistance when compared to other tested LR. PHP with water and methanol demonstrates the least thermal resistance at all LR and inclination angles, but water is more suitable for applications with high heat load and methanol – for low-power applications where start-up and transferring to pulsating mode at lower heat flux densities are necessary. Pentane, while less efficient, may still be suitable for specific low-power applications for which early start-up and low sensibility to inclination angle are the most important features. The findings provide valuable guidance for designing advanced thermal management systems for electronics cooling leveraging PHP technology.

6.4 Conclusions

The operating characteristics of pulsating heat pipes (PHPs) are influenced by multiple factors, including length ratio (LR), inclination angle, and working fluid properties. The following conclusions summarize the key findings related to average HZ temperature, temperature difference and thermal resistance under various operating conditions.

1. The length ratio (LR) of the pulsating heat pipe (PHP) has a notable impact on heat transfer characteristics, influencing average heating zone (HZ) temperature. In most cases, increasing LR leads to a rise in the average HZ temperature due to a higher internal pressure and saturation temperature. However, higher LR also promotes lower thermal resistance by increasing the number of active nucleation sites, reducing start-up heat flux, and enhancing two-phase heat transfer.

2. The inclination angle plays a critical role in PHP efficiency by influencing the movement of the working fluid. A vertical bottom-heated orientation ($+90^\circ$) provides the most effective heat transfer due to pushing action of vapor formations on liquid slugs and gravity-assisted fluid circulation, reducing average HZ temperature, temperature difference and thermal resistance and maintaining stable oscillations of the working fluid. As the inclination angle decreases, the difficulty in vapor escape from the heating zone increases, leading to higher HZ temperatures and greater thermal resistance. The horizontal configuration (0°) exhibits the least efficient heat and mass transfer, with significant temperature and thermal resistance rising because of vapor stagnation in HZ. While water and methanol show strong inclination-dependent performance, pentane is less sensitive to inclination angle variations in the range from $+90^\circ$ to $+45^\circ$ due to its low viscosity and enhanced vapor motion.

3. The choice of working fluid significantly affects PHP performance, as different fluids exhibit distinct thermal characteristics based on their nucleation site critical radius, latent heat of vaporization. PHP with methanol demonstrates the least average heating zone temperatures and temperature difference, its thermal resistance is almost equal to that one of PHP with water. But PHP with methanol reaches the same values of thermal resistance at significantly lower heat flux density than PHP with water. This is due to low critical radius of nucleation sites of methanol which leads to higher number of active nucleation sites than that of water at the same heat flux densities, enabling earlier pulsating motion. Despite the least among all tested liquids critical radius of nucleation sites for pentane, PHP with this heat carrier suffers from excessive vapor generation,

leading to high average HZ temperatures, greater thermal resistance, and lower heat transfer efficiency.

CONCLUSIONS

As a result of this study, an experimental investigation was carried out to analyze the start-up and transient characteristics of pulsating heat pipes (PHPs) across diverse geometrical and operational conditions. These characteristics are regarded as key parameters of PHP intended for electronics cooling because they directly affect beginning of PHP working and its transition to the most effective pulsating mode of operation and, thus, influence PHP thermal behavior. A dedicated experimental setup was designed, incorporating copper PHPs with five turns, varying heating zone lengths, and multiple inclination angles to systematically evaluate their performance under different working conditions. The study focused on the influence of PHP length ratio, inclination angle, and thermophysical properties of heat carriers on critical aspects such as startup and transient heat transfer characteristics, pulsation stability, dry-out limits and heat transfer characteristics of PHP.

The findings from this research play a vital role in the advancement of PHP technology, enabling the development of more efficient thermal management solutions particularly relevant for electronics cooling and high-performance heat dissipation applications, where compact, lightweight, and energy-efficient thermal systems are essential. The key findings of this study are summarized as follows:

1. As a result of PHP performance analysis, main PHP operational modes were defined as follows: heat conductivity, thermosyphone, transition, and pulsating mode. The least efficient mode is heat conductivity mode when heat is transferred only by heat conductivity of PHP casing because of absence of heat carrier movement inside PHP. Pulsating mode demonstrates the highest heat transfer efficiency due to stable pulsating movement of heat carrier between HZ and CZ which provides two-phase heat transfer. Start-up characteristics (heat flux density and temperature) correspond to beginning of heat carrier movement inside PHP and transient heat flux density – to beginning of pulsating mode. Values of start-up and dry-out input heat flux and borders of all

operational modes are strongly dependent on length ratio (LR), inclination angle and heat carrier properties.

2. PHP length ratio significantly affects start-up and transient behavior. A higher LR (0.481) requires 1.5-2.5 times higher heat input to start-up for water and 1.4-2 times higher heat input for transition into pulsating mode for water and methanol than a lower LR (0.069), but it doesn't influence on start-up and transient characteristics for pentane. From other hand, in most cases, it provides lower amplitude of temperature pulsations and 1.2-1.5 times higher dry-out heat input. The least LR (0.069) enables start-up at low heat input but suffered from early dry-out, highlighting a trade-off between quick activation and working at high heat loads.

3. Working fluid selection influences start-up time, pulsation amplitude and stability, operating mode borders and dry-out limits. Using of heat carriers with low heat of vaporization and saturation temperature, such as methanol and pentane, provides low values of start-up and transient heat input fluxes and shifts borders of operational modes toward lower heat inputs but dry-out occurs also at lower heat input fluxes. PHP with pentane has the most stable pulsations with the least amplitude. Water also provides stable pulsations but with the highest amplitude. Amplitude of pulsations for methanol PHP is in between two previous but pulsations are very unstable.

4. A 50-fold increase in vapor density results in 2 times decreasing of start-up heat flux density, 1.5-1.8 times decreasing in start-up temperature and decreasing of transient heat flux density, due to decreasing of work necessary for bubble formation during boiling process. Increasing of liquid thermal conductivity leads to increasing of start-up and transient characteristics. Increasing of such liquid properties as: surface tension, viscosity, and density increases start-up temperature, start-up and transient heat flux density, as they introduce greater resistance to bubble formation and heat carrier movement. Liquids with high heat capacity and heat of vaporization need more energy for heating up to saturation and evaporation and, thus, higher start-up and transient characteristics.

5. Inclination angle significantly affects PHP start-up and transient behavior. At horizontal orientation (0°), PHP requires the highest start-up and transient heat flux density, because conditions for vapor to leave HZ are the most unfavorable. With increasing of inclinations angle from 0° to $+90^\circ$ these conditions become more favorable and start-up and transient heat flux density decreases. PHP with water successfully starts at all LR, whereas PHP with pentane fails to start in horizontal orientation and PHP with methanol starts only with LR of 0.069. All tested PHP configurations failed to start at -45° and -90° inclination angles.

6. The impact of LR on start-up heat flux density varies with inclination angle and heat carrier properties. At $+90^\circ$ inclination, increasing LR reduces start-up heat flux density for all fluids due to the shortened adiabatic zone (AZ), which lowers hydraulic resistance and allows easier vapor transport to the condensation zone (CZ). At $+45^\circ$ inclination, water and methanol (and water also at 0°) exhibit a non-monotonic trend, where the least start-up heat flux density is observed at $LR = 0.242$. This occurs because such LR provides well balanced conditions for both returning of liquid to HZ by capillary force and immediate active boiling for initiating of heat carrier pulsating movement. Pentane follows the same trend at $+45^\circ$ as at $+90^\circ$.

7. Increasing of PHP length ratio leads to increasing of average heating zone (HZ) temperature due to higher internal pressure and saturation temperature. However, higher LR also enhances heat transfer efficiency by improving number of active and potential nucleation sites density and, thus, decreases PHP temperature difference and thermal resistance.

8. A vertical bottom-heated orientation ($+90^\circ$) provides the most effective heat and mass transfer due to pushing action of vapor formations on liquid slugs and gravity-assisted fluid circulation, reducing average HZ temperature, temperature difference and thermal resistance and maintaining stable oscillations of the working fluid. As the inclination angle decreases, the difficulty in vapor escape from the HZ increases, leading to higher HZ temperatures and greater thermal resistance. The horizontal configuration (0°) exhibits the least efficient heat and mass transfer, with significant temperature and

thermal resistance rising because of vapor stagnation in HZ. While water and methanol show strong inclination-dependent performance, pentane is less sensitive to inclination angle variations in the range from $+90^\circ$ to $+45^\circ$ due to its low viscosity and enhanced vapor motion.

9. PHP with methanol demonstrates the least average HZ temperatures and temperature difference, its thermal resistance is almost equal to that one of PHP with water. PHP with pentane suffers from excessive vapor generation, leading to high average HZ temperatures, greater thermal resistance, and lower heat transfer efficiency. The differences between heat transfer characteristics of PHP with tested heat carriers are caused by differences in their heat of vaporization and critical radius of nucleation sites.

10. For the first time, empirical dimensionless correlation is proposed for predicting start-up and transient heat flux density in PHPs. It has an accuracy of $\pm 23\%$ and can be used for water, alcohols, and organic fluids as heat carriers in the range of heat flux density from 150 to 4200 W/m², PHP inner diameter 1-2 mm, LR range from 0.069 to 0.481, inclination angle from $+45^\circ$ to $+90^\circ$.

11. For practical applications, using of PHP with LR of 0.481 can be recommended because such LR provides the least start-up, transient characteristics, temperature difference and thermal resistance. Water can be used for high-load applications where high start-up, transient characteristics and high pulsations amplitude are acceptable. If low start-up and transient heat flux density are crucial it is better to use methanol but with regard to its dry-out at low heat input.

REFERENCES

- [1] G. E. Moore, ‘Cramming more components onto integrated circuits, Reprinted from Electronics, volume 38, no.8, *IEEE Solid-State Circuits Soc. Newsl.*, vol. 11, no. 3, pp. 33–35, 2006.
- [2] S. M. Sohel Murshed and C. A. Nieto de Castro, ‘A critical review of traditional and emerging techniques and fluids for electronics cooling’, *Renew. Sustain. Energy Rev.*, vol. 78, pp. 821–833, 2017.
- [3] A. Faghri, ‘Heat Pipes: Review, Opportunities and Challenges’, *Front. Heat Pipes*, vol. 5, no. 1, 2014.
- [4] Akachi H., Structure of heat pipe, US patent 4921041, 1990..
- [5] H. Han, X. Cui, Y. Zhu, and S. Sun, ‘A comparative study of the behavior of working fluids and their properties on the performance of pulsating heat pipes (PHP)’, *Int. J. Therm. Sci.*, vol. 82, no. 1, pp. 138–147, 2014.
- [6] M. B. Shafii, A. Faghri, and Y. Zhang, ‘Thermal modeling of unlooped and looped pulsating heat pipes’, *J. Heat Transfer*, vol. 123, no. 6, pp. 1159–1172, 2001.
- [7] G. M. Khandekar, S. Schneider, M., ‘Mathematical Modeling of Pulsating Heat Pipes: State of the art and future challenges’, *ISHMT-ASME-joint Int. Conf. Heat Mass Transf. Kolkata, India*, vol. 60, no. c, pp. 856–862, 2002.
- [8] M. Groll, S. Khandekar, Pulsating heat pipes: Progress and Prospects’, *Energy*, vol. 3, no. i, pp. 1–8, 2003.
- [9] Q. Cai, C. L. Chen, and J. F. Asfia, ‘Operating characteristic investigations in pulsating heat pipe’, *J. Heat Transfer*, vol. 128, no. 12, pp. 1329–1334, 2006.
- [10] P. Charoensawan, S. Khandekar, M. Groll, and P. Terdtoon, ‘Closed loop pulsating heat pipes - Part A: Parametric experimental investigations’, *Appl. Therm. Eng.*, vol. 23, no. 16, pp. 2009–2020, 2003.

- [11] X. Han, X. Wang, H. Zheng, X. Xu, and G. Chen, ‘Review of the development of pulsating heat pipe for heat dissipation’, *Renew. Sustain. Energy Rev.*, vol. 59, pp. 692–709, 2016.
- [12] Akachi H., US patent 5490558, 1996.
- [13] S. R. Hosoda M, Nishio S, ‘Meandering closed- loop heat-transport tube propagation phenomena of vapor plug’, in *Proceedings of 5th ASME/JSME joint thermal engineering conference*, pp. 737–44, 1999.
- [14] H. T. M. Dobson R. T., ‘Lumped parameter analysis of closed and open oscillatory heat pipes’, in *Proceedings of the 11th International Heat Pipe Conference*, pp. 137–142, 1999.
- [15] P. Charoensawan and P. Terdtoon, ‘Thermal performance of horizontal closed-loop oscillating heat pipes’, *Appl. Therm. Eng.*, vol. 28, no. 5–6, pp. 460–466, 2008.
- [16] H. Yang, S. Khandekar, and M. Groll, ‘Operational limit of closed loop pulsating heat pipes’, *Appl. Therm. Eng.*, vol. 28, no. 1, pp. 49–59, 2008.
- [17] H. Yang, S. Khandekar, and M. Groll, ‘Performance characteristics of pulsating heat pipes as integral thermal spreaders’, *Int. J. Therm. Sci.*, vol. 48, no. 4, pp. 815–824, 2009.
- [18] S. Wang and S. Nishio, ‘Heat Transport Characteristics in Closed Loop Oscillating Heat Pipes’, *Heat Transfer Summer Conference*, Vol. 47349, pp. 805–810, 2005.
- [19] M. B. Shafii, A. Faghri, and Y. Zhang, ‘Analysis of heat transfer in unlooped and looped pulsating heat pipes’, *Int. J. Numer. Methods Heat Fluid Flow*, vol. 12, no. 5, pp. 585–609, 2002.
- [20] M. Saha, C. M. Feroz, F. Ahmed, and T. Mujib, ‘Thermal performance of an open loop closed end pulsating heat pipe’, *Heat Mass Transf. und g*, vol. 48, no. 2, pp. 259–265, 2012.
- [21] R. R. Riehl, ‘Characteristics of an open loop pulsating heat pipe’, *SAE Tech. Pap.*, no. 724, 2004.
- [22] D. Mangini, M. Mameli, A. Georgoulas, L. Araneo, S. Filippeschi, and M. Marengo, ‘A pulsating heat pipe for space applications: Ground and microgravity experiments’, *Int. J. Therm. Sci.*, vol. 95, pp. 53–63, 2015.

- [23] V. Ayel *et al.*, ‘Experimental study of a closed loop flat plate pulsating heat pipe under a varying gravity force’, *Int. J. Therm. Sci.*, vol. 96, pp. 23–34, 2015.
- [24] M. Mameli, V. Manno, S. Filippeschi, and M. Marengo, ‘Thermal instability of a Closed Loop Pulsating Heat Pipe: Combined effect of orientation and filling ratio’, *Exp. Therm. Fluid Sci.*, vol. 59, pp. 222–229, 2014.
- [25] J. Qu, Q. Wang, and Q. Sun, ‘Lower limit of internal diameter for oscillating heat pipes: A theoretical model’, *Int. J. Therm. Sci.*, vol. 110, pp. 174–185, 2016.
- [26] N. Waowaew, P. Terdtoon, S. Maezawa, P. Kamonpet, and W. Klongpanich, ‘Correlation to predict heat transfer characteristics of a radially rotating heat pipe at vertical position’, *Appl. Therm. Eng.*, vol. 23, no. 8, pp. 1019–1032, 2003.
- [27] L. Quan and L. Jia, ‘Experimental Study on Heat Transfer Characteristic of Plate Pulsating Heat Pipe’, *International conference on Micro/Nanoscale Heat Transfer*, pp. 361–366, Vol. 43918, 2009.
- [28] J. Lee, Y. Joo, and S. J. Kim, ‘Effects of the number of turns and the inclination angle on the operating limit of micro pulsating heat pipes’, *Int. J. Heat Mass Transf.*, vol. 124, pp. 1172–1180, 2018.
- [29] M. Mameli, L. Araneo, S. Filippeschi, L. Marelli, R. Testa, and M. Marengo, ‘Thermal response of a closed loop pulsating heat pipe under a varying gravity force’, *Int. J. Therm. Sci.*, vol. 80, no. 1, pp. 11–22, 2014.
- [30] M. Li, L. Li, and D. Xu, ‘Effect of number of turns and configurations on the heat transfer performance of helium cryogenic pulsating heat pipe’, *Cryogenics (Guildf.)*, vol. 96, no. April, pp. 159–165, 2018.
- [31] N. Kammuang-Lue, P. Sakulchangsatjatai, C. Sriwiset, and P. Terdtoon, ‘Investigation and prediction of optimum meandering turn number of vertical and horizontal closed-loop pulsating heat pipes’, *Therm. Sci.*, vol. 22, no. 1, pp. 273–284, 2018.
- [32] H. Y. Noh and S. J. Kim, ‘Numerical simulation of pulsating heat pipes: Parametric investigation and thermal optimization’, *Energy Convers. Manag.*, vol. 203, p. 112237, 2020.

- [33] S. Khandekar, ‘Thermofluid dynamic study of flat-plate closed-loop pulsating heat pipes’, *Microscale Thermophys. Eng.*, vol. 6, no. 4, pp. 303–317, 2003.
- [34] C. Hua, X. Wang, X. Gao, H. Zheng, X. Han, and G. Chen, ‘Experimental research on the start-up characteristics and heat transfer performance of pulsating heat pipes with rectangular channels’, *Appl. Therm. Eng.*, vol. 126, pp. 1058–1062, 2017.
- [35] J. Qu, H. Y. Wu, and Q. Wang, ‘Experimental investigation of silicon-based micro-pulsating heat pipe for cooling electronics’, *Nanoscale Microscale Thermophys. Eng.*, vol. 16, no. 1, pp. 37–49, 2012.
- [36] Z. Li, L. Jia, and W. B. Wei, ‘Experimental study on natural convection cooling of LED based on plate pulsating heat pipe’, *K. Cheng Je Wu Li Hsueh Pao/Journal Eng. Thermophys.*, vol. 34, no. 7, pp. 1361–1364, 2013.
- [37] J. Lee and S. J. Kim, ‘Effect of channel geometry on the operating limit of micro pulsating heat pipes’, *Int. J. Heat Mass Transf.*, vol. 107, pp. 204–212, 2017.
- [38] K. Mehta, N. Mehta, and V. Patel, ‘Experimental investigation of the thermal performance of closed loop flat plate oscillating heat pipe’, *Exp. Heat Transf.*, vol. 34, no. 1, pp. 85–103, 2021.
- [39] A. Takawale, S. Abraham, A. Sielaff, P. S. Mahapatra, A. Pattamatta, and P. Stephan, ‘A comparative study of flow regimes and thermal performance between flat plate pulsating heat pipe and capillary tube pulsating heat pipe’, *Appl. Therm. Eng.*, vol. 149, pp. 613–624, 2019.
- [40] B. Markal, A. C. Candere, M. Avci, and O. Aydin, ‘Effect of double cross sectional ratio on performance characteristics of pulsating heat pipes’, *Int. Commun. Heat Mass Transf.*, vol. 127, p. 105583, 2021.
- [41] Y. Zhang and A. Faghri, ‘Advances and unsolved issues in pulsating heat pipes’, *Heat Transf. Eng.*, vol. 29, no. 1, pp. 20–44, 2008.
- [42] B. Holley and A. Faghri, ‘Analysis of pulsating heat pipe with capillary wick and varying channel diameter’, *Int. J. Heat Mass Transf.*, vol. 48, no. 13, pp. 2635–2651, 2005.

- [43] S. Liu, J. Li, X. Dong, and H. Chen, ‘Experimental study of flow patterns and improved configurations for pulsating heat pipes’, *J. Therm. Sci.*, vol. 16, no. 1, pp. 56–62, 2007.
- [44] K. Park and H. B. Ma, ‘Nanofluid effect on heat transport capability in a well-balanced oscillating heat pipe’, *J. Thermophys. Heat Transf.*, vol. 21, no. 2, pp. 443–445, 2007.
- [45] E. Sedighi, A. Amarloo, and B. Shafii, ‘Numerical and experimental investigation of flat-plate pulsating heat pipes with extra branches in the evaporator section’, *Int. J. Heat Mass Transf.*, vol. 126, pp. 431–441, 2018.
- [46] Morris, ‘Experimental Investigation of the Heat Transfer Capability and Thermal Performace of Dual Layer Pulsating Heat Pipes’, University of Rhode Island, 2012.
- [47] A. A. Hathaway, C. A. Wilson, and H. B. Ma, ‘Experimental investigation of uneven-turn water and acetone oscillating heat pipes’, *J. Thermophys. Heat Transf.*, vol. 26, no. 1, pp. 115–122, 2012.
- [48] K. H. Chien, Y. T. Lin, Y. R. Chen, K. S. Yang, and C. C. Wang, ‘A novel design of pulsating heat pipe with fewer turns applicable to all orientations’, *Int. J. Heat Mass Transf.*, vol. 55, no. 21–22, pp. 5722–5728, 2012.
- [49] C. Y. Tseng, K. S. Yang, K. H. Chien, M. S. Jeng, and C. C. Wang, ‘Investigation of the performance of pulsating heat pipe subject to uniform/alternating tube diameters’, *Exp. Therm. Fluid Sci.*, vol. 54, pp. 85–92, 2014.
- [50] C. Y. Tseng, K. S. Yang, K. H. Chien, S. K. Wu, and C. C. Wang, ‘A novel double pipe pulsating heat pipe design to tackle inverted heat source arrangement’, *Appl. Therm. Eng.*, vol. 106, pp. 697–701, 2016.
- [51] G. H. Kwon and S. J. Kim, ‘Operational characteristics of pulsating heat pipes with a dual-diameter tube’, *Int. J. Heat Mass Transf.*, vol. 75, pp. 184–195, 2014.
- [52] D. Zhang, Z. He, E. Jiang, C. Shen, and J. Zhou, ‘A review on start-up characteristics of the pulsating heat pipe’, *Heat Mass Transf.*, Vol. 57, pp. 723–35, 2021.

- [53] J. Lim and S. J. Kim, ‘Effect of a channel layout on the thermal performance of a flat plate micro pulsating heat pipe under the local heating condition’, *Int. J. Heat Mass Transf.*, vol. 137, pp. 1232–1240, 2019.
- [54] Y. He, D. Jiao, G. Pei, X. Hu, and L. He, ‘Experimental study on a three-dimensional pulsating heat pipe with tandem tapered nozzles’, *Exp. Therm. Fluid Sci.*, vol. 119, 2020.
- [55] J. Wang, H. Ma, and Q. Zhu, ‘Effects of the evaporator and condenser length on the performance of pulsating heat pipes’, *Appl. Therm. Eng.*, vol. 91, pp. 1018–1025, 2015.
- [56] J. Kim and S. J. Kim, ‘Experimental investigation on the effect of the condenser length on the thermal performance of a micro pulsating heat pipe’, *Appl. Therm. Eng.*, vol. 130, pp. 439–448, 2018.
- [57] M. Dilawar and A. Pattamatta, ‘A parametric study of oscillatory two-phase flows in a single turn Pulsating Heat Pipe using a non-isothermal vapor model’, *Appl. Therm. Eng.*, vol. 51, no. 1–2, pp. 1328–1338, 2013.
- [58] Z. Gan *et al.*, ‘Experimental Study on a Hydrogen Closed Loop Pulsating Heat Pipe with Different Adiabatic Lengths’, *Heat Transf. Eng.*, vol. 40, no. 3–4, pp. 205–214, 2019.
- [59] Q. Li, C. Wang, Y. Wang, Z. Wang, H. Li, and C. Lian, ‘Study on the effect of the adiabatic section parameters on the performance of pulsating heat pipes’, *Appl. Therm. Eng.*, vol. 180, p. 115813, 2020.
- [60] Z. Deng, Y. Zheng, X. Liu, B. Zhu, and Y. Chen, ‘Experimental study on thermal performance of an anti-gravity pulsating heat pipe and its application on heat recovery utilization’, *Appl. Therm. Eng.*, vol. 125, pp. 1368–1378, 2017.
- [61] H. Kargarsharifabad, S. J. Mamouri, M. B. Shafii, and M. T. Rahni, ‘Experimental investigation of the effect of using closed-loop pulsating heat pipe on the performance of a flat plate solar collector’, *J. Renew. Sustain. Energy*, vol. 5, no. 1, 2013.
- [62] D. Bastakoti, H. Zhang, W. Cai, and F. Li, ‘Numerical analysis of effects of surface tension and viscosity on 3 dimensional pulsating heat pipe’, *Am. Soc. Mech. Eng. Fluids Eng. Div. FEDSM*, vol. 3, pp. 1–7, 2018.

- [63] M. Kumar, R. Kant, A. K. Das, and P. K. Das, ‘Effect of Surface Tension Variation of the Working Fluid on the Performance of a Closed Loop Pulsating Heat Pipe’, *Heat Transf. Eng.*, vol. 40, no. 7, pp. 509–523, 2019.
- [64] M. Xing, R. Wang, and R. Xu, ‘Experimental study on thermal performance of a pulsating heat pipe with surfactant aqueous solution’, *Int. J. Heat Mass Transf.*, vol. 127, pp. 903–909, 2018.
- [65] A. Gandomkar, K. Kalan, M. Vandadi, M. B. Shafii, and M. H. Saidi, ‘Investigation and visualization of surfactant effect on flow pattern and performance of pulsating heat pipe’, *J. Therm. Anal. Calorim.*, vol. 139, no. 3, pp. 2099–2107, 2020.
- [66] J. Wang, J. Xie, and X. Liu, ‘Investigation on the performance of closed-loop pulsating heat pipe with surfactant’, *Appl. Therm. Eng.*, vol. 160, p. 113998, 2019.
- [67] K. Bao, X. Wang, Y. Fang, X. Ji, X. Han, and G. Chen, ‘Effects of the surfactant solution on the performance of the pulsating heat pipe’, *Appl. Therm. Eng.*, vol. 178, p. 115678, 2020.
- [68] M. Alhuyi Nazari, M. H. Ahmadi, R. Ghasempour, and M. B. Shafii, ‘How to improve the thermal performance of pulsating heat pipes: A review on working fluid’, *Renew. Sustain. Energy Rev.*, vol. 91, no. November 2017, pp. 630–638, 2018.
- [69] X. Liu, Y. Chen, and M. Shi, ‘Dynamic performance analysis on start-up of closed-loop pulsating heat pipes (CLPHPs)’, *Int. J. Therm. Sci.*, vol. 65, pp. 224–233, 2013.
- [70] J. Qu, H. Wu, and P. Cheng, ‘Start-up, heat transfer and flow characteristics of silicon-based micro pulsating heat pipes’, *Int. J. Heat Mass Transf.*, vol. 55, no. 21–22, pp. 6109–6120, 2012.
- [71] P. Srikrishna, N. Siddharth, S. U. M. Reddy, and G. S. V. L. Narasimham, ‘Experimental investigation of flat plate closed loop pulsating heat pipe’, *Heat Mass Transf.*, vol. 55, no.9, pp. 2637-2649, 2019.
- [72] Z. Xue and W. Qu, ‘Experimental study on effect of inclination angles to ammonia pulsating heat pipe’, *Chinese J. Aeronaut.*, vol. 27, no. 5, pp. 1122–1127, 2014.

- [73] S. Khandekar, N. Dollinger, and M. Groll, ‘Understanding operational regimes of closed loop pulsating heat pipes: An experimental study’, *Appl. Therm. Eng.*, vol. 23, no. 6, pp. 707–719, 2003.
- [74] Y. Zhu, X. Cui, H. Han, and S. Sun, ‘The study on the difference of the start-up and heat-transfer performance of the pulsating heat pipe with water-acetone mixtures’, *Int. J. Heat Mass Transf.*, vol. 77, pp. 834–842, 2014.
- [75] P. R. Pachghare and A. M. Mahalle, ‘Thermo-hydrodynamics of closed loop pulsating heat pipe: An experimental study’, *J. Mech. Sci. Technol.*, vol. 28, no. 8, pp. 3387–3394, 2014.
- [76] H. Han, X. Cui, Y. Zhu, T. Xu, Y. Sui, and S. Sun, ‘Experimental study on a closed-loop pulsating heat pipe (CLPHP) charged with water-based binary zeotropes and the corresponding pure fluids’, *Energy*, vol. 109, pp. 724–736, 2016.
- [77] W. Wang, X. Cui, and Y. Zhu, ‘Heat transfer performance of a pulsating heat pipe charged with acetone-based mixtures’, *Heat Mass Transf.*, vol. 53, no. 6, pp. 1983–1994, 2017.
- [78] R. Xu, C. Zhang, H. Chen, Q. Wu, and R. Wang, ‘Heat transfer performance of pulsating heat pipe with zeotropic immiscible binary mixtures’, *Int. J. Heat Mass Transf.*, vol. 137, pp. 31–41, 2019.
- [79] R. Zamani, K. Kalan, and M. B. Shafii, ‘Experimental investigation on thermal performance of closed loop pulsating heat pipes with soluble and insoluble binary working fluids and a proposed correlation’, *Heat Mass Transf.*, vol. 55, no. 2, pp. 375–384, 2019.
- [80] C. Y. Tsai, H. T. Chien, P. P. Ding, B. Chan, T. Y. Luh, and P. H. Chen, ‘Effect of structural character of gold nanoparticles in nanofluid on heat pipe thermal performance’, *Mater. Lett.*, vol. 58, no. 9, pp. 1461–1465, 2004.
- [81] H. B. Ma, C. Wilson, Q. Yu, K. Park, U. S. Choi, and M. Tirumala, ‘An experimental investigation of heat transport capability in a nanofluid oscillating heat pipe’, *J. Heat Transfer*, vol. 128, no. 11, pp. 1213–1216, 2006.

- [82] Y. H. Lin, S. W. Kang, and H. L. Chen, 'Effect of silver nano-fluid on pulsating heat pipe thermal performance', *Appl. Therm. Eng.*, vol. 28, no. 11–12, pp. 1312–1317, 2008.
- [83] R. R. Riehl and N. Dos Santos, 'Water-copper nanofluid application in an open loop pulsating heat pipe', *Appl. Therm. Eng.*, vol. 42, pp. 6–10, 2012.
- [84] V. K. Karthikeyan, K. Ramachandran, B. C. Pillai, and A. Brusly Solomon, 'Effect of nanofluids on thermal performance of closed loop pulsating heat pipe', *Exp. Therm. Fluid Sci.*, vol. 54, pp. 171–178, 2014.
- [85] J. Qu and H. Wu, 'Thermal performance comparison of oscillating heat pipes with SiO₂/water and Al₂O₃/water nanofluids', *Int. J. Therm. Sci.*, vol. 50, no. 10, pp. 1954–1962, 2011.
- [86] S. Rudresha and V. Kumar, 'CFD Analysis and Experimental Investigation on Thermal Performance of Closed loop Pulsating Heat pipe using different Nanofluids Experiments Apparatus and procedure .', *Int. J. Adv. Res.*, vol. 2, no. 8, pp. 753–760, 2014.
- [87] M. A. Nazari, R. Ghasempour, M. H. Ahmadi, G. Heydarian, and M. B. Shafii, 'Experimental investigation of graphene oxide nanofluid on heat transfer enhancement of pulsating heat pipe', *Int. Commun. Heat Mass Transf.*, vol. 91, pp. 90–94, 2018.
- [88] A. Akbari and M. H. Saidi, 'Experimental investigation of nanofluid stability on thermal performance and flow regimes in pulsating heat pipe', *J. Therm. Anal. Calorim.*, vol. 135, no. 3, pp. 1835–1847, 2019.
- [89] M. Gonzalez and Y. J. Kim, 'Experimental study of a pulsating heat pipe using nanofluid as a working fluid', in *Fourteenth Intersociety Conference on Thermal and Thermomechanical Phenomena in Electronic Systems (ITherm)*, 2014, pp. 541–546.
- [90] F. M. Ali, W. M. M. Yunus, and Z. A. Talib, 'Study of the effect of particles size and volume fraction concentration on the thermal conductivity and thermal diffusivity of Al₂O₃ nanofluids', *Int. J. Phys. Sci.*, vol. 8, no. 28, pp. 1442–1457, 2013.

- [91] H. J. Kim, S. H. Lee, J. H. Lee, and S. P. Jang, ‘Effect of particle shape on suspension stability and thermal conductivities of water-based bohemite alumina nanofluids’, *Energy*, vol. 90, pp. 1290–1297, 2015.
- [92] V. K. Karthikeyan, K. Ramachandran, B. C. Pillai, and A. Brusly Solomon, ‘Understanding thermo-fluidic characteristics of a glass tube closed loop pulsating heat pipe: flow patterns and fluid oscillations’, *Heat Mass Transf.*, vol. 51, no. 12, pp. 1669–1680, 2015.
- [93] M. Mohammadi, M. Mohammadi, and M. B. Shafii, ‘Experimental investigation of a pulsating heat pipe using ferrofluid (magnetic nanofluid)’, *J. Heat Transfer*, vol. 134, no. 1, pp. 14–16, 2012.
- [94] H. R. Goshayeshi, M. Goodarzi, M. R. Safaei, and M. Dahari, ‘Experimental study on the effect of inclination angle on heat transfer enhancement of a ferrofluid in a closed loop oscillating heat pipe under magnetic field’, *Exp. Therm. Fluid Sci.*, vol. 74, pp. 265–270, 2016.
- [95] E. R. Babu, H. N. Reddappa, and G. V. Gnanendra Reddy, ‘Effect of Filling Ratio on Thermal Performance of Closed Loop Pulsating Heat Pipe’, *Mater. Today Proc.*, vol. 5, no. 10, pp. 22229–22236, 2018.
- [96] M. L. Rahman, M. Chowdhury, N. A. Islam, S. M. Mufti, and M. Ali, ‘Effect of filling ratio and orientation on the thermal performance of closed loop pulsating heat pipe using ethanol’, *AIP Conf. Proc.*, vol. 1754, 2016.
- [97] D. Yin, H. Rajab, and H. B. Ma, ‘Theoretical analysis of maximum filling ratio in an oscillating heat pipe’, *Int. J. Heat Mass Transf.*, vol. 74, pp. 353–357, 2014.
- [98] B. Y. Tong, T. N. Wong, and K. T. Ooi, ‘Closed-loop pulsating heat pipe’, *Appl. Therm. Eng.*, vol. 21, no. 18, pp. 1845–1862, 2001.
- [99] G. Spinato, N. Borhani, and J. R. Thome, ‘Operational regimes in a closed loop pulsating heat pipe’, *Int. J. Therm. Sci.*, vol. 102, pp. 78–88, 2016.
- [100] V. M. Patel and H. B. Mehta, ‘Channel wise displacement-velocity-frequency analysis in acetone charged multi-turn Closed Loop Pulsating Heat Pipe’, *Energy Convers. Manag.*, vol. 195, no. May, pp. 367–383, 2019.

- [101] P. Cheng and H. Ma, 'A mathematical model of an oscillating heat pipe', *Heat Transf. Eng.*, vol. 32, no. 11–12, pp. 1037–1046, 2011.
- [102] V. S. Nikolayev, 'A dynamic film model of the pulsating heat pipe', *J. Heat Transfer*, vol. 133, no. 8, pp. 1–9, 2011.
- [103] J. Jo, J. Kim, and S. J. Kim, 'Experimental investigations of heat transfer mechanisms of a pulsating heat pipe', *Energy Convers. Manag.*, vol. 181, no. December 2018, pp. 331–341, 2019.
- [104] I. Yoon *et al.*, 'Neutron phase volumetry and temperature observations in an oscillating heat pipe', *Int. J. Therm. Sci.*, vol. 60, pp. 52–60, 2012.
- [105] S. Jun and S. J. Kim, 'Experimental investigation on the thermodynamic state of vapor plugs in pulsating heat pipes', *Int. J. Heat Mass Transf.*, vol. 134, pp. 321–328, 2019.
- [106] V. M. Patel, Gaurav, and H. B. Mehta, 'Influence of working fluids on startup mechanism and thermal performance of a closed loop pulsating heat pipe', *Appl. Therm. Eng.*, vol. 110, pp. 1568–1577, 2017.
- [107] M. Mameli, M. Marengo, and S. Khandekar, 'Local heat transfer measurement and thermo-fluid characterization of a pulsating heat pipe', *Int. J. Therm. Sci.*, vol. 75, pp. 140–152, 2014.
- [108] W. Jiansheng, W. Zhenchuan, and L. Meijun, 'Thermal performance of pulsating heat pipes with different heating patterns', *Appl. Therm. Eng.*, vol. 64, no. 1–2, pp. 209–212, 2014.
- [109] D. S. Jang, H. J. Chung, Y. Jeon, and Y. Kim, 'Thermal performance characteristics of a pulsating heat pipe at various nonuniform heating conditions', *Int. J. Heat Mass Transf.*, vol. 126, pp. 855–863, 2018.
- [110] D. Torresin, F. Agostini, A. Mularczyk, B. Agostini, and M. Habert, 'Double condenser pulsating heat pipe cooler', *Appl. Therm. Eng.*, vol. 126, pp. 1051–1057, 2017.
- [111] S. Khandekar and M. Groll, 'An insight into thermo-hydrodynamic coupling in closed loop pulsating heat pipes', *Int. J. Therm. Sci.*, vol. 43, no. 1, pp. 13–20, 2004.

- [112] S. Jun and S. J. Kim, 'Comparison of the thermal performances and flow characteristics between closed-loop and closed-end micro pulsating heat pipes', *Int. J. Heat Mass Transf.*, vol. 95, pp. 890–901, 2016.
- [113] S. Jun and S. J. Kim, 'Experimental study on a criterion for normal operation of pulsating heat pipes in a horizontal orientation', *Int. J. Heat Mass Transf.*, vol. 137, pp. 1064–1075, 2019.
- [114] I. Nekrashevych and V. S. Nikolayev, 'Pulsating heat pipe simulations: Impact of PHP orientation', *Microgravity Science and Technology*, Vol. 31, no. 3, pp. 241-8, 2019.
- [115] S. Khandekar, A. P. Gautam, and P. K. Sharma, 'Multiple quasi-steady states in a closed loop pulsating heat pipe', *Int. J. Therm. Sci.*, vol. 48, no. 3, pp. 535–546, 2009.
- [116] J. R. Taylor, 'An Introduction to Error Analysis: The Study of Uncertainties in Physical Measurements', 2nd ed. Sausalito, CA, USA: University Science Books, 1997.
- [117] Klein, S. A., & Alvarado, F. L. (2002). Engineering equation solver. F-Chart Software, Madison, WI, 1.
- [118] S. J. Kline, F. A. McClintock, Describing uncertainties in single-sample experiments, *Mech. Eng.* 75 (1) (1953) 3-8.
- [119] P. Griffith, J.D. Wallis The Role of Surface Conditions in Nucleate Boiling Technical Report, Massachusetts Institute of Technology, 1958.
- [120] C.J. Han, P. Griffith 'The mechanism of heat transfer in nucleate pool boiling', *Int. J. Heat and Mass Transfer*, vol. 8, iss. 6, pp. 887-904, 1965.
- [121] J.R. Howell, R. Siegel 'Incipience, growth and detachment of boiling bubbles in saturated water from artificial nucleation sites of known geometry and size' *In: Proc. 3d Int. Heat Transfer Conf.* New York: Sci. Press, vol. 4, pp. 12-23, 1966.
- [122] G.S. Dzakowich, W. Frost 'An analytical description of the waiting period between successive vapor bubbles formed during nucleate boiling'. *In Proc. 1968 Heat Transfer and Fluid Mechanics Inst.* Stanford: Stanford Univ. press, pp. 98-115, 1968.

ANNEX A: List of Publications

Journal Articles:

1. Mane, K.V., Alekseik, Y. Comprehensive parametric and design review for reducing pulsating heat pipes dependence on space orientation. *Archives of Thermodynamics*, 2024, 45(2), p. 165-182. DOI: <https://doi.org/10.24425/ather.2024.150863> (**SCOPUS Q3**).
2. Mane, K., & Alekseik, Y. The combined effect of heating zone length and inclination angle on start-up, transient, and operational characteristics of a pulsating heat pipe. *Refrigeration Engineering and Technology*, 2024, 60(3), p. 156-167. DOI: <https://doi.org/10.15673/ret.v60i3.2997>

Conference Proceedings:

1. Mane K.V., Alekseik Y. Influence of PHP channel design on start-up and gravity: a review. *Modern Problems of Scientific Support of Energy. Materials of the XIX Scientific and Practical Conference of Young Scientists and Students*, Kyiv, April 20–23, 2021, Kyiv: KPI, Polytechnic Publishing House, 2021, Vol. 1, p. 125-126.
2. Mane K., Alekseik Y. Influence of heating zone length on thermal performance of pulsating heat pipe. *Modern Problems of Scientific Support for Energy. Proceedings of the XX International Scientific and Practical Conference of Young Scientists and Students*, Kyiv, April 25–28, 2023. Kyiv: KPI, Polytechnic Publishing House, 2023, Vol. 1, p. 107-108.
3. Mane K.V., Alekseik Y. Pulsating heat pipe sensitivity to space orientation: zone length and heat carrier influence. *Modern Problems of Scientific Support for Energy. Proceedings of the XXI International Scientific and Practical Conference of Young Scientists and Students*, Kyiv, April 23–26, 2024. Kyiv: KPI, Polytechnic Publishing House, 2024, Vol.1, p. 70-72.
4. Alekseik Ye.S, Mane K.V. Influence of the heat carrier and the length of the heating zone of a pulsating heat pipe on the limits of the main operating modes at

different inclination angles. Proceedings of the XXV International Scientific and Practical Conference of Modern Information and Electronic Technologies, May 27–29, 2024, Odessa, Ukraine, pp. 72-73

ANNEX B: The act of implementation in the educational process

ПОГОДЖЕНО

ЗАТВЕРДЖУЮ


Завідувач кафедри

Директор

атомної енергетики

Навчально-наукового інституту

атомної та теплової енергетики

 Валерій ТУЗ


 Свєтєлєн ПИСЬМЕННИЙ
2025 р.

АКТ

Про використання в навчальному процесі кафедри атомної енергетики
Навчально-наукового інституту атомної та теплової енергетики
Національного технічного університету України
«Київський політехнічний інститут імені Ігоря Сікорського»
результатів дисертаційної роботи Манє Кішора Вішванатха (Mane Kishor Vishwanath)
«Визначення параметрів ефективного застосування пульсаційних теплових труб в системах
охолодження електронної техніки» (Determination of parameters of effective use of pulsation
heat pipes in cooling systems of electronic equipment)

Комісія у складі професора кафедри атомної енергетики д.т.н., проф. Кондратюка В.А. (голова комісії), доцента кафедри атомної енергетики к.т.н. доц. Воробйова М.В. та професора кафедри атомної енергетики д.т.н. проф. Кравця В.Ю. розглянула стан використання матеріалів дисертаційної роботи Манє Кішора Вішванатха (Mane Kishor Vishwanath) при підготовці PhD за напрямком 142 Енергетичне машинобудування та 143 Атомна енергетика.

Комісія прийшла до висновку, що матеріали дисертаційної роботи Манє Кішора Вішванатха (Mane Kishor Vishwanath) входять до складу:

- дисципліни «Кінетика фазових перетворень в енергетичному обладнанні», лекційні заняття: «Звичайні теплові труби. Мініатюрні і мікротеплові труби. Конструкція. Особливості роботи. Газорегульовані теплові труби. Контурні теплові труби. Пульсаційні теплові труби. Конструкція. Особливості роботи.» та «Теплопередавальні характеристики пульсаційних теплових труб в залежності від робочих параметрів».

 Голова комісії д.т.н., проф.  Вадим КОНДРАТЮК

 Члени комісії к.т.н., доц.  Микита ВОРОБЙОВ

 д.т.н., проф.  Володимир КРАВЕЦЬ